



US Army Corps  
of Engineers

AD-A187 240

DTIC FILE COPY

MISCELLANEOUS PAPER GL-87-25



# AN EXAMINATION OF SLOPE STABILITY COMPUTATION PROCEDURES FOR SUDDEN DRAWDOWN

by

Stephen G. Wright

Geotechnical Engineering Department  
University of Texas at Austin  
Austin, Texas 78712

and

J. M. Duncan

Department of Civil Engineering  
Virginia Polytechnic Institute  
Blacksburg, Virginia 24061



DTIC  
SELECTED  
NOV 06 1987  
S D  
CD

September 1987

Final Report

Approved For Public Release Distribution Unlimited

Prepared for DEPARTMENT OF THE ARMY  
US Army Corps of Engineers  
Washington, DC 20314-1000

Under Computer Applications in  
Geotechnical Engineering (CAGE) Project  
Contract Nos. DACW39-86-M-0982, DACW39-86-M-1731

Monitored by Geotechnical Laboratory  
US Army Engineer Waterways Experiment Station  
PO Box 631, Vicksburg, Mississippi 39180-0631



Destroy this report when no longer needed. Do not return  
it to the originator.

The findings in this report are not to be construed as an official  
Department of the Army position unless so designated  
by other authorized documents.

The contents of this report are not to be used for  
advertising, publication, or promotional purposes.  
Citation of trade names does not constitute an  
official endorsement or approval of the use of  
*such commercial products.*

Unclassified

SECURITY CLASSIFICATION OF THIS PAGE

| REPORT DOCUMENTATION PAGE  |       |  |  | Form Approved<br>OMB No 0704 0188<br>Exp Date Jun 30 1986 |                        |
|--|-------|--|--|---|------------------------|
| 1a REPORT SECURITY CLASSIFICATION<br>Unclassified  |       | 1b RESTRICTIVE MARKINGS  |  |   |                        |
| 2a SECURITY CLASSIFICATION AUTHORITY   |       | 3 DISTRIBUTION/AVAILABILITY OF REPORT  |  |   |                        |
| 2b DECLASSIFICATION/DOWNGRADING SCHEDULE   |       | Approved for public release;<br>distribution unlimited                           |  |   |                        |
| 4 PERFORMING ORGANIZATION REPORT NUMBER(S)   |       | 5 MONITORING ORGANIZATION REPORT NUMBER(S)                                       |  |   |                        |
|  |       | Miscellaneous Paper GL-87-25   |  |   |                        |
| 6a NAME OF PERFORMING ORGANIZATION<br>See reverse  |       | 6b OFFICE SYMBOL<br>(if applicable)  | 7a NAME OF MONITORING ORGANIZATION<br>USAEWES<br>Geotechnical Laboratory               |   |                        |
| 6c ADDRESS (City, State, and ZIP Code)<br>Austin, TX 78712 and<br>Blacksburg, VA 24061   |       | 7b ADDRESS (City, State, and ZIP Code)<br>PO Box 631<br>Vicksburg, MS 39180-0631 |  |   |                        |
| 8a NAME OF FUNDING / SPONSORING ORGANIZATION<br>US Army Corps of Engineers   |       | 8b OFFICE SYMBOL<br>(if applicable)  | 9 PROCUREMENT INSTRUMENT IDENTIFICATION NUMBER<br>DACW39-86-M-0982<br>DACW39-86-M-1731 |   |                        |
| 8c ADDRESS (City, State, and ZIP Code)<br>Washington, DC 20314-1000  |       | 10 SOURCE OF FUNDING NUMBERS   |  |   |                        |
|  |       | PROGRAM ELEMENT NO   | PROJECT NO   | TASK NO   | WORK UNIT ACCESSION NO |
| 11 TITLE (Include Security Classification)<br>An Examination of Slope Stability Computation Procedures for Sudden Drawdown   |       |  |  |   |                        |
| 12 PERSONAL AUTHOR(S)<br>Wright, Stephen G., and Duncan, J. M.   |       |  |  |   |                        |
| 13a TYPE OF REPORT<br>Final Report   |       | 13b TIME COVERED<br>FROM to  |  | 14 DATE OF REPORT (Year Month Day)<br>September 1987      | 15 PAGE COUNT<br>177   |
| 16 SUPPLEMENTARY NOTATION<br>Available from National Technical Information Service, 5825 Port Royal Road,<br>Springfield, VA 22161.  |       |  |  |   |                        |
| 17 COSATI CODES  |       |  | 18 SUBJECT TERMS (Continue on reverse if necessary and identify by block number)       |   |                        |
| FIELD  | GROUP | SUB GROUP  | effective stress analysis  | Slope stability   |                        |
|  |       |  | Pore pressure coefficients   | Sudden drawdown   |                        |
|  |       |  | Shear strength envelopes   | Two-stage analysis  |                        |
| 19 ABSTRACT (Continue on reverse if necessary and identify by block number)<br>"Sudden" or "rapid" drawdown is considered to occur when reservoir or other adjacent water levels are lowered at such a rate that little or no drainage occurs in an earth slope at the time the water level is being lowered. Slope stability analyses are routinely performed to calculate the factor of safety for earth slopes subjected to this condition. Several different procedures exist and are currently used by designers to compute slope stability for the case of sudden drawdown. These various procedures are based on fundamentally different approaches and are known to produce different results in at least some instances. The procedures, the assumptions employed, and the numerical results obtained using these procedures are the subject of this paper.<br>The various procedures differ primarily in the manner in which the drawdown rate is defined and can be grouped into two general categories. The first category includes those procedures which are based on the use of effective stress. The second category includes procedures require that pore water pressure can be estimated at the end of drawdown. |       |  |  |   |                        |
| 20 DISTRIBUTION STATEMENT (If available)   |       |  | 21 LIMITATION OF ABSTRACT  |   |                        |
| <input checked="" type="checkbox"/> UNCLASSIFIED   |       |  | <input type="checkbox"/> UNCLASSIFIED  |   |                        |
| 22 NAME OF RESPONSIBLE ORGANIZATION  |       |  | 23 DISTRIBUTION STATEMENT (If available)   |   |                        |
| US Army Corps of Engineers   |       |  | <input type="checkbox"/> UNCLASSIFIED  |   |                        |

6a. NAME OF PERFORMING ORGANIZATION.

Geotechnical Engineering Center, Civil Engineering Department, University of Texas at Austin and Department of Civil Engineering, Virginia Polytechnic Institute

19. ABSTRACT (Continued).

and the differences among the various effective stress procedures are related directly to differences in the procedures used to estimate pore water pressures. The second category of procedures for sudden drawdown analysis is comprised of two-stage procedures: one set (stage) of calculations is performed for conditions existing immediately prior to drawdown and is used to estimate effective stresses and corresponding undrained strengths; the second set (stage) of computations is performed for conditions immediately after drawdown and employs undrained shear strengths estimated from the first set of computations.

This study provides a basis for a number of important conclusions regarding the accuracy and the degree of conservatism of the procedures for analyzing rapid drawdown slope stability. From these results, the best procedure should have the following characteristics:

- a. The procedure should employ a measure of shear strength and pore pressure that reflects the actual properties of the soils in the slopes.
- b. The procedures should employ a soundly based technique for relating shear strength to effective consolidation pressures.
- c. The procedure should not include strength components due to negative pore water pressures to avoid overestimating factors of safety for conditions where partial drainage occurs during drawdown.

A method with these characteristics can be conceived as a combination of methods currently in use. It could be described as being a modification of the method currently used by the US Army Corps of Engineers, the modification being an adoption of Lowe and Karafiath's procedure for representing the undrained strength of the soil rather than using the R-envelope as is now done.

|               |   |
|---------------|---|
| Accession     |   |
| NTIS          | J |
| DTIC          |   |
| Unannounced   |   |
| Justification |   |
| By            |   |
| Date          |   |
| Dist          |   |
| A-1           |   |



## PREFACE

Although considerable advances have been made during the past several years in the understanding of shear strength and computation procedures for estimating slope stability, the procedures for estimating slope stability during sudden drawdown have remained relatively poorly understood. The lack of understanding of procedures for slope stability computations for sudden drawdown became especially evident to one of the writers (Wright) during recent efforts to develop a computer program for slope stability for the US Army Corps of Engineers (CE). Rather than settle for adoption of a procedure in the computer program somewhat arbitrarily, without understanding the potential differences among procedures, the US Army Engineer Waterways Experiment Station (WES) contracted (Contract Nos. DACW39-86-M-0982 and DACW39-86-M-1731) with the writers to prepare a state-of-the-art paper on the subject of stability computations for sudden drawdown. The results of that effort are presented in this paper.

An initial draft of this paper was first prepared by Dr. Stephen G. Wright and reviewed by Dr. J. M. Duncan. A separate draft set of comments, conclusions, and recommendations was subsequently prepared by Dr. Duncan. The two drafts were then combined in the final form presented herein. Various CE personnel and consultants also reviewed the original draft of this paper and offered many useful suggestions and comments. Their contributions are gratefully acknowledged and, to the extent feasible, their suggestions have been incorporated into this paper.

The writers express their appreciation to the members of the Computer Applications in Geotechnical Engineering (CAGE) Committee of the CE for their many comments and useful suggestions. Special appreciation is extended to Messrs. Dale Munger, Office, Chief of Engineers (OCE); and Earl Edris, Engineering Group, Soil Mechanics Division, Geotechnical Laboratory (GL), WES; Professors Tom Wolff, Michigan State University; and Milton Harr, Purdue University, for their many detailed comments on the first draft of this report. The interest and support of the CE provided both the catalyst and means that made this study possible.

The report was funded by the CAGE project sponsored by OCE. Mr. William E. Strohm, Jr., Engineering Geology and Rock Mechanics Division, GL, was Principal Investigator of the CAGE project. At WES, the work was

under the management of the Soil Mechanics Division (SMD), GL.

The Contract Monitor was Mr. Earl Edris. Mr. Clifford L. McAnear was Chief, SMD; and Dr. William F. Marcuson III was Chief, GL, during the preparation of this report.

COL Dwayne G. Lee, CE, is Commander and Director of WES. Dr. Robert W. Whalin is Technical Director.

## TABLE OF CONTENTS

|  |    |
|--|----|
| PREFACE.....   | 1  |
| LIST OF FIGURES.....   | 6  |
| LIST OF TABLES.....  | 11 |
| NOMENCLATURE.....  | 12 |
| SECTION 1 - INTRODUCTION.....                                    | 15 |
| Background and General Assumptions.....                          | 15 |
| Organization of Report.....                                      | 17 |
| SECTION 2 - EFFECTIVE STRESS (ONE-STEP) ANALYSIS PROCEDURES..... | 19 |
| Shear Strength Parameters.....                                   | 19 |
| Estimation of Pore Water Pressures.....                          | 23 |
| Bishop-Morgenstern Procedure.....                                | 23 |
| Transient Flow Solutions.....                                    | 34 |
| Discussion of assumptions.....                                   | 36 |
| Soil is saturated.....   | 37 |
| Single effective stress component.....                           | 37 |
| Constant total stress ( $\Delta\bar{\sigma} = -\Delta u$ ).....  | 38 |
| Simplified Procedures Based on Water Flow.....                   | 39 |
| Procedures Based on Dupuit Assumptions.....                      | 39 |
| Procedures Based on Steady-State Flow.....                       | 41 |
| Empirical Procedures Based on Experience.....                    | 43 |
| Discussion.....  | 43 |
| Summary.....   | 50 |
| SECTION 3 - TWO-STAGE ANALYSIS PROCEDURES.....                   | 52 |
| Introduction.....  | 52 |
| Stage 1 Stability Calculations.....                              | 52 |
| Stage 2 Stability Calculations.....                              | 54 |

|  |    |
|--|----|
| Corps of Engineers' Procedure.....                                   | 55 |
| Lowe and Karafiath's Procedure.....                                  | 62 |
| Discussion.....  | 71 |
| R-envelope versus $\tau_{ff}-\bar{\sigma}_{fc}$ line.....            | 71 |
| R-envelope construction.....   | 77 |
| SECTION 4 - ESTIMATION OF ACU STRENGTH ENVELOPES FROM ICU TESTS..... | 82 |
| Taylor's Procedure.....  | 83 |
| $\tau_{ff}$ versus $\bar{\sigma}_{fc}$ envelopes.....                | 84 |
| Pore pressure coefficients, $\bar{A}_f$ .....                        | 85 |
| Lowe and Karafiath's Procedure.....                                  | 85 |
| $\tau_{ff}$ versus $\bar{\sigma}_{fc}$ envelopes.....                | 86 |
| Pore pressure coefficients, $\bar{A}_f$ .....                        | 87 |
| Modified Karafiath Procedure.....                                    | 87 |
| $\tau_{ff}$ versus $\bar{\sigma}_{fc}$ envelopes.....                | 87 |
| Pore pressure coefficients, $\bar{A}_f$ .....                        | 88 |
| Extension of Noorany and Seed's Study.....                           | 89 |
| $\tau_{ff}$ versus $\bar{\sigma}_{fc}$ envelopes.....                | 89 |
| Pore pressure coefficients, $\bar{A}_f$ .....                        | 90 |
| Extension of H. Benjamin's Study.....                                | 90 |
| $\tau_{ff}$ versus $\bar{\sigma}_{fc}$ envelopes.....                | 90 |
| Pore pressure coefficients, $\bar{A}_f$ .....                        | 90 |
| Linear Interpolation Procedure.....                                  | 91 |
| $\tau_{ff}$ versus $\bar{\sigma}_{fc}$ envelopes.....                | 91 |
| Pore pressure coefficients, $\bar{A}_f$ .....                        | 92 |
| Comparison of Procedures.....  | 93 |
| Pilarcitos Dam Soil.....   | 93 |
| $\tau_{ff}$ versus $\bar{\sigma}_{fc}$ envelopes.....                | 94 |

|  |     |
|--|-----|
| $\bar{A}_f$ versus $\bar{\sigma}_{fc}$ .....               | 94  |
| Other soils.....   | 94  |
| $\tau_{ff}$ versus $\bar{\sigma}_{fc}$ envelopes.....      | 108 |
| $\bar{A}_f$ versus $\bar{\sigma}_{fc}$ .....               | 108 |
| Discussion.....  | 108 |
| SECTION 5 - AN ALTERNATE APPROACH FOR SUDDEN DRAWDOWN..... | 120 |
| Validity of Skempton's Pore Pressure Equation.....         | 121 |
| Finite Element Computations.....                           | 127 |
| Pore Pressure Coefficients.....                            | 129 |
| Pore Pressure Computations.....                            | 131 |
| Stability Computations.....                                | 132 |
| Summary.....   | 132 |
| SECTION 6 - COMPARATIVE EXAMPLES AND CALCULATIONS.....     | 134 |
| Effective Stress Procedures.....                           | 134 |
| Analyses for Pilarcitos Dam.....                           | 144 |
| Parametric Studies.....                                    | 153 |
| SECTION 7 - SUMMARY, CONCLUSIONS AND RECOMMENDATIONS.....  | 161 |
| Effective Stress Analysis Procedures.....                  | 161 |
| Two-Stage Analysis Procedures.....                         | 162 |
| Conclusions.....   | 163 |
| Recommendations.....                                       | 167 |
| REFERENCES .....   | 170 |

## LIST OF FIGURES

|              |   |    |
|--------------|---|----|
| Figure 2.1 - | Effective Stress Paths with Failure Envelopes for (a) "Stress Path Tangency" and (b) "Peak Principal Stress Difference" Failure Criteria.....   | 21 |
| Figure 2.2 - | Changes in Water Levels Used to Compute Major Principal Stress Changes in Bishop's and Morgenstern's Procedure..  | 25 |
| Figure 2.3 - | Representation of Pore Water Pressures After Drawdown for Bishop's and Morgenstern's Procedure.....   | 27 |
| Figure 2.4 - | Mohr's Circle of Stress Showing Principal Stress Changes for Sudden Drawdown.....   | 30 |
| Figure 2.5 - | Variation of the Pore Pressure Coefficient $B$ with the Value of $A$ for Various Values of the Ratio, $\Delta\sigma_1/\Delta\sigma_3$ .....   | 31 |
| Figure 2.6 - | Major and Minor Principal Stress Changes Due to Sudden Drawdown for an Element of Soil at the Slope Face.....   | 33 |
| Figure 2.7 - | Comparison of Factors of Safety Calculated Using Effective Stresses with Measured Pore Water Pressures and Pore Water Pressures Estimated Using Bishop's and Morgenstern's Procedure (After Winkley, 1982)..... | 48 |
| Figure 3.1 - | Schematic Illustration of the Two Stages Considered in Analyses by Two-Stage Procedures for Sudden Drawdown....   | 53 |
| Figure 3.2 - | Bilinear Shear Strength Envelope Used in Corps of Engineers' Procedure for Sudden Drawdown Stability Calculations.....  | 56 |
| Figure 3.3 - | Bilinear Shear Strength Envelope Used in Corps of Engineers' Procedure for Steady-Seepage Stability Calculations.....   | 57 |
| Figure 3.4 - | Family of Shear Strength Envelopes for Various Anisotropic Consolidation Stress Ratios, $K_c (= \bar{\sigma}_{1c}/\bar{\sigma}_{3c})$ , Used in Lowe and Karafiath's Procedure.....                             | 63 |
| Figure 3.5 - | Orientation of Major Principal Stress at Consolidation ( $\bar{\sigma}_{1c}$ ) Assumed in Lowe and Karafiath's Procedure.....   | 66 |
| Figure 3.6 - | Relationship between Stresses on the Shear Plane and the Principal Stresses at Consolidation for Lowe and Karafiath's Procedure.....  | 67 |
| Figure 3.7 - | Mohr's Circles for Stresses at Failure for (a) the Minor Principal Stress Approaching Zero, and (b) the Effective Stress on the Failure Plane Approaching Zero.....   | 69 |
| Figure 3.8 - | Circles of Stress and the Corresponding R-Envelope.....   | 73 |

|               |  |     |
|---------------|--|-----|
| Figure 3.9 -  | Relationship between the R-Envelope and the Line Representing the Relationship between $\tau_{ff}$ and $\bar{\sigma}_{fc}$ for Isotropic Consolidation.....  | 74  |
| Figure 3.10 - | R-Envelope Constructed through Points Corresponding to Stresses on the Failure Plane.....  | 78  |
| Figure 4.1 -  | Shear Strength Envelopes ( $\tau_{ff}$ vs. $\bar{\sigma}_{fc}$ ) for Various Effective Principal Consolidation Stress Ratios ( $K_c$ ) Estimated from Strength Parameters for Isotropic Consolidation Using Taylor's Procedure.....  | 95  |
| Figure 4.2 -  | Shear Strength Envelopes ( $\tau_{ff}$ vs. $\bar{\sigma}_{fc}$ ) for Various Effective Principal Consolidation Stress Ratios ( $K_c$ ) Estimated from Strength Parameters for Isotropic Consolidation Using Lowe and Karafiath's Procedure.....  | 96  |
| Figure 4.3 -  | Shear Strength Envelopes ( $\tau_{ff}$ vs. $\bar{\sigma}_{fc}$ ) for Various Effective Principal Consolidation Stress Ratios ( $K_c$ ) Estimated from Strength Parameters for Isotropic Consolidation Using the Modified form of Lowe and Karafiath's Procedure.....   | 97  |
| Figure 4.4 -  | Shear Strength Envelopes ( $\tau_{ff}$ vs. $\bar{\sigma}_{fc}$ ) for Various Effective Principal Consolidation Stress Ratios ( $K_c$ ) Estimated from Strength Parameters for Isotropic Consolidation Using the Extension of Noorany and Seed's Procedure.....   | 98  |
| Figure 4.5 -  | Shear Strength Envelopes ( $\tau_{ff}$ vs. $\bar{\sigma}_{fc}$ ) for Various Effective Principal Consolidation Stress Ratios ( $K_c$ ) Estimated from Strength Parameters for Isotropic Consolidation Using the Extension of Benjamin's Study...   | 99  |
| Figure 4.6 -  | Shear Strength Envelopes ( $\tau_{ff}$ vs. $\bar{\sigma}_{fc}$ ) for Various Effective Principal Consolidation Stress Ratios ( $K_c$ ) Estimated from Strength Parameters for Isotropic Consolidation Using Linear Interpolation.....  | 100 |
| Figure 4.7 -  | Variation in the Pore Pressure Coefficient, $\bar{A}_f$ , with Effective Normal Stress on the Failure Plane at Consolidation, $\bar{\sigma}_{fc}$ , for Various Effective Principal Consolidation Stress Ratios ( $K_c$ ) Estimated from Strength Parameters for Isotropic Consolidation Using Taylor's Procedure.....             | 101 |
| Figure 4.8 -  | Variation in the Pore Pressure Coefficient, $\bar{A}_f$ , with Effective Normal Stress on the Failure Plane at Consolidation, $\bar{\sigma}_{fc}$ , for Various Effective Principal Consolidation Stress Ratios ( $K_c$ ) Estimated from Strength Parameters for Isotropic Consolidation Using Lowe and Karafiath's Procedure..... | 102 |

|               |   |      |
|---------------|---|------|
| Figure 4.9 -  | Variation in the Pore Pressure Coefficient, $A_f$ , with Effective Normal Stress on the Failure Plane at Consolidation, $\bar{\sigma}_{fc}$ , for Various Effective Principal Consolidation Stress Ratios ( $K_c$ ) Estimated from Strength Parameters for Isotropic Consolidation Using the Modified Form of Lowe and Karafiath's Procedure..... | .103 |
| Figure 4.10 - | Variation in the Pore Pressure Coefficient, $A_f$ , with Effective Normal Stress on the Failure Plane at Consolidation, $\bar{\sigma}_{fc}$ , for Various Effective Principal Consolidation Stress Ratios ( $K_c$ ) Estimated from Strength Parameters for Isotropic Consolidation Using the Extension of Noorany and Seed's Procedure.....       | .104 |
| Figure 4.11 - | Variation in the Pore Pressure Coefficient, $A_f$ , with Effective Normal Stress on the Failure Plane at Consolidation, $\bar{\sigma}_{fc}$ , for Various Effective Principal Consolidation Stress Ratios ( $K_c$ ) Estimated from Strength Parameters for Isotropic Consolidation Using the Extension of Benjamin's Study.....                   | .105 |
| Figure 4.12 - | Variation in the Pore Pressure Coefficient, $A_f$ , with Effective Normal Stress on the Failure Plane at Consolidation, $\bar{\sigma}_{fc}$ , for Various Effective Principal Consolidation Stress Ratios ( $K_c$ ) Estimated from Strength Parameters for Isotropic Consolidation Using Linear Interpolation.....                                | .106 |
| Figure 4.13 - | Shear Strength Envelopes ( $\tau_{ff}$ vs. $\bar{\sigma}_{fc}$ ) for an Effective Principal Consolidation Stress Ratio ( $K_c$ ) of 3.42 Estimated from Strength Parameters for Isotropic Consolidation Using Several Procedures: Material Property Set No. 1.....  | .109 |
| Figure 4.14 - | Shear Strength Envelopes ( $\tau_{ff}$ vs. $\bar{\sigma}_{fc}$ ) for an Effective Principal Consolidation Stress Ratio ( $K_c$ ) of 2.06 Estimated from Strength Parameters for Isotropic Consolidation Using Several Procedures: Material Property Set No. 2.....  | .110 |
| Figure 4.15 - | Shear Strength Envelopes ( $\tau_{ff}$ vs. $\bar{\sigma}_{fc}$ ) for an Effective Principal Consolidation Stress Ratio ( $K_c$ ) of 2.27 Estimated from Strength Parameters for Isotropic Consolidation Using Several Procedures: Material Property Set No. 3.....  | .111 |
| Figure 4.16 - | Shear Strength Envelopes ( $\tau_{ff}$ vs. $\bar{\sigma}_{fc}$ ) for an Effective Principal Consolidation Stress Ratio ( $K_c$ ) of 2.35 Estimated from Strength Parameters for Isotropic Consolidation Using Several Procedures: Material Property Set No. 4.....  | .112 |

Figure 4.17 - Variation in the Pore Pressure Coefficient,  $\bar{A}_f$ , with Effective Normal Stress on the Failure Plane at Consolidation,  $\bar{\sigma}_{fc}$ , for an Effective Principal Consolidation Stress Ratio ( $K_c$ ) of 3.42 Estimated from Strength Parameters for Isotropic Consolidation Using Several Procedures: Material Property Set No. 1.....113

Figure 4.18 - Variation in the Pore Pressure Coefficient,  $\bar{A}_f$ , with Effective Normal Stress on the Failure Plane at Consolidation,  $\bar{\sigma}_{fc}$ , for an Effective Principal Consolidation Stress Ratio ( $K_c$ ) of 2.06 Estimated from Strength Parameters for Isotropic Consolidation Using Several Procedures: Material Property Set No. 2.....114

Figure 4.19 - Variation in the Pore Pressure Coefficient,  $\bar{A}_f$ , with Effective Normal Stress on the Failure Plane at Consolidation,  $\bar{\sigma}_{fc}$ , for an Effective Principal Consolidation Stress Ratio ( $K_c$ ) of 2.27 Estimated from Strength Parameters for Isotropic Consolidation Using Several Procedures: Material Property Set No. 3.....115

Figure 4.20 - Variation in the Pore Pressure Coefficient,  $\bar{A}_f$ , with Effective Normal Stress on the Failure Plane at Consolidation,  $\bar{\sigma}_{fc}$ , for an Effective Principal Consolidation Stress Ratio ( $K_c$ ) of 2.35 Estimated from Strength Parameters for Isotropic Consolidation Using Several Procedures: Material Property Set No. 4..... 116

Figure 5.1 - Comparison of Skempton's Pore Pressure Coefficient,  $\bar{A}_f$ , from Triaxial Compression and Triaxial Extension Tests (After Van Saun, 1985)..... 125

Figure 5.2 - Comparison of Henkel's Pore Pressure Coefficient,  $a/2$ , from Triaxial Compression and Triaxial Extension Tests (After Van Saun, 1985)..... 126

Figure 5.3 - Stresses Representing "Unloading" of Slope Face Due to Sudden Drawdown..... 128

Figure 6.1 - Parameters Used in First Series of Comparative Analyses Employing Effective Stress Procedures..... 135

Figure 6.2 - Piezometric Line Used to Represent Pore Water Pressures by Bishop's and Morgenstern's Procedure..... 137

Figure 6.3 - Schematic Illustration of Pre-Drawdown and Post-Drawdown Boundary Conditions Used for Finite Element Solution of Steady-State Flow Equations..... 138

Figure 6.4 - Flow Paths for Drainage of Upstream Slope for (a) Embankment on Impervious Foundation, and (b) Embankment on Relatively Pervious Foundation..... 140

Figure 6.5 - Cross-Section of Lokvarka Dam (From Nonveiller, 1957).. 141

Figure 6.6 - Equipotential Lines From Solution of Steady-State Flow Equations for Lokvarka Dam Core After Full, Instantaneous Drawdown (From Adams, 1982).....142

Figure 6.7 - Idealized Cross-Section Used for Analyses of Pilarcitos Dam.....145

Figure 6.8 - Critical Shear Surface For Pilarcitos Dam Based on Effective Stress Analyses with Pore Pressures Calculated Using Stresses from Finite Element Computations and Pore Pressure Coefficients Estimated from the R-Envelope Using Taylor's Procedure.....147

Figure 6.9 - Critical Shear Surface For Pilarcitos Dam Based on the Corps of Engineers' Procedure.....148

Figure 6.10 - Critical Shear Surface For Pilarcitos Dam Based on Lowe and Karafiath's Procedure - Using Linear Interpolation to Estimate Strength Envelopes for Anisotropic Consolidation from Strength Parameters for Isotropic Consolidation..... 149

Figure 6.11 - Critical Shear Surface For Pilarcitos Dam Based on a Two-Stage Analysis Employing a Single  $\tau_{ff}$  vs.  $\bar{\sigma}_{fc}$  Envelope..... 150

## LIST OF TABLES

|   |     |
|---|-----|
| Table 2.1 - Embankment Dams Studied by Winkley (1982).....  | 46  |
| Table 2.2 - Comparison of Factors of Safety Computed Using Measured Pore Water Pressures and Pore Water Pressures Estimated by Bishop's and Morgenstern's Procedure (From Winkley, 1982).....   | 47  |
| Table 3.1 - Comparison of the Slope and Intercept for the $\tau_{ff} - \bar{\sigma}_{fc}$ Envelopes with the Strength Parameters from the R Envelope ( $c_R$ and $\phi_R$ ).....  | 76  |
| Table 3.2 - Comparison of the Shear Strength Parameters for R-Envelopes Drawn Tangent to Circles of Stress ( $c_R$ , $\phi_R$ ) and R-Envelopes Drawn Through Points Corresponding to Stresses on the Failure Plane ( $c_{Rf}$ , $\phi_{Rf}$ )..... | 80  |
| Table 4.1 - Summary of Four Sets of Soil Properties Used to Compare Procedures for Estimating Shear Strength Envelopes for Anisotropic Consolidation.....   | 107 |
| Table 6.1 - Summary of Factors of Safety Calculated by Effective Stress Methods for Selected Examples.....  | 143 |
| Table 6.2 - Summary of Factors of Safety for Pilarcitos Dam Calculated by Various Procedures.....   | 151 |
| Table 6.3 - Summary of Four Sets of Soil Properties Used for Comparative Calculations with Various Procedures.....  | 154 |
| Table 6.4 - Summary of Factors of Safety Calculated by Various Procedures Methods for Four Sets of Material Properties - 1.5:1 Slope.....   | 156 |
| Table 6.5 - Summary of Factors of Safety Calculated by Various Procedures Methods for Four Sets of Material Properties - 3.5:1 Slope.....   | 157 |

## NOMENCLATURE

### English Letters

- a - Henkel's pore pressure coefficient
- $a_v$  - coefficient of compressibility
- A - Skempton's pore pressure coefficient
- $\bar{A}$  - Skempton's pore pressure coefficient (= AB)
- $\bar{A}_f$  - value of  $\bar{A}$  at failure
- B - Skempton's pore pressure coefficient
- $\bar{B}$  - Skempton's pore pressure coefficient (=  $\Delta u / \Delta \sigma_1$ )
- $\bar{c}$  - cohesion intercept for effective stress envelope (from either R or S tests)
- $c_R$  - "cohesion" intercept for R-envelope drawn tangent to circles of stress
- $c_{Rf}$  - "cohesion" intercept for R-envelope drawn through points on circle of stress representing stresses on the failure plane
- e - void ratio
- g - acceleration due to gravity
- h - total head
- $\Delta h_w$  - change in height of water due to drawdown directly above the point of interest
- k - coefficient of permeability
- $K_c$  - effective principal stress ratio at consolidation ( $\bar{\sigma}_{1c} / \bar{\sigma}_{3c}$ )
- $K_f$  - effective principal stress ratio at failure ( $\bar{\sigma}_{1f} / \bar{\sigma}_{3f}$ )
- n - porosity
- $n_e$  - effective porosity
- $S_R$  - degree of saturation
- $S_s$  - specific storage
- $\bar{u}$  - excess pore water pressure above final static value
- $\Delta u$  - change in pore water pressure due to undrained shear

$\Delta u_f$  - change in pore water pressure due to undrained shear - at the time of failure

#### Greek Letters

- $\alpha$  - compressibility of soil skeleton,  $- dn/d\bar{\sigma}$
- $\beta$  - compressibility of fluid,  $d\rho/du$
- $\gamma_w$  - unit weight of water
- $\theta_\tau$  - angle of inclination of  $\tau_{ff}$  vs.  $\bar{\sigma}_{fc}$  envelope
- $\lambda_{c\phi}$  - dimensionless coefficient ( $= \gamma H \tan \bar{\phi} / \bar{c}$ )
- $\rho$  - mass density of fluid,  $\gamma_w/g$
- $\bar{\sigma}$  - effective normal stress
- $\sigma_1$  - total major principal stress
- $\bar{\sigma}_1$  - effective major principal stress
- $\bar{\sigma}_{1c}$  - effective major principal stress at the time of consolidation
- $\bar{\sigma}_{1f}$  - effective major principal stress at failure
- $\sigma_3$  - total minor principal stress
- $\bar{\sigma}_3$  - effective minor principal stress
- $\bar{\sigma}_{3c}$  - effective minor principal stress at the time of consolidation
- $\bar{\sigma}_{3cl}$  - effective minor principal stress at consolidation in an isotropically consolidated undrained test which produces a  $\bar{\sigma}_3$  and corresponding  $\bar{\sigma}_1/\bar{\sigma}_3$  during shear equivalent to those in an anisotropically consolidated shear test at the time of consolidation.
- $\bar{\sigma}_{3f}$  - effective minor principal stress at failure
- $\bar{\sigma}_{fc}$  - effective normal stress on the failure plane at the time of consolidation.
- $\bar{\sigma}_{ff}$  - effective normal stress on the failure plane at failure
- $\Delta\sigma_1$  - major principal stress change (largest, most positive change in normal stress)
- $\Delta\sigma_2$  - intermediate principal stress change
- $\Delta\sigma_3$  - minor principal stress change (smallest, most negative change in normal stress)

- $\tau$  - shear stress
- $\tau_{fc}$  - shear stress on the failure plane at the time of consolidation
- $\tau_{ff}$  - shear stress on the failure plane at failure
- $\tau_0$  - intercept of  $\tau_{ff}$  vs.  $\bar{\sigma}_{fc}$  envelope
- $\bar{\phi}$  - angle of internal friction for effective stress envelope (from either R or S tests)
- $\phi_R$  - slope of the R-envelope when drawn tangent to circles of stress
- $\phi_{Rf}$  - slope of the R-envelope when drawn through points on circle of stress representing stresses on the failure plane
- $\psi_1, \psi_2$  - pore pressure coefficients used in Lowe and Karafiath's procedure for estimating effects of anisotropic consolidation on undrained shear strengths using results of tests with isotropic consolidation

SECTION 1  
INTRODUCTION  
(Wright)

"Sudden" or "rapid" drawdown is considered to occur when reservoir or other adjacent water levels are lowered at such a rate that little or no drainage occurs in an earth slope while the water level is being lowered. Slope stability analyses are routinely performed to calculate the factor of safety for earth slopes subjected to this condition. Frequently the design of such earth slopes is governed by the sudden drawdown condition rather than by other conditions, such as those immediately after construction and with steady state seepage.

Several different procedures exist and are currently used by designers to compute slope stability for the case of sudden drawdown. These various procedures are based on fundamentally different approaches and are known to produce different results in at least some instances. The procedures, the assumptions employed and the numerical results obtained using these procedures are the subject of this paper.

BACKGROUND AND GENERAL ASSUMPTIONS

Most stability computations for sudden drawdown are based on several common assumptions. First, most procedures are based on the assumption that the drawdown is instantaneous. As the soil drains, the shear strength will change and, eventually, will approach values corresponding to the fully "drained" or steady seepage condition. By considering the case of instantaneous drawdown as well as the steady seepage condition it is assumed that the worst condition will be detected and can be used to judge the design. Intermediate conditions

between the undrained and fully drained condition are usually ignored. Only the condition of instantaneous drawdown with no drainage will be considered in this paper. Stability computations for the steady seepage condition are routinely performed and do not need to be covered here. Although partial drainage during drawdown is not covered in this paper, the techniques usually used are based on solutions to governing equations for transient flow, which are discussed in Section 2 of this paper.

Procedures for sudden drawdown stability computations are also all based on the assumption that the soil is saturated. This assumption is consistent with the usual assumption that sudden drawdown will follow a period of relatively steady reservoir or river levels and the soil will have ample opportunity to become saturated. Although there are probably many cases where the soil does not become saturated, especially when drawdown follows the first filling of a reservoir or an unprecedented flood, the possibility still exists that the soil will at some time become saturated. Shear strengths will be at their minimum values when such saturation occurs, and, accordingly the assumption of saturated conditions appears to be appropriate for design. However, the fact that the soil may not be saturated at the time of some failures may need to be recognized when actual failures are examined.

Factors of safety calculated by the various procedures for sudden drawdown will also be influenced by the particular limit equilibrium slope stability analysis procedure employed. For example, the ordinary Method of Slices will typically underestimate the factor of safety while the Corps of Engineers' Modified Swedish procedure may overestimate the factor of safety in comparison to the values obtained using procedures

based on more rational assumptions. However, most of the differences among factors of safety caused by the procedures used to compute the factor of safety can be eliminated by use only of procedures which satisfy complete static equilibrium. Such complete equilibrium procedures are readily available and have been implemented in many computer programs for slope stability analysis, including the program UTEXAS2 which is currently being implemented by the Corps of Engineers. Accordingly, the subject of assumptions and differences among various limit equilibrium procedures is of little concern and is ignored for the balance of this paper. It will be assumed that any of the various procedures discussed for stability analysis for sudden drawdown would be used with a limit equilibrium procedure which satisfies complete static equilibrium.

#### ORGANIZATION OF REPORT

Procedures for stability calculations for sudden drawdown can be separated into two general groups: (1) Effective stress procedures, and (2) Two-stage procedures. Effective stress procedures are based on defining shear strengths in terms of effective stresses and require that pore water pressures immediately after drawdown be determined. Effective stress procedures are described and discussed in Section 2. Two-stage analysis procedures require that two separate sets of stability calculations be performed. The first set is performed for conditions just before drawdown to compute the effective stresses, which are then used to estimate undrained shear strengths for subsequent undrained loading. The undrained shear strengths are then used in the second set of computations to compute the factor of safety after the water table has been lowered. Two-stage analysis procedures are presented in Section 3.

3. One of the two-stage analysis procedures (Lowe and Karafiath's , 1960a) as well as an alternative effective stress analysis procedure which is developed and presented in this paper take into account the fact that the soil is consolidated anisotropically under unequal principal stresses ( $\bar{\sigma}_{1c}$ ,  $\bar{\sigma}_{3c}$ ) before drawdown. Procedures for estimating the effects of anisotropic consolidation from the results of laboratory tests employing isotropic consolidation are discussed in Section 4. The alternative effective stress procedure considered in this paper is presented in Section 5. Results of several series of comparative calculations for the factor of safety are presented in Section 6. Finally, a summary and recommendations are presented in Section 7.

SECTION 2  
EFFECTIVE STRESS (ONE-STEP) ANALYSIS PROCEDURES  
(Wright)

Effective stress analysis procedures are based on expressing the shear strength in terms of effective stresses. Accordingly, analyses are based on effective stresses and pore water pressures must be estimated for the condition immediately after drawdown. The only difference between an effective stress analysis for conditions after drawdown and an effective stress analysis for long-term, steady seepage conditions is in the pore water pressures and surface loads used in the computations. In the case of sudden drawdown analyses the pore water pressures should represent the pressures expected immediately after drawdown; for long-term, steady-state seepage analyses the pore water pressures represent those associated with steady seepage.

SHEAR STRENGTH PARAMETERS

Effective stress shear strength parameters may be determined from either consolidated-undrained tests with pore water pressure measurements or from consolidated-drained tests. In the case of consolidated-undrained tests two candidate criteria exist for defining "failure" and determining the effective stress shear strength parameters: Failure may be defined to be either at the point of maximum principal stress difference,  $(\sigma_1 - \sigma_3)_{\max}$ , or at the point where the effective stress path becomes tangent to the failure envelope (Fig.

2.1)<sup>1</sup>. In the case of rapid drawdown the loading is considered to be undrained. Consequently, it is fundamentally more correct to define failure and the corresponding effective stress shear strength parameters at the point of peak principal stress difference; the peak principal stress difference represents the point of peak load (shear resistance) for undrained loading. However, differences between the effective stress shear strength parameters at the point of peak principal stress difference and stress path tangency are likely to be relatively small for compacted soils and soils with low sensitivities. Such soils are the most likely types of fine-grained soils encountered in earth dams and riverbank slopes where drawdown is significant.

Consolidated-drained shear test procedures may also be used to determine the effective stress shear strength parameters. Fundamentally, the effective stress shear strength parameters determined in consolidated-drained shear tests should be different from those applicable to undrained loading associated with rapid drawdown for two reasons: First, the effective stress strength parameters determined in consolidated-drained shear tests correspond to points of stress path tangency on the effective stress failure envelope,  $(\bar{\sigma}_1/\bar{\sigma}_3)_{\max.}$ ; the effective stress strength parameters applicable at failure for undrained

---

<sup>1</sup>If no cohesion ( $\bar{c}$ ) intercept exists, the point where the effective stress path becomes tangent to the failure envelope coincides with the point of maximum effective principal stress ratio,  $(\bar{\sigma}_1/\bar{\sigma}_3)_{\max.}$ . Thus, "maximum effective principal stress ratio" and "stress path tangency" are synonymous failure criteria. If a cohesion intercept exists, the two failure criteria are not identical, and it is fundamentally more correct to use the point of stress path tangency, although the point of effective principal stress ratio is often taken to be the point of failure for convenience.

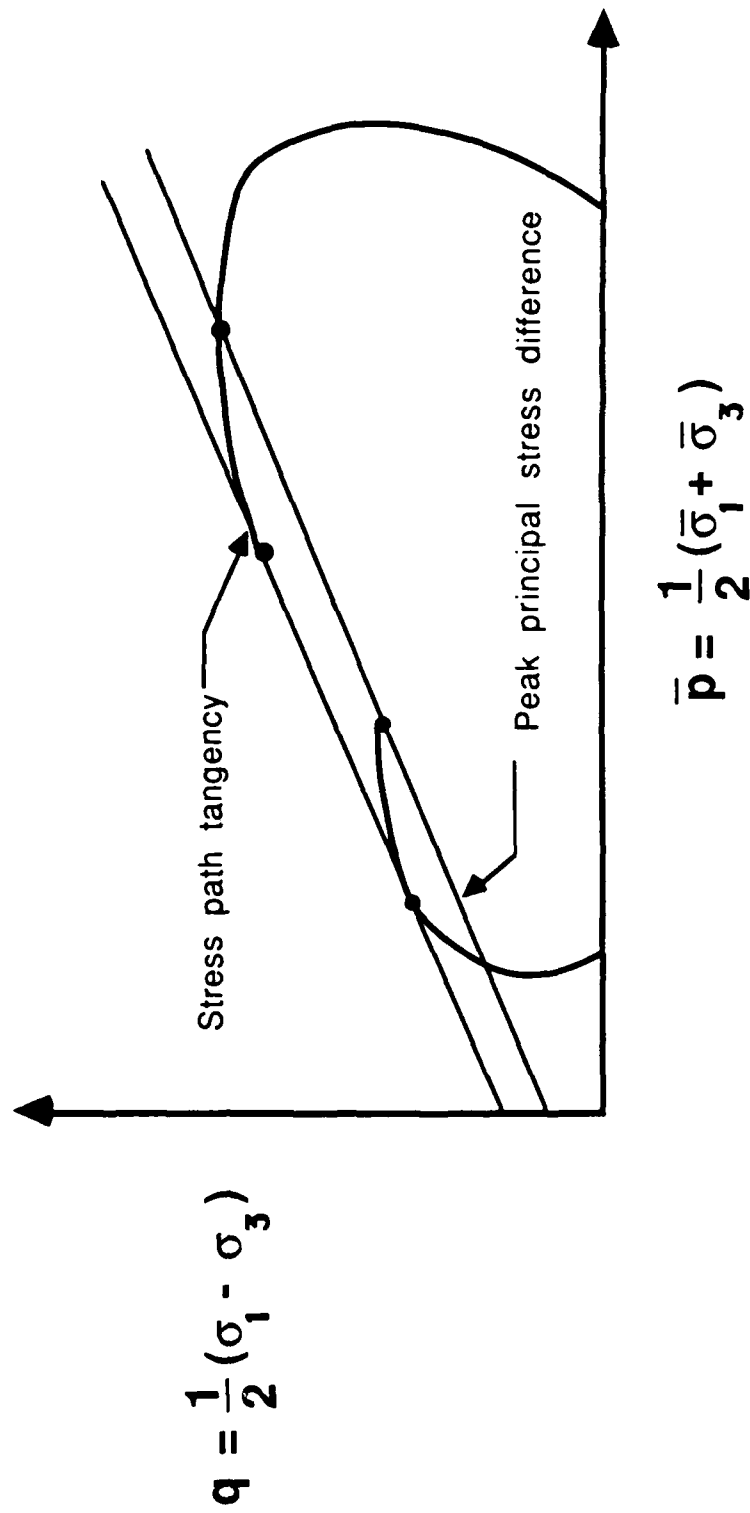


Figure 2.1 - Effective Stress Paths with Failure Envelopes for  
 (a) "Stress Path Tangency" and  
 (b) "Peak Principal Stress Difference" Failure Criteria

loading are those corresponding to the peak principal stress difference,  $(\sigma_1 - \sigma_3)_{\max.}$ . Secondly, in consolidated-drained shear tests a portion of the load applied to cause failure goes into producing volume change and the strength parameters measured reflect this additional energy required to produce the volume changes (Bishop and Eldin, 1953; Bishop, 1954a; Rowe, 1962; Rowe, Barden and Lee, 1964). For undrained loading as in the cases of sudden drawdown and consolidated-undrained shear tests in the laboratory, no energy is used to produce volume changes and, accordingly, any measured shear strength parameters do not reflect such added energy. Consequently, the effective stress shear strength parameters determined from consolidated-drained and consolidated-undrained shear tests will not be identical.

Effective stress shear strength parameters determined for a particular soil will clearly differ depending on the test procedures (drained vs. undrained) employed and the manner in which failure is selected. In addition to the two failure criteria discussed earlier, a limiting strain, e. g. 15 percent, is sometimes selected as the point defining failure in a laboratory shear test. Thus, a third potential "failure criterion" is introduced and further differences among shear strength parameters may exist. Additional differences may also be caused by the type of laboratory shear device employed (triaxial shear, direct shear, direct simple shear and plane strain). In most cases all of the factors discussed pertaining to laboratory measurements of shear strength will probably be overshadowed by scatter in data and the variability of most soils in the field. However, all of the factors will contribute to at least some extent to the computed results and may influence conclusions drawn in any particular instance.

## ESTIMATION OF PORE WATER PRESSURES

All of the effective stress analysis procedures require that pore water pressures at the end of drawdown be estimated. At least four fundamentally different approaches have been used to estimate the pore water pressures. The first procedure was first suggested by Bishop (1954b) and later employed by Morgenstern (1963) using Skempton's (1954) pore pressure coefficients. The procedure involves estimating the pore water pressures by first estimating what the pore pressures would be before drawdown and then estimating the changes in pore water pressure which would occur during drawdown. The changes in pore water pressure are estimated by estimating the changes in total stress and relating the changes in total stress to changes in pore water pressure using Skempton's pore pressure coefficients. The second approach to estimating pore water pressures involves solving either analytically or numerically the basic governing differential equation for the transient (non-steady) flow of water associated with the drawdown of the reservoir. Procedures based on the second approach generally employ solutions developed for either soil consolidation or groundwater flow. The third approach is actually a simplification of the second approach, consisting of representing the flow as steady-state flow for selected instants of time following drawdown. The fourth approach is the least well-defined approach and essentially encompasses those approaches in which the pore water pressures are estimated based on past experience and judgement.

### BISHOP-MORGENSTERN PROCEDURE

Bishop's (1954b) and Morgenstern's (1963) procedure for estimating pore water pressures after drawdown is based on Skempton's pore pressure

coefficient,  $B$ , and estimated changes in total stress during drawdown.

The pore pressure coefficient  $B$  is defined as,

$$B = \frac{\Delta u}{\Delta \sigma_1} \quad 2.1$$

where  $\Delta u$  is the change in pore water pressure and  $\Delta \sigma_1$  is the major principal stress change. Thus, the change in pore water pressure during drawdown can be expressed as,

$$\Delta u = B \Delta \sigma_1 \quad 2.2$$

The smaller the value of  $B$ , the smaller the changes in pore water pressure during drawdown. Because the changes are expected to represent decreases in pressure the smaller the decrease in pressure during drawdown, the higher will be the final values of pore water pressure. Higher values of pressure correspond directly to lower factors of safety. Thus, the factor of safety will decrease as  $B$  becomes smaller, all other factors remaining the same. Bishop and Morgenstern each considered probable values for  $B$  and suggested that a value of unity represented a lower-bound and, thus, conservative value. Consequently, and based on Eq. 2.2, the change in pore water pressure becomes equal to the major principal stress change,  $\Delta \sigma_1$  ( $B = 1.0$  in Eq. 2.2).

Bishop and Morgenstern also assumed that the major principal stress change,  $\Delta \sigma_1$ , was equal to the change in total vertical stress on the slope directly above any particular point of interest. Thus,

$$\Delta \sigma_1 = \Delta h_w \gamma_w \quad 2.3$$

where  $\Delta h_w$  is the change in height of water above the surface of the slope directly above the point of interest (Fig. 2.2) and  $\gamma_w$  is the unit weight of water. Combining Eqs. 2.2 and 2.3 and setting  $B$  equal to unity then gives,

$$\Delta u = \Delta h_w \gamma_w \quad 2.4$$

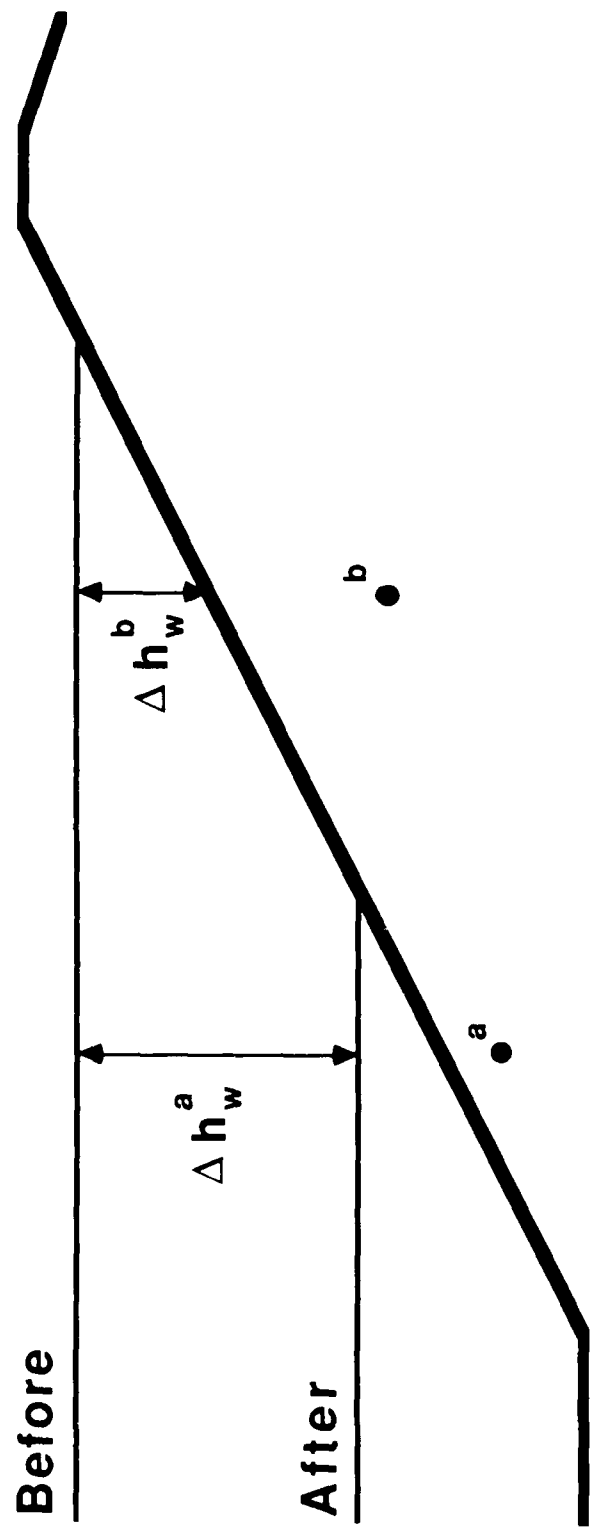


Figure 2.2 - Changes in Water Levels Used to Compute Major Principal Stress  
Changes in Bishop's and Morgenstern's Procedure

Bishop and Morgenstern also assumed that the head loss in the slope prior to drawdown is small and can be ignored. The consequence of this assumption combined with the previous assumptions and Eq. 2.4 is that the pore pressures after drawdown can be expressed by a simple piezometric surface as illustrated in Fig. 2.3. The piezometric surface is coincident with the surface of the slope above the level of the drawdown and is coincident with the reservoir surface at and below the level of the drawdown. Pore water pressures are simply the product of the unit weight of water and the depth below the final piezometric surface.

Bishop's and Morgenstern's procedure involves the following four assumptions:

- (1) The head loss due to seepage in the slope before drawdown is negligible.
- (2) Skempton's (1954) equation and pore pressure coefficients can be used to compute changes in pore water pressures.
- (3) The pore pressure coefficient  $B$  is equal to unity.
- (4) The major principal stress change,  $\Delta\sigma_1$ , is equal to the change in vertical stress on the surface of the slope directly above any point of interest.

The assumption that the head loss in the slope is negligible appears to be reasonable inasmuch as slides due to sudden drawdown are typically shallow. In addition the assumption of negligible head loss is made primarily for simplicity; the concepts employed in Bishop's and Morgenstern's procedure could be easily extended to include head losses in the slope before drawdown if they were important. Bishop's and Morgenstern's procedure is also based on the fundamental assumption that

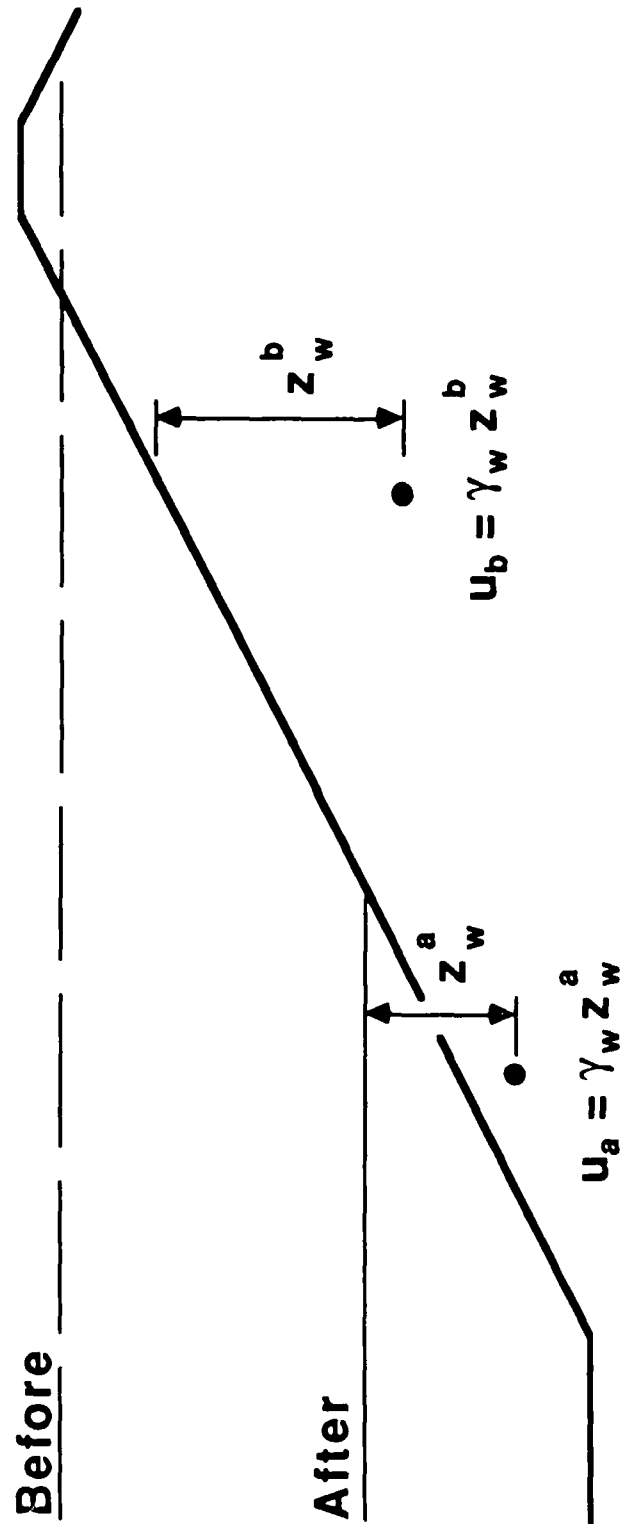


Figure 2.3 - Representation of Pore Water Pressures After Drawdown for Bishop's and Morgenstern's Procedure

Skempton's (1954) equation for pore water pressures can be applied to predicting pore water pressures in earth slopes due to sudden drawdown. For the present this will be considered valid and the use of Skempton's equation is discussed in further detail in Section 5 of this paper. However, the remaining two assumptions listed above require some further discussion at this point.

The assumption that the pore pressure coefficient,  $B$ , is equal to unity is best examined by considering Skempton's original expression for the changes in pore water pressure due to undrained loading. Skempton expressed the change in pore pressure during undrained loading as,

$$\Delta u = B\Delta\sigma_3 + AB(\Delta\sigma_1 - \Delta\sigma_3) \quad 2.5$$

where,  $\Delta u$  is the change in pore water pressure,  $\Delta\sigma_1$  and  $\Delta\sigma_3$ , are the major and minor principal stress changes, respectively, and  $A$  and  $B$  are pore pressure coefficients. The coefficient  $B$  represents tendencies for pore water pressures to change due to a change in all-around (isotropic) pressure; while the coefficient  $A$  represents tendencies for pore water pressures to change due to a change in shear stress (principal stress difference). By dividing both sides of Eq. 2.5 through by the major principal stress change ( $\Delta\sigma_1$ ) and rearranging terms the following equation can be written:

$$\frac{\Delta u}{\Delta\sigma_1} = B\left[1 - (1 - A)\left(1 - \frac{\Delta\sigma_3}{\Delta\sigma_1}\right)\right] \quad 2.6$$

The quantity on the left-hand side of this equation is equal to the pore pressure coefficient,  $B$ . In the case of most saturated soils the value of  $B$  will be essentially unity and, thus,

$$B = \left[1 - (1 - A)\left(1 - \frac{\Delta\sigma_3}{\Delta\sigma_1}\right)\right] \quad 2.7$$

Accordingly, the pore pressure coefficient  $B$  can be related to the pore pressure coefficient  $A$  and the principal stress changes,  $\Delta\sigma_1$  and  $\Delta\sigma_3$ . At this point the "principal stress changes,"  $\Delta\sigma_1$  and  $\Delta\sigma_3$ , which have been used in Eqs. 2.1 through 2.7 should be distinguished from "changes in principal stress." The major principal stress change,  $\Delta\sigma_1$ , in these equations represents the largest algebraic (most positive) change in stress. In the case of drawdown, the changes in normal stress are likely to all be negative in value. Thus, the least negative value is the major principal stress change, while the most negative value is the minor principal stress change (Fig. 2.4). Accordingly, the absolute value of the major principal stress change,  $\Delta\sigma_1$ , is likely to be smaller than the absolute value of the minor principal stress change,  $\Delta\sigma_3$ . Referring to Eq. 2.7 it is then likely that both  $\Delta\sigma_1$  and  $\Delta\sigma_3$  will be negative and the absolute value of  $\Delta\sigma_3$  will be larger than the absolute value of  $\Delta\sigma_1$ . Thus, the ratio,  $\Delta\sigma_3/\Delta\sigma_1$ , will be greater than unity. Consequently, the value  $B$  given by Eq. 2.7 will always be greater than unity for all values of  $A$  less than or equal to unity. Most compacted soils as well as natural soils in slopes likely to be subjected to sudden drawdown would be expected to produce values of  $A$  which are less than unity. Accordingly, Bishop's and Morgenstern's assumption that a conservative lower-bound value for  $B$  is unity appears to be valid. The degree of conservatism associated with this assumption may be seen by examining values of  $B$  computed for various values of  $A$  and ratio of principal stress change ( $\Delta\sigma_3/\Delta\sigma_1$ ) as shown in Fig. 2.5. Referring to this figure it can be seen that the values of  $B$  are at least unity and in many cases may be several times greater than unity. For example, if the ratio of principal stress changes is 2.0 and  $A$  is 0.2, a value which is certainly

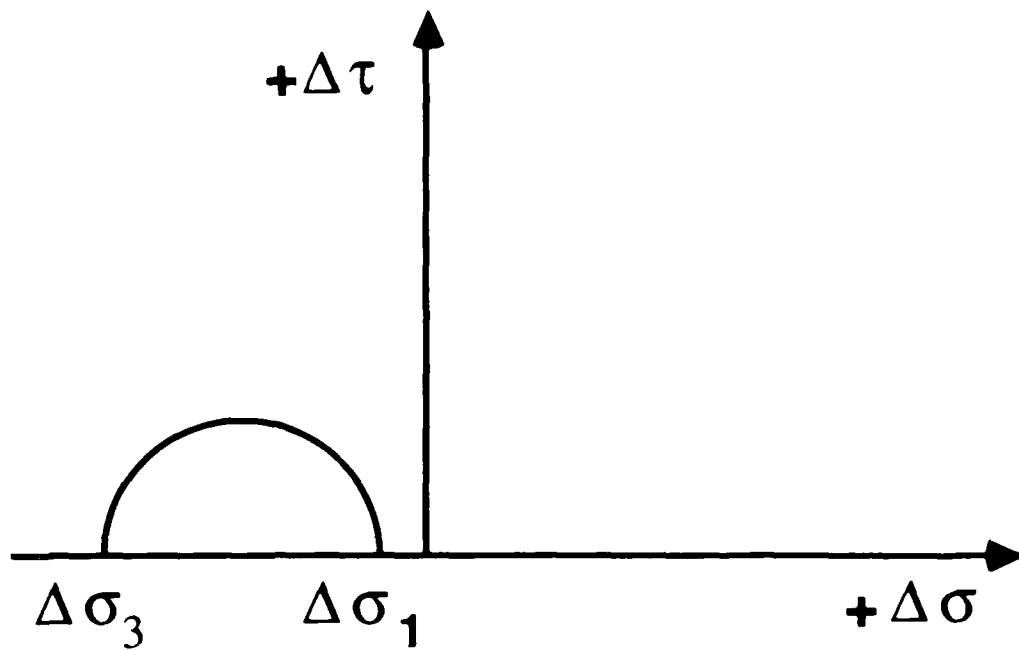


Figure 2.4 - Mohr's Circle of Stress Showing Principal Stress Changes for Sudden Drawdown

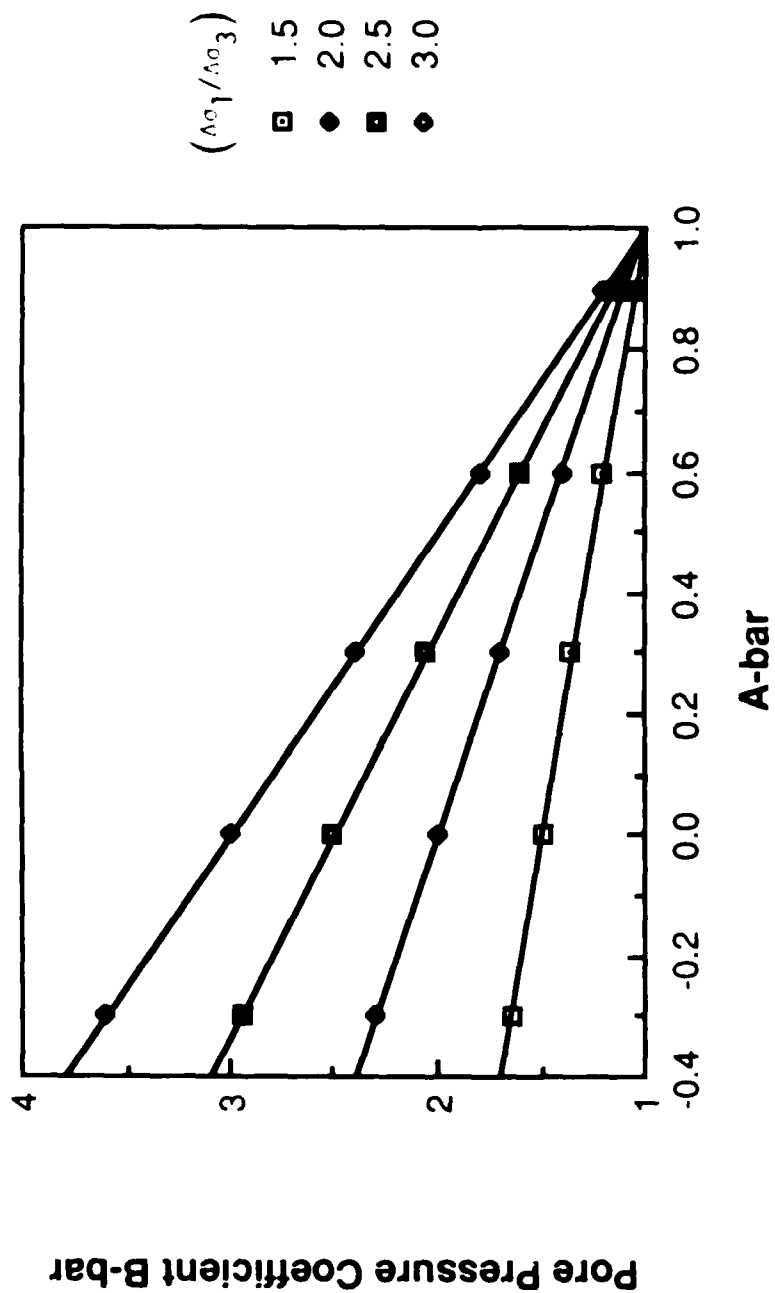


Figure 2.5 - Variation of the Pore Pressure Coefficient  $\bar{B}$  with the Value of  $\bar{A}$  for Various Values of the Ratio,  $\sigma_1/\sigma_3$

reasonable for a compacted clay at low confining pressures, the value of  $B$  is 1.80. This value (1.80) is approaching twice the value assumed by Morgenstern. Consequently, the change in pore water pressure during drawdown would be nearly twice the value predicted based on Bishop's and Morgenstern's assumed values.

The final assumption to be considered in Bishop's and Morgenstern's procedure is that the major principal stress change is equal to the change in vertical stress directly above any point of interest. At the face of the slope the change in stress normal (perpendicular) to the face of the slope will be equal to the change in water pressure (or vertical stress) on the face of the slope. The change in normal stress on the face of the slope will be negative but greater in magnitude than the change in normal stress on a plane perpendicular to the slope face. Thus, at the face of the slope the change in vertical stress,  $\Delta h_w \gamma_w$  will actually be equal to the minor principal stress change,  $\Delta \sigma_3$ , while the major principal stress change,  $\Delta \sigma_1$ , will be smaller in absolute value than the change in vertical stress (Fig. 2.6). The consequence of this will be that the actual change in pore pressure computed from Eq. 2.2 would be smaller than what is computed by Morgenstern's assumption, provided that all other factors remain the same, including the assumption that  $B$  is unity.

Based on the above discussion it appears that Bishop's and Morgenstern's procedure may underestimate the actual value of  $B$  while at the same time the major principal stress change,  $\Delta \sigma_1$ , is overestimated. Consequently, it is entirely possible that two errors may compensate each other in the procedure.

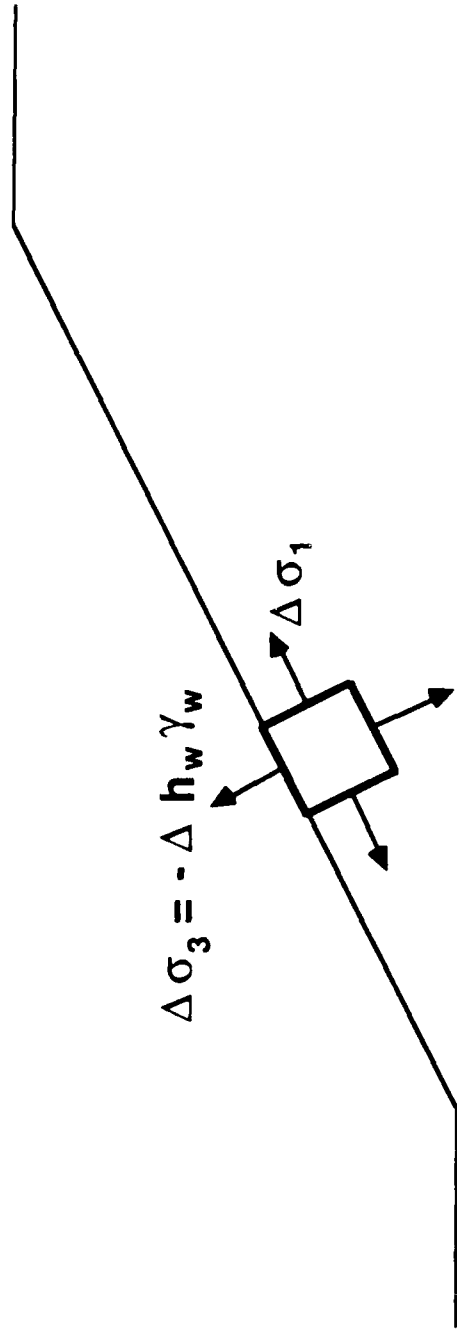


Figure 2.6 - Major and Minor Principal Stress Changes Due to Sudden Drawdown for an Element of Soil at the Slope Face

## TRANSIENT FLOW SOLUTIONS

During the past 15 years the writer has gained the impression that in a number of instances pore water pressures due to drawdown have been estimated from theoretical solutions based on the equations of transient flow. Although the details of the solutions are not available, the solutions appear to have been based generally on numerical solutions of the equations for consolidation or groundwater flow. In this section the governing equations for transient flow are presented and the assumptions employed in the classical versions of these equations for soil consolidation and groundwater flow are examined. Requirements for correct modeling in the case of sudden drawdown are also presented.

The general governing partial differential equation which must be satisfied for two-dimensional transient (time-dependent) flow in porous media is,

$$\rho k \left( \frac{\partial^2 h}{\partial x^2} + \frac{\partial^2 h}{\partial y^2} \right) = n S_R \frac{\partial \rho}{\partial t} + \rho S_R \frac{\partial n}{\partial t} + n \rho \frac{\partial S_R}{\partial t} \quad 2.8$$

where,  $h$  is total head,  $n$  is porosity,  $\rho$  is the mass density of the fluid ( $\gamma_w/g$ ), and  $S_R$  is the degree of saturation (e. g. Freeze and Cherry, 1979). The partial derivatives on the left are taken with respect to the spatial coordinates ( $x$  and  $y$ ); the partial derivatives on the right-hand side are taken with respect to time ( $t$ ). In the case of saturated flow ( $S_R = 100\% - \partial S_R / \partial t = 0$ ) and an incompressible fluid ( $\partial \rho / \partial t = 0$ ), Eq. 2.8 reduces to

$$\rho k \left( \frac{\partial^2 h}{\partial x^2} + \frac{\partial^2 h}{\partial y^2} \right) = \rho \frac{\partial n}{\partial t} \quad 2.9$$

In order to solve Eq. 2.9 either the head ( $h$ ) must be related to the porosity ( $n$ ), or the porosity must be related to the head. The most

widely employed procedure for relating porosity to head follows the one employed in the classical consolidation theory first suggested by Terzaghi. This approach can be derived by first expressing the partial derivative of porosity with respect to time as,

$$\frac{\partial n}{\partial t} = \frac{1}{1 + e_0} \frac{\partial e}{\partial \bar{\sigma}} \frac{\partial \bar{\sigma}}{\partial u} \frac{\partial u}{\partial h} \frac{\partial h}{\partial t} \quad 2.10$$

where,  $\partial e / \partial \bar{\sigma}$  represents the change in void ratio with respect to effective stress,  $\partial \bar{\sigma} / \partial u$  represents the change in effective stress with respect to pore pressure,  $\partial u / \partial h$  represents the change in pore pressure with respect to total head, and  $\partial h / \partial t$  represents the change in total head with respect to time. The change in void ratio with respect to change in effective stress can be expressed by the coefficient of compressibility,  $a_v$ , where,

$$a_v = - \frac{\partial e}{\partial \bar{\sigma}} \quad 2.11$$

The change in effective stress is assumed to be equal in magnitude and opposite in sign to the change in pore water pressure. Thus,

$$\frac{\partial \bar{\sigma}}{\partial u} = - 1.0 \quad 2.12$$

The change in pore pressure with respect to head can be expressed as,

$$\frac{\partial u}{\partial h} = \gamma_w \quad 2.13$$

Substituting Eqs. 2.11, 2.12 and 2.13 into 2.10 gives,

$$\frac{\partial n}{\partial t} = \frac{1}{1 + e_0} a_v \gamma_w \frac{\partial h}{\partial t} \quad 2.14$$

Finally, substituting Eq. 2.14 into Eq. 2.9 and rearranging terms gives.

$$\frac{\partial^2 h}{\partial x^2} + \frac{\partial^2 h}{\partial y^2} = \frac{a_v \gamma_w}{k (1 + e_0)} \frac{\partial h}{\partial t} \quad 2.15$$

In the case of one-dimensional flow Eq. 2.15 reduces to,

$$\frac{\partial^2 h}{\partial x^2} = \frac{a_v \gamma_w}{k (1 + e_0)} \frac{\partial h}{\partial t} \quad 2.16$$

which is Terzaghi's classical equation for one-dimensional equation expressed in terms of total head. Equation 2.16 can also be expressed in terms of excess pore pressure,  $\bar{u}$ , as,

$$\frac{\partial^2 \bar{u}}{\partial x^2} = \frac{a_v \gamma_w}{k (1 + e_0)} \frac{\partial \bar{u}}{\partial t} \quad 2.17$$

An alternate form of Eq. 2.15 is often used in modeling groundwater problems. The equation for two-dimensional transient flow is written as,

$$\frac{\partial^2 h}{\partial x^2} + \frac{\partial^2 h}{\partial y^2} = \frac{S_s}{k} \frac{\partial h}{\partial t} \quad 2.18$$

where,  $S_s$  is the "specific storage." The specific storage is expressed as,

$$S_s = \gamma_w (\alpha + n\beta) \quad 2.19$$

where,  $\alpha$  and  $\beta$  are the compressibilities of the soil skeleton and water, respectively. That is,

$$\alpha = - \frac{dn}{d\sigma} \quad 2.20$$

and,

$$\beta = \frac{dp}{du} \quad 2.21$$

Equations 2.15 and 2.18 are fundamentally identical except that Eq. 2.18 also takes into account the compressibility of water. Solutions to the two equations should be essentially identical.

#### Discussion of Assumptions

Equation 2.15 is based on the assumption that the water is incompressible, which is a reasonable assumption for all practical

purposes. Equations 2.15 and 2.18 are also based on a number of other important assumptions:

1. The soil is saturated and remains saturated during flow.
2. Darcy's Law is valid (Assumed in deriving Eq. 2.8).
3. The void ratio is related to a single effective normal stress component ( $\bar{\sigma}$ ), regardless of the state of stress, including shear stresses.
4. The change in effective stress is equal in magnitude to the change in pore water pressure, regardless of changes in total stress.

The assumption that the fluid is incompressible and Darcy's Law is valid seems acceptable. However, the remaining three assumptions listed may not be valid and are discussed in further detail below.

Soil is saturated. In the case of drawdown the soil may become partly saturated above the phreatic surface as drainage occurs. Accordingly, the third term,  $n\rho\partial S_R/\partial t$ , in the governing equation (Eq. 2.8) for transient flow must be retained. This requires that a relationship be established between the degree of saturation of the soil and the total head in the soil. Although such relationships can be determined, they require that additional soil parameters be evaluated. Such relationships between degree of saturation and total head do not appear to have been included in past uses of the transient flow equations for predicting pore water pressures during sudden drawdown.

Single effective stress component. The assumption that the change in volume (void ratio) is related to a single effective normal stress component ignores the fact that shear stresses produce volume change and, accordingly, for undrained or partially drained loading shear

stresses will affect the pore water pressures. Correct representation of the relationship between effective stress and volume change requires that a complete constitutive (stress-strain) model be used and that all components of stress be considered. For two-dimensional plane-strain conditions three stress components must be considered:  $\bar{\sigma}_x$ ,  $\bar{\sigma}_y$ , and  $\tau_{xy}$ . Constitutive models based on Hooke's law are not valid for the present problem because they do not properly model the volume change behavior of soil during shear and, accordingly, they will not predict proper changes in pore water pressures. During the past decade considerable progress has been made in developing constitutive models based on plasticity theory, which can account for shear induced volume changes. Such models show considerable promise; however, they do not appear to have been coupled with the equations for transient flow and applied to the case of reservoir drawdown.

Constant total stress ( $\Delta\bar{\sigma} = -\Delta u$ ). The assumption that changes in effective stress are equal to the changes in pore water pressure is invalid for cases where there is a significant change in total stress. For example, at the immediate face of a slope which is subjected to rapid drawdown the total stress and pore water pressure change by the same amount, while the effective stress remains unchanged. Any solution based on the assumption that the change in effective stress is equal to the change in pore pressure is clearly not valid in this case. Changes in total stress and their effects on the effective stress are easily accounted for in the case of one-dimensional problems: For example in Terzaghi's classical problem of one-dimensional consolidation the change in total stress can be assumed to be constant over any vertical distance. In two dimensions the changes in total stress will vary from

point to point in the slope and can only be computed from a complete stress analysis. By coupling the stresses with the equations of transient flow as discussed in the previous paragraph, changes in total stress should automatically be taken into account; however, as noted above such coupled solutions have not generally been used.

#### SIMPLIFIED PROCEDURES BASED ON WATER FLOW

A number of procedures for estimating pore pressures have been developed based on various simplified hydraulic flow solutions. These procedures and solutions can be generally grouped into two categories: The first category of solutions is based on the Dupuit assumptions and a simplified differential equation for flow. The second set of procedures is based on a solution of the governing partial differential equation for two-dimensional steady-state flow. These procedures and the assumptions employed are reviewed below.

##### Procedures Based on Dupuit Assumptions.

Procedures based on the Dupuit assumptions employ some form of the following partial differential equation:

$$kh \frac{\partial^2 h}{\partial x^2} + k \left( \frac{\partial h}{\partial x} \right)^2 = n \frac{\partial h}{\partial t} \quad 2.22$$

This equation is based on the Dupuit assumptions that (1) equipotential lines are vertical, and (2) the hydraulic gradient is equal to the slope of the phreatic surface (line of seepage) and does not vary in the vertical direction. In addition the equation is based on a number of other assumptions:

1. Darcy's Law is valid.
2. The soil is saturated below the phreatic surface at any time.
3. The flow is horizontal in the x direction.

4. The soil or slope in which flow is occurring is homogeneous and underlain by an impervious base. Although not apparent from Eq. 2.22, "h" represents not only head, but also the elevation of the phreatic surface above the assumed impervious base. Thus, Eq. 2.22 is not a general governing differential equation for one-dimensional flow where x may represent a direction other than horizontal.

5. The soil is assumed to be incompressible, i. e. there is no volume change even though the pore pressures (heads) may change with time.

6. The drainage of the soil in the zone where the free surface is changing with time is represented by the effective porosity,  $n_e$ . ASTM (1986) defines effective porosity as "The ratio of: (1) the volume of the voids of a soil or rock mass that can be drained by gravity, to (2) the total volume of the mass." In the case of Eq. 2.22 as the phreatic surface drops from an elevation,  $h_1$ , to a new elevation,  $h_2$ , the volume of water that drains from the soil is equal to the product of  $n_e$  and the total volume of soil between the elevations  $h_1$  and  $h_2$ .

Equation 2.22 is usually simplified by ignoring the second term on the left-hand side involving products of derivatives, which gives,

$$kh \frac{\partial^2 h}{\partial x^2} = n \frac{\partial h}{\partial t} \quad 2.23$$

Equation 2.23 is also sometimes written as,

$$k \frac{\partial^2 h^2}{\partial x^2} = 2n \frac{\partial h}{\partial t} \quad 2.24$$

Browzin (1961) developed a simple analytical solution for Eq. 2.23 while Desai and Sherman (1971) presented a numerical solution. Several other published solutions (Brahma and Harr, 1963; Newlin and Rossier, 1967) have been based on further simplification of Eq. 2.23 achieved by replacing the quantity "h" in the first term by a constant quantity,  $\bar{h}$ , representing the average height of the phreatic surface above the impervious base:

$$k\bar{h}\frac{\partial^2 h}{\partial x^2} = n \frac{\partial h}{\partial t} \quad 2.25$$

The various solutions to Eqs. 2.23 or 2.25 have been directed toward determining the drop in the phreatic surface due to partial drainage during drawdown, rather than toward determining the pore water pressures at the end of a sudden, instantaneous drawdown. However, regardless of the degree of drainage, the pore water pressures are defined by the location of the phreatic surface and the assumption of vertical equipotential lines. For an instantaneous drawdown the pore pressures should be identical to those determined using Bishop's and Morgenstern's procedures, although the two approaches (Bishop-Morgenstern and Dupuit-based flow solutions) represent totally different approaches fundamentally. By either procedure the pore pressures are simply calculated by taking the distance from the surface of the slope (or reservoir level if below the final drawdown level) and multiplying the distance by the unit weight of water.

#### Procedures Based on Steady-State Flow.

A number of procedures have employed the solutions for steady-state flow for the purpose of calculating pore water pressures and flow velocities during drawdown. In the case of isotropic materials the

following Laplace equation is the governing equation which must be solved:

$$\frac{\partial^2 h}{\partial x^2} + \frac{\partial^2 h}{\partial y^2} = 0 \quad 2.26$$

Cedergren (1948) appears to have been one of the first to apply this equation to the case of drawdown. He constructed flow nets to solve the equation and suggested an approach for accounting for partial drainage and the drop in the phreatic surface during or after drawdown. He first constructed a flow net for the original reservoir level and steady-seepage (pre-drawdown) condition. Next, using the original location of the phreatic surface but with a new reservoir level representing drawdown at the slope face he constructed a new flow net. For the new flow net the portion of the upstream slope between the original and new reservoir levels as well as the phreatic surface were now considered zero pressure, drainage (discharge) boundaries. Based on the velocities of flow in a direction perpendicular to the phreatic surface (obtained from the new flow net), Cedergren estimated the amount of water which would have flowed away from the original phreatic surface for a selected increment of time. This allowed a new position for the phreatic surface to be estimated and the process was repeated. This process was repeated in selected increments of time until the desired final solution in time was obtained. If appropriate, additional changes in the reservoir level could be considered at any stage in the process. Desai (1972, 1977) used the same approach employed by Cedergren, but employed the finite element, rather than graphical (flow net) procedures to solve the Laplace equation (Eq. 2.26).

Although procedures based on the governing equation for steady-state flow appear to have been used in a number of instances to

obtain pore pressures associated with reservoir drawdown, there appears to be no fundamental basis for the use of such procedures. As shown previously the governing equation for transient flow is,

$$\rho k \left( \frac{\partial^2 h}{\partial x^2} + \frac{\partial^2 h}{\partial y^2} \right) = n S_R \frac{\partial p}{\partial t} + \rho S_R \frac{\partial n}{\partial t} + n \rho \frac{\partial S_R}{\partial t} \quad 2.8$$

Equation 2.8 is clearly not the same as Eq. 2.26 and only by ignoring significant terms on the right-hand side of Eq. 2.8 do the two equations become identical.

#### EMPIRICAL PROCEDURES BASED ON EXPERIENCE

Pore pressures due to sudden drawdown appear to be predicted sometimes using various empirical procedures based on the results from either model tests or field measurements. For example, Nagy (1967) presented a series of charts showing the critical rate of drawdown (required to cause instability) for various slope angles, effective stress friction angles and mean soil grain diameter. Nagy considered the mean grain diameter to suitably characterize the soil permeability (and presumably soil volume change characteristics) and developed his chart based on the results of a series of model experiments. Although empirical procedures based on experimental measurements and field experience can be used to predict pore water pressures for use in sudden drawdown analyses, the lack of sufficient data and the complexity of the problem appears to have limited the use of this approach to at most a few isolated cases.

#### DISCUSSION

None of the procedures examined for estimating pore pressures due to sudden drawdown can be justified on theoretical bases; only the procedure developed by Bishop (1954b) and Morgenstern (1963) even

attempts to account for changes in pore water pressure which occur due to induced shear stress during drawdown. However, even Bishop's and Morgenstern's procedure does not account for differences among various soils. Instead Bishop and Morgenstern adopted what they considered to be conservative assumptions.

The only way in which any of the effective stress procedures can be checked is by comparison of results obtained using the procedures with measured results for actual dams. Such comparisons may take several forms. Pore pressures may be measured and compared directly with values which are predicted by the various theoretical and empirical approaches. This is difficult to accomplish and due to point-to-point variations in pore pressures it is difficult to judge the overall validity of various approaches. Another approach is to examine case histories where slope failures occurred due to drawdown and to compute the factor of safety by various procedures. Wong, Duncan and Seed (1983) computed the factors of safety for two dams which failed by sliding due to sudden drawdown: Pilarcitos Dam and the Walter Bouldin Dam. They found that the factor of safety computed by Bishop's and Morgenstern's procedures were 1.15 and 0.98, respectively. These values (1.15, 0.98) are sufficiently close to unity for these dams which failed to suggest that the pore pressures predicted were reasonably correct. Wong, Duncan and Seed only considered Bishop's and Morgenstern's procedure for predicting pore water pressures and, thus, no assessment was made of other effective stress procedures. Analyses like those performed by Wong, Duncan and Seed are very useful; however, the number of well-documented case histories of actual slope failures due to sudden drawdown is small and such analyses are seldom performed.

Much of the existing field data pertaining to embankment performance during sudden drawdown consists of measured pore pressures in stable embankments. Winkley (1982) examined measured pore pressure data for eight embankment dams and dikes reported in the literature and summarized in Table 2.1. He computed factors of safety for these eight dams using measured pore pressure information and pore pressures based on Bishop's and Morgenstern's procedure. Because sufficient strength data were generally not available for the dams, Winkley assumed several sets of strength values and computed the factor of safety for each set; there was no way of establishing which set of values was actually correct, because the slopes were stable and the factor of safety was not known. The factors of safety are summarized in Table 2.2 for each slope and set of shear strength values used. Factors of safety computed employing pore pressures estimated by Bishop's and Morgenstern's procedure are plotted versus the corresponding values computed using the measured pore pressure data in Fig. 2.7. A total of 30 pairs of values are plotted; only 6 of the factors of safety which were computed using estimated pore water pressures exceed those based on the measured pore pressures. The mean ratio of factors of safety based on estimated-to-measured values is 0.98, with a standard deviation of 0.09. The results shown in Fig. 2.7 confirm Bishop's and Morgenstern's hypothesis that their procedure is conservative and are in substantial agreement with the results of Wong, Duncan and Seed for embankments which failed.

Few comparative studies appear to have been conducted employing pore pressures estimated by procedures other than Bishop's and Morgenstern's. Some insight into the probable relationship between the

TABLE 2.1

## EMBANKMENT DAMS STUDIED BY WINKLEY (1982)

| Name                 | Height<br>of Dam<br>(ft.) | Upstream<br>Slope | Amount<br>of<br>Drawdown<br>(ft.) | Duration<br>of<br>Drawdown<br>(days) | Ref.                         |
|----------------------|---------------------------|-------------------|-----------------------------------|--------------------------------------|------------------------------|
| Sir Adam Peak Dike   | 52                        | 2.5:1             | 25                                | 1                                    | Brazett<br>(1961)            |
| Lokvarka Dam         | 537                       | 1.9:1             | 53.5<br>77.8                      | -<br>-                               | Nonveiller<br>(1957)         |
| Glen Shira Lower Dam | 53                        | 3.0:1             | 16<br>24<br>30                    | 2<br>3<br>4                          | Patton &<br>Semple<br>(1961) |
| Alcova Dam           | 239                       | 3.0:1             | 126.6                             | 49                                   | Glover et<br>al (1948)       |
| Castiletto Dam       | 246                       | 3.0:1             | 194                               | 180                                  | Meyer-<br>Peter<br>(1964)    |
| Sardis Dam           | 97                        | 3.5:1             | 15                                | 81                                   | Corps of<br>Engrs.<br>(1967) |
| Grenada Dam          | 80                        | 4.5:1             | 16                                | 90                                   | Corps of<br>Engrs.<br>(1970) |
| Goscheneralp         | 345                       | 4.0:1             | 283                               | 70                                   | Meyer-<br>Peter<br>(1964)    |

TABLE 2.2

COMPARISON OF FACTORS OF SAFETY COMPUTED USING MEASURED PORE WATER PRESSURES AND PORE WATER PRESSURES ESTIMATED BY BISHOP'S AND MORGENSTERN'S PROCEDURE (From Winkley, 1982)

| Dam                         | (Assumed Factor of Strength Values)<br>$\lambda_{c\phi}$ | Safety (Meas. Data) | Factor of Safety (Bishop-Morgenstern) | $\frac{F_{Bishop}}{F_{Meas.}}$ |
|-----------------------------|--|---------------------|---------------------------------------|--------------------------------|
| Sir Adam Peak Dike          | 11.8   | 1.06                | 1.36                                  | 1.28                           |
| Sir Adam Peak Dike          | 5.9  | 1.39                | 1.45                                  | 1.04                           |
| Sir Adam Peak Dike          | 3.9  | 1.79                | 1.75                                  | 0.98                           |
| Sir Adam Peak Dike          | 3  | 2.09                | 2.04                                  | 0.98                           |
| Lokvarka - Drawdown No. 1   | 35.8   | 1.29                | 1.25                                  | 0.97                           |
| Lokvarka - Drawdown No. 1   | 17.9   | 1.32                | 1.29                                  | 0.98                           |
| Lokvarka - Drawdown No. 1   | 11.9   | 1.36                | 1.32                                  | 0.97                           |
| Lokvarka - Drawdown No. 1   | 8.9  | 1.39                | 1.36                                  | 0.98                           |
| Lokvarka - Drawdown No. 2   | 35.8   | 1.28                | 1.25                                  | 0.98                           |
| Lokvarka - Drawdown No. 2   | 17.9   | 1.31                | 1.26                                  | 0.96                           |
| Lokvarka - Drawdown No. 2   | 11.9   | 1.35                | 1.29                                  | 0.96                           |
| Lokvarka - Drawdown No. 2   | 8.9  | 1.39                | 1.32                                  | 0.95                           |
| Glen Shira - Drawdown No. 1 | 0  | 1.46                | 1.65                                  | 1.13                           |
| Glen Shira - Drawdown No. 1 | 12   | 1.48                | 1.52                                  | 1.03                           |
| Glen Shira - Drawdown No. 2 | 0  | 1.45                | 1.66                                  | 1.14                           |
| Glen Shira - Drawdown No. 2 | 12   | 1.49                | 1.38                                  | 0.93                           |
| Glen Shira - Drawdown No. 3 | 0  | 1.73                | 1.77                                  | 1.02                           |
| Glen Shira - Drawdown No. 3 | 12   | 1.43                | 1.37                                  | 0.96                           |
| Alcova                      | 54.4   | 1.16                | 0.95                                  | 0.82                           |
| Alcova                      | 27.2   | 1.25                | 1.02                                  | 0.82                           |
| Alcova                      | 18.1   | 1.33                | 1.09                                  | 0.82                           |
| Alcova                      | 13.6   | 1.31                | 1.15                                  | 0.88                           |
| Castiletto                  | 56   | 2.11                | 2.03                                  | 0.96                           |
| Castiletto                  | 14   | 2.15                | 2.07                                  | 0.96                           |
| Sardis Dam                  | 20   | 2.19                | 2.19                                  | 1.00                           |
| Sardis Dam                  | 5  | 2.19                | 2.19                                  | 1.00                           |
| Grenada                     | 18   | 1.75                | 1.65                                  | 0.94                           |
| Grenada                     | 4.5  | 2.26                | 2.16                                  | 0.96                           |
| Goscheneralp                | 78.5   | 2.62                | 2.61                                  | 1.00                           |
| Goscheneralp                | 19.6   | 2.63                | 2.62                                  | 1.00                           |

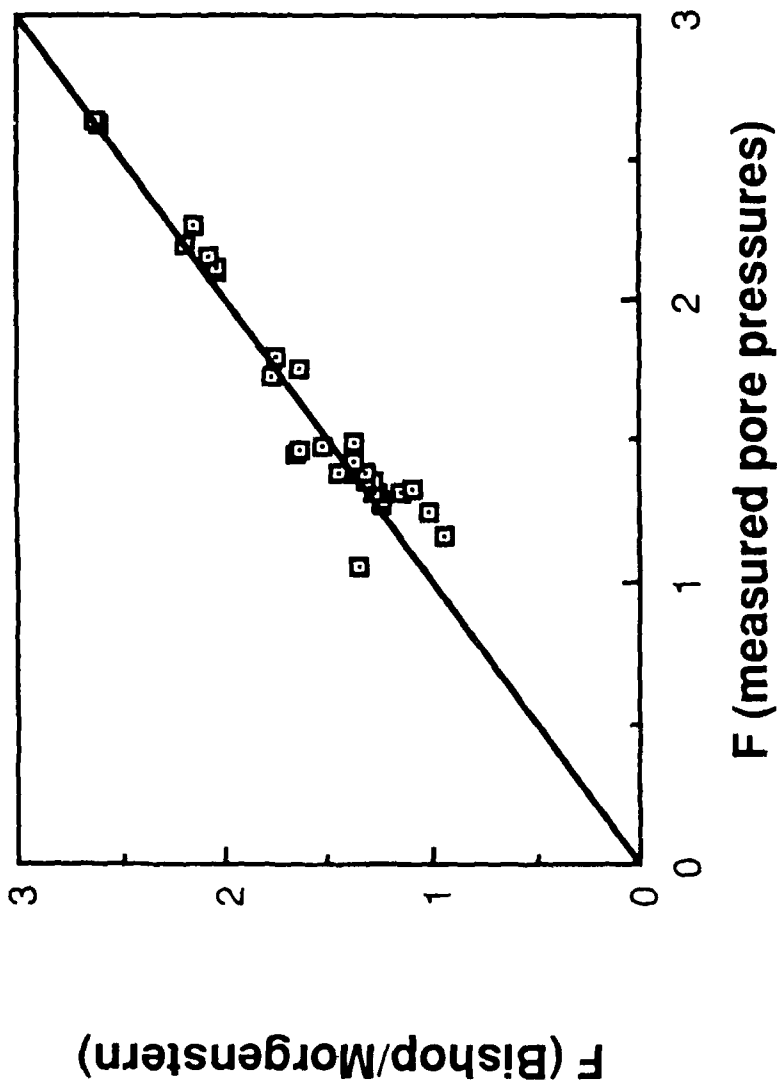


Figure 2.7 - Comparison of Factors of Safety Calculated Using Effective Stresses with Measured Pore Water Pressures and Pore Water Pressures Estimated Using Bishop's and Morgenstern's Procedure (After Winkley, 1982)

pore pressures obtained using Bishop's and Morgenstern's approach and the procedures based on various solutions of equations of hydraulic flow appears in the early work of Glover, Gibbs and Daehn (1948). They first observed:

".... the removal of the reservoir load caused an immediate change in both the contact pressures [effective stress] and the pore pressures. The latter assume a distribution resembling that due to a gravity flow system but with a pressure gradient in the vertical direction considerably less. This distribution will rapidly revert to the gravity flow system as soon as enough percolation can take place to satisfy the tendency of the grain structure to change volume. The pore pressure distribution referred to herein as a gravity flow system is one which can be maintained by gravity forces only as distinguished from a system wherein the pore pressures are influenced by an unsatisfied tendency of the grain structure to expand."

Although they failed to recognize that the soil may exhibit a tendency to compress due to shear, rather than expand, Glover et al, recognized that pore pressures will be influenced by the tendency of the soil to change volume and will differ from those associated with gravity flow. However, based on their assumption that the soil would tend to expand they continued:

"The gravity flow system will exhibit an approximately hydrostatic pressure increase along a vertical line. .... It is concluded that no pore pressure distribution less favorable to stability than the gravity flow system will be encountered, following a drawdown, no matter how rapidly it may be accomplished."

Thus, while recognizing that pore pressures will be influenced by tendencies for the soil to change volume, they considered the assumption of a gravity flow condition, i. e. that Eq. 2.26 can be considered the governing equation, should be conservative. Morgenstern (1963) also noted that Terzaghi and Peck suggested as a first approximation that horizontal flow and vertical equipotential lines could be assumed for conditions after sudden drawdown and that the assumption led to essentially identical pore pressures to those obtained using Bishop's

and Morgenstern's approach. Also as noted earlier the transient flow procedures based on the Dupuit assumptions lead to pore pressures identical to those obtained by Bishop's and Morgenstern's procedure. Consequently, it appears that pore pressures predicted using at least a number of the procedures based on equations of hydraulic flow are identical to those based on Bishop's and Morgenstern's approach. It then also follows that the validity of the procedures may be comparable to the validity of Bishop's and Morgenstern's procedure.

#### SUMMARY

Effective stress analysis procedures all require that the pore pressures be estimated for conditions at the end of sudden drawdown; the various effective stress "procedures" differ only in the manner in which the pore water pressures are estimated. Several procedures for estimating pore water pressures have been developed and discussed in the previous sections. Based on the discussion several important conclusions can be drawn:

- (1) The various procedures for estimating pore water pressures are based on totally different approaches and assumptions and none can be verified strictly on theoretical grounds due to the simplifying nature of the assumptions employed.
- (2) Bishop's and Morgenstern's procedure has produced good agreement with measured field data including cases of slope failure.
- (3) Bishop's and Morgenstern's procedure is the easiest procedure to use to estimate pore water pressures.
- (4) Several of the approximate procedures based on equations of hydraulic flow yield pore pressures which are identical to those

obtained by Bishop's and Morgenstern's procedures and, thus, such procedures based on hydraulic flow should show equally good agreement with field performance data.

(5) None of the existing procedures for predicting pore water pressures account for the differences among various soil types and their tendency to change volume and generate pore water pressures during shear. Only Bishop's and Morgenstern's procedure even considers pore pressures generated during shear.

(6) Numerical analyses which couple the equilibrium equations for the stresses with the governing equation of hydraulic flow offer the most promising alternative for obtaining a fundamentally, rigorous solution to the problem of predicting pore water pressures due to sudden drawdown. However, such an approach is extremely complex, which may account for the fact that the approach has not been used to predict pore pressures due to sudden drawdown.

SECTION 3  
TWO-STAGE ANALYSIS PROCEDURES  
(Wright)

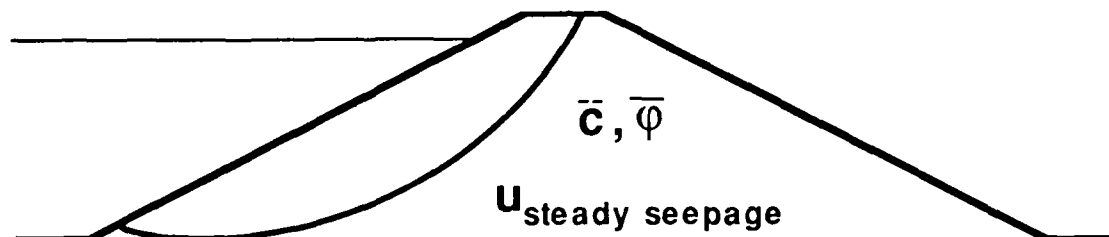
INTRODUCTION

Two separate sets of stability calculations are performed in the two-stage analysis procedures (Fig. 3.1). The first set of computations is performed for conditions just prior to drawdown. The purpose of the first set of computations is to estimate the stresses under which the soil is consolidated before drawdown and the corresponding values of undrained shear strength. The second set of computations is performed for conditions immediately after drawdown using the loads after drawdown and the undrained shear strengths established from the first set of computations. The two sets of computations are performed for a selected, individual shear (sliding) surface; various trial shear surfaces are selected until the one producing the minimum factor of safety (after drawdown) is found. The most critical shear surface found in this manner will usually be different from the most critical shear surface for conditions before drawdown (steady seepage, etc.).

Stage 1 Stability Computations

The first set of stability computations in the two-stage procedures is performed using shear strength parameters and loads representing conditions in the slope just prior to drawdown. The shear strength parameters are expressed in terms of effective stresses and would normally be obtained from either consolidated-drained (CD, S) tests or consolidated-undrained (CU, R) tests with pore pressure measurements. The pore water pressures used in the first set of stability computations

### (a) Stage 1 - Before Drawdown



### (b) Stage 2 - After Drawdown

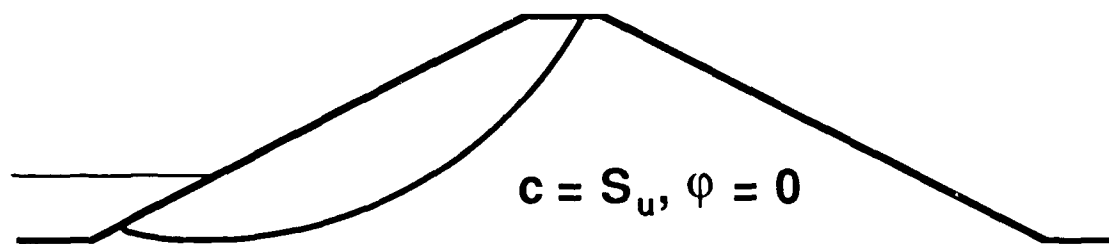


Figure 3.1 - Schematic Illustration of the Two Stages Considered in Analyses by Two-Stage Procedures for Sudden Drawdown

are determined either from a steady state seepage analysis or calculated directly from the reservoir level before drawdown, neglecting head losses in the slope. The purpose of the first set of stability calculations is to compute the stresses on the shear surface prior to drawdown. The factor of safety calculated in the first set of computations is of no interest; however, the factor of safety must ordinarily be calculated as part of the limit equilibrium solution for the stresses. Once the stresses have been calculated they are used to estimate the undrained shear strength,  $s_u$ , at the shear surface. The undrained shear strength is estimated for each slice and, ordinarily, will be different for each slice because the stresses vary from slice to slice. Several procedures have been used to estimate the undrained shear strength along the shear surface; the differences in these procedures constitute the primary difference among the various two-stage procedures of analysis and are described in further detail in the various subsections below.

#### Stage 2 Stability Calculations

The second set of stability computations is performed for conditions immediately after drawdown. For all but freely draining materials the shear strengths used are those estimated based on the first set of computations and are represented as " $\phi = 0$ " strengths ( $c = s_u$ ,  $\phi = 0$ ). Total stresses are used; pore pressures are not considered explicitly. In the case of freely-draining materials effective stresses are used; the shear strength parameters are identical to those used in the first set of computations and pore pressures representing those after drawdown are used. Regardless of whether materials are freely draining or not, any surface loads due to water which remains after

drawdown are applied for the second set of computations. The factor of safety calculated in the second set of computations is the factor of safety after drawdown.

#### CORPS OF ENGINEERS' PROCEDURE

The Corps of Engineers' procedure is based on the use of a composite (bilinear) shear strength envelope which represents the minimum of the R and S envelopes, from consolidated-drained and consolidated-undrained shear tests, respectively, as shown in Fig. 3.2. The Corps of Engineers' Stability Manual (Engineer Manual 1110-2-1902) indicates that the same composite (bilinear) shear strength envelope is used for both the first and the second states of the computations, although it is not clear that procedures in the Manual are always followed in practice. In general geotechnical engineering practice, including possibly the Corps of Engineers' own practice, it appears that at least three variations of the Corps of Engineers' procedure might be adopted for the shear strength used in the first stage computations:

1. The S ("drained," effective stress) envelope could be adopted exclusively to define the shear strength in the first stage computations. This would be consistent with the general concept that the first stage computations in two-stage analysis procedures represent conditions with steady-seepage before drawdown and the conventional geotechnical practice of employing the S envelope for such conditions.
2. A bilinear envelope representing the S envelope or a line of " $(R + S)/2$ ," whichever is less, as shown in Fig. 3.3. Such an envelope as the one illustrated in Fig. 3.3 is recommended by the Corps of Engineers for the steady-seepage stability condition.

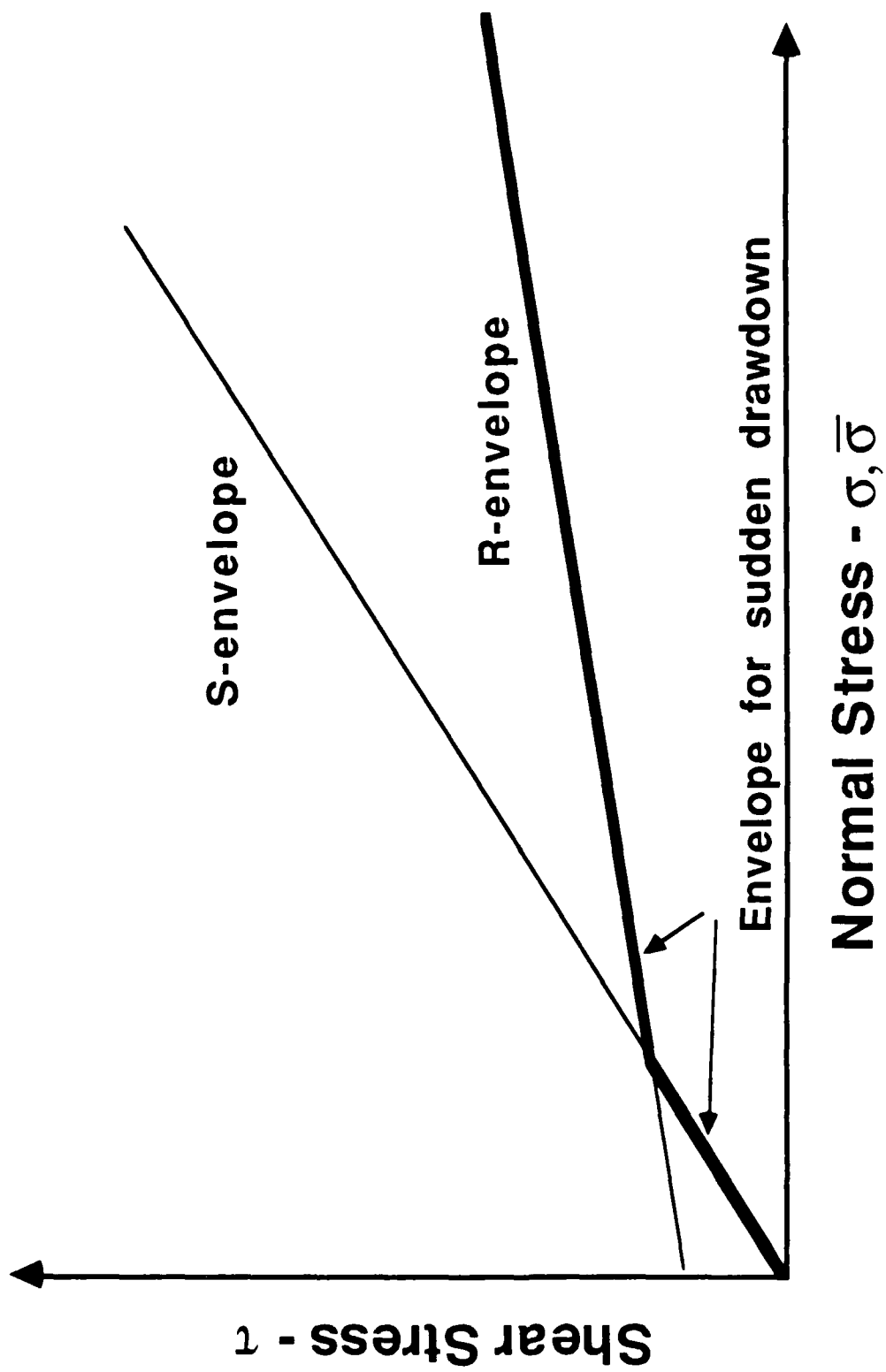


Figure 3.2 - Bilinear Shear Strength Envelope Used in Corps of Engineers' Procedure for Sudden Drawdown Stability Calculations

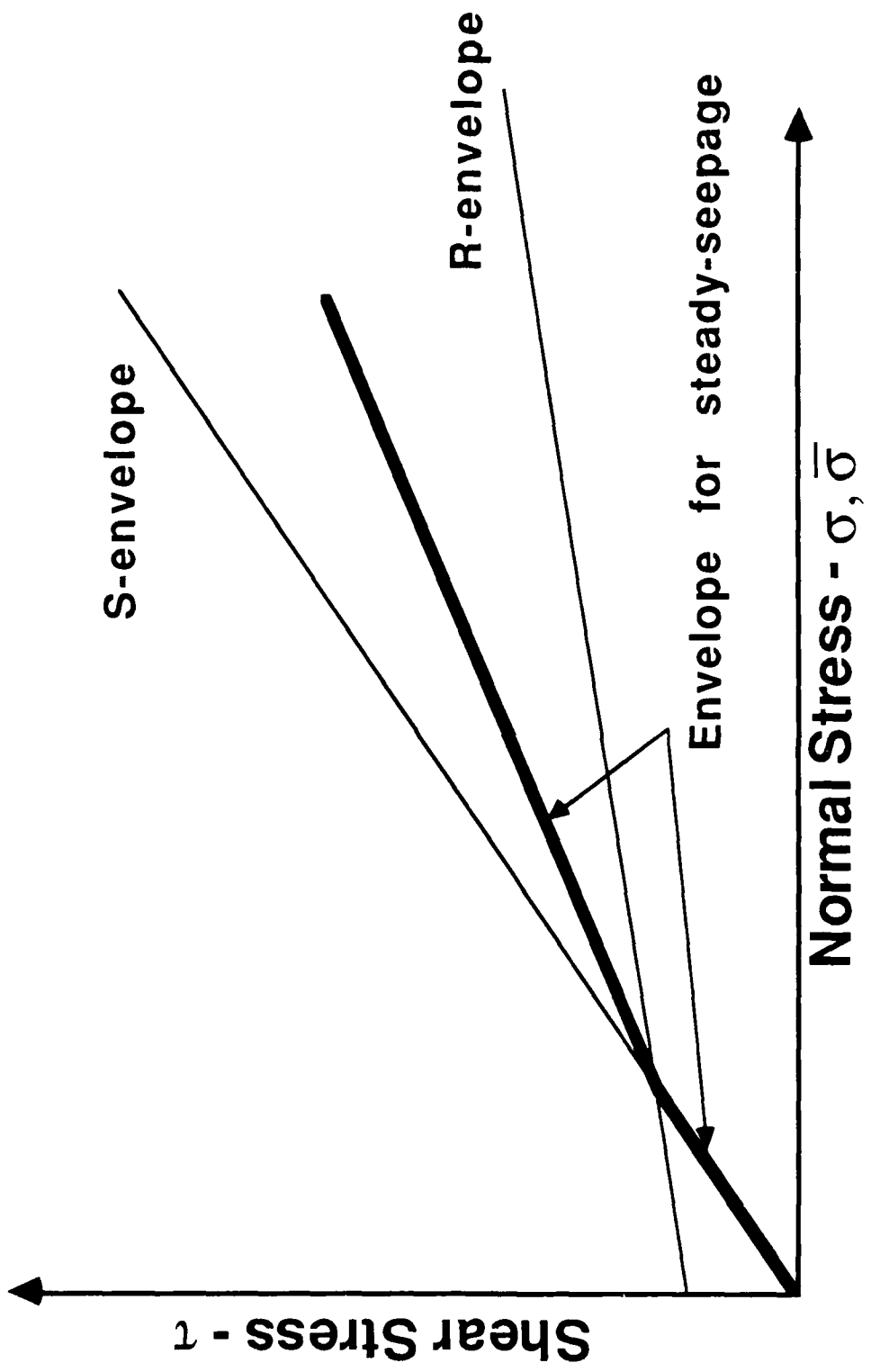


Figure 3.3 - Bilinear Shear Strength Envelope Used in Corps of Engineers' Procedure for Steady-Seepage Stability Calculations

Thus, use of the envelope would again be consistent with the concept that the first stage stability computations are performed to represent conditions with steady seepage before drawdown, and would be consistent with the Corps of Engineers' recommendations for the steady-seepage condition.

3. The composite (bilinear) envelope used for the second stage computations and shown in Fig. 3.2 could be used for the first stage computations as discussed earlier above and, apparently, intended by the procedure given in Corps of Engineers (1970).

Inasmuch as the first-stage computations are only used to compute the effective normal stress on the shear surface it is probably not important as to which of the three alternatives is selected to describe the failure envelope. However, some differences among computed factors of safety can be expected depending on the envelope selected.

Several alternatives may be used in the first-stage computations to estimate the pore pressures in the slope before drawdown. The most fundamentally correct approach is to estimate pore pressures based on either graphical (flow net) or numerical solutions for the steady state seepage through the slope prior to drawdown. A simpler approach is to ignore head losses in the slope in which case the water surface adjacent to the slope can be extended horizontally into the slope and treated as a horizontal piezometric line to define pore pressures at all points within the slope. Examples presented in the Corps of Engineers' Stability Manual indicate that head losses are ignored, i. e. a horizontal water surface is assumed to exist before drawdown. In this case effective stresses can be accounted for in either of two ways: (1)

submerged unit weights can be used below the water surface and total unit weights can be used above the water surface, or (2) total unit weights can be used for all materials and pore pressures can be calculated using the upstream reservoir surface as a piezometric surface for the entire slope. The approach employing submerged unit weights is only valid when there are no seepage forces (no hydraulic gradient). The writer recommends use of total unit weights and pore water pressures in all cases because seepage forces are then ignored and the potential for errors due to their inadvertent omission are eliminated.

Use of a horizontal water surface, rather than accounting for head losses in the slope due to steady seepage will lead to higher values of estimated pore pressure and, thus, lower effective stresses. Consequently, the undrained shear strengths which are estimated using the effective stresses will be lower when a horizontal water surface is assumed and, thus, will be in error on the safe side. The negligible head losses in the upstream slope of relatively homogeneous slopes, especially at the shallow depths where most drawdown failures may occur, probably justify ignoring such head losses. By ignoring such head losses the analyses are often substantially simplified and any errors are in the direction of increased safety.

The first-stage computations are used to calculate the effective normal stresses along the shear surface. Inasmuch as some procedure of slices is ordinarily used, the effective normal stresses will be calculated at the base of each individual slice; the effective normal stress is computed by dividing the total normal force on the base of the slice by the area of the base of the slice and subtracting the pore

water pressure<sup>1</sup>. Once the effective normal stress is calculated the bilinear shear strength envelope (Fig. 3.2) is used to determine an appropriate value of shear strength. The shear strength determined in this manner is then considered to represent an undrained shear strength for use in the second stage stability computations.

Second stage computations are performed once appropriate undrained shear strengths have been estimated from the first stage computations. In general, the second stage computations are performed in an identical fashion for all two-stage analysis procedures once undrained shear strengths have been estimated. More specifically, the Corps of Engineers' Stability Manual suggests two limit equilibrium analysis procedures for computing the factor of safety for the second stage: (1) the Modified Swedish procedure, and (2) the Ordinary Method of Slices. Several observations may be made with regard to the recommendation of these two procedures:

1. Although the Ordinary Method of Slices is not generally considered to be an accurate procedure, in the special case of sudden drawdown (saturated soil, undrained loading) the friction angle ( $\phi$ ) is zero for the second stage computations. In this case ( $\phi = 0$ ) the factor of safety calculated using the Ordinary Method of Slices will be identical to the value calculated by any

---

<sup>1</sup>The reader is referred to Wright (1986b) for the specific equations used to compute the normal force on the base of slices in the various limit equilibrium procedures employed in UTEXAS2 (Wright, 1986a). In the case where submerged unit weights are used for soil below the water table, the normal force which is calculated on the base of the slice will be the effective normal force and the pore water pressures should not be subtracted.

procedure which satisfies complete static equilibrium. Thus, the value for the factor of safety should be as accurate as any that can be obtained by limit equilibrium procedures.

2. While accurate for the second-stage computations, the factor of safety computed by the Ordinary Method of Slices will not be the same as the one computed by the Corps of Engineers' Modified Swedish procedure, because the Modified Swedish procedure does not satisfy moment equilibrium.

3. The Ordinary Method of Slices is restricted to use with circular shear surfaces. Thus, the Modified Swedish procedure would apparently be used for noncircular shear surfaces according to the Stability Manual (excluding those special cases where the Corps' Wedge Method is used).

4. In cases where some portions of a slope may be freely draining and, thus, shear strengths might be represented as "drained" and expressed in terms of effective stresses for the second stage computations, the Stability Manual is unclear regarding use of the Ordinary Method of Slices. All illustrations of applications using the Ordinary Method of Slices in the Stability Manual apply only to soils which are not drained. The Ordinary Method of Slices can lead to large errors when effective stresses are used.

In general, it is not clear in the Corps of Engineers' procedure if all soils are to be considered undrained, or if portions of the soil which are freely draining are to be considered as "drained." Consequently, it is not clear regarding the manner in which strengths might be represented in a cross-section of a zoned earth dam for portions which are freely draining. For example, it is not clear if the bilinear

envelope used for conventional steady-seepage analyses (Fig. 3.3) is to be used for freely-draining materials or if the conventional S envelope by itself is to be used in these cases.

#### LOWE AND KARAFIATH'S PROCEDURE

Lowe and Karafiath (1960a) developed their procedure to account for the fact that the soil is consolidated anisotropically prior to drawdown. Although Lowe and Karafiath did not elaborate on the first-stage stability computations, the first-stage computations are generally performed as conventional steady-state seepage stability computations. Effective stress shear strength parameters are determined employing either consolidated-drained (CD, S) shear test procedures or consolidated-undrained (CU, R) test procedures with pore pressure measurements; pore pressures are determined by either an appropriate steady-state seepage analysis or by neglecting head losses and using the reservoir surface as a horizontal piezometric line.

The principal unique feature of Lowe and Karafiath's procedure involves the use of a family of shear strength envelopes to estimate the undrained shear strength for the second-stage stability computations (Fig. 3.4). Each shear strength envelope corresponds to a given effective principal stress ratio at consolidation,  $K_c (= \bar{\sigma}_{1c}/\bar{\sigma}_{3c})$ ; the family of envelopes is developed from laboratory tests employing anisotropic consolidation and several, selected effective principal stress ratios. Each envelope expresses the variation in undrained shear strength ( $\tau_{ff}$ ) with effective normal stress on the failure plane at the time of consolidation ( $\bar{\sigma}_{fc}$ ) for a given consolidation stress ratio ( $K_c$ ). The undrained shear strength is the shear stress on the failure plane at failure and can be computed from

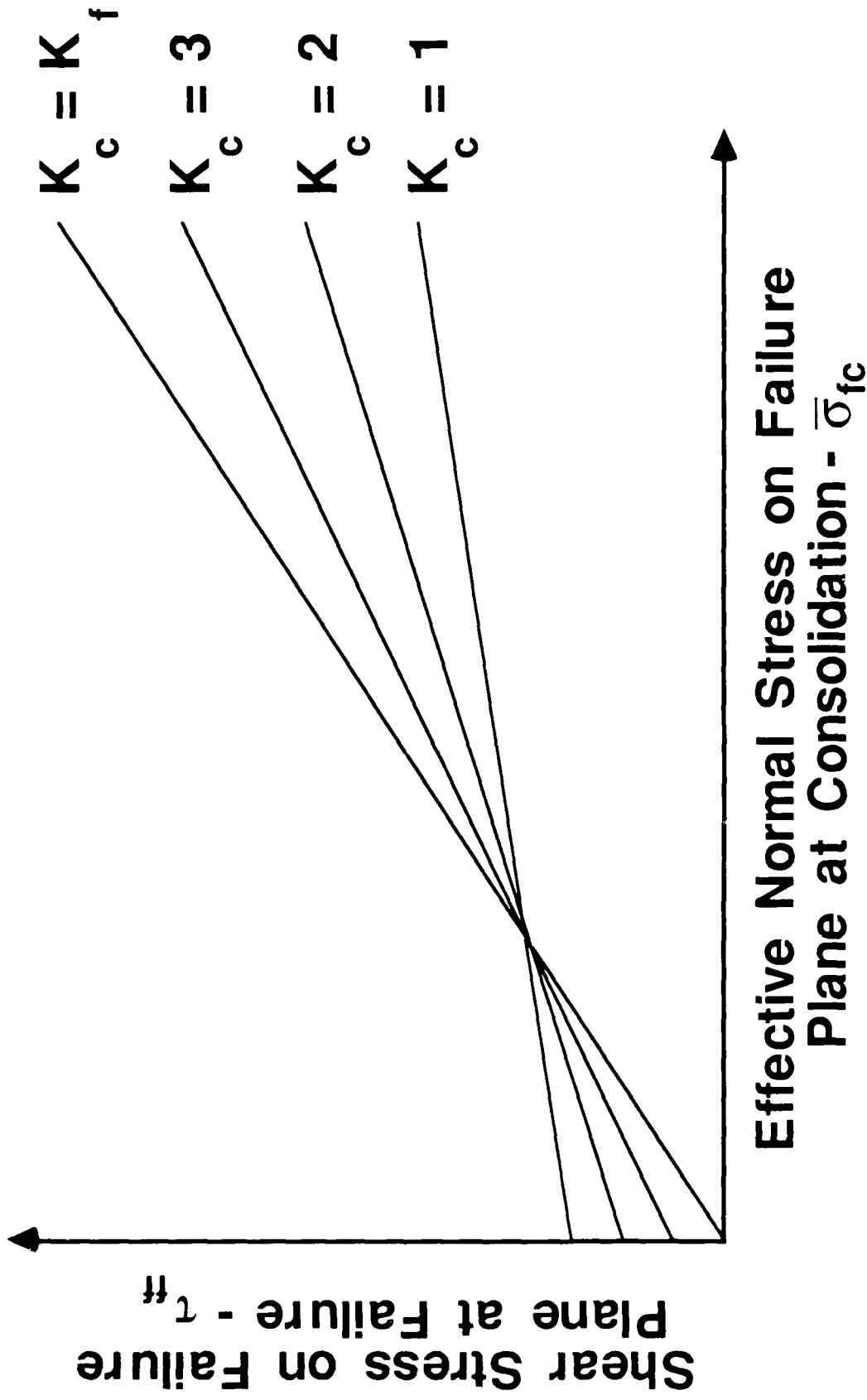


Figure 3.4 - Family of Shear Strength Envelopes for Various Anisotropic Consolidation Stress Ratios,  $K_c (= \bar{\sigma}_{1c}/\bar{\sigma}_{3c})$ , Used in Lowe and Karafiath's Procedure

$$\tau_{ff} = \frac{(\sigma_{1f} - \sigma_{3f})}{2} \cos \bar{\phi} \quad 3.1$$

where,  $\sigma_{1f}$  and  $\sigma_{3f}$  represent the major and minor principal stresses, respectively, at failure and  $\bar{\phi}$  is the friction angle in terms of effective stresses. The effective normal stress on the failure plane at consolidation can be computed from:

$$\bar{\sigma}_{fc} = \frac{(\bar{\sigma}_{1c} + \bar{\sigma}_{3c})}{2} - \frac{(\bar{\sigma}_{1c} - \bar{\sigma}_{3c})}{2} \sin \bar{\phi} \quad 3.2$$

where,  $\bar{\sigma}_{1c}$  and  $\bar{\sigma}_{3c}$  represent the major and minor principal effective stresses at consolidation, respectively. Values of both  $\tau_{ff}$  and  $\bar{\sigma}_{fc}$  can be calculated from the data from any triaxial shear test and plotted on a diagram like the one shown in Fig. 3.4. The lowest value of effective principal stress ratio for which failure envelopes can be determined is unity, which corresponds to an isotropic state of stress at consolidation and is the usual stress state employed in consolidated-undrained triaxial shear tests. The upper limit on the effective principal stress ratio to which a soil can be consolidated is equal to the effective principal stress ratio at failure in a consolidated-drained shear test. Accordingly, the failure envelope corresponding to the maximum effective principal stress ratio at consolidation is identical to the conventional (effective stress) failure envelope from consolidated-drained shear tests (Note:  $\tau_{fc} = \tau_{ff}$  and  $\bar{\sigma}_{fc} = \bar{\sigma}_{ff}$  in the case of consolidated-drained shear tests).

Fundamentally, Lowe and Karafiath's procedure requires that several series of consolidated-undrained shear tests be performed using each of several different effective principal stress ratios for consolidation. However, several simplified procedures have been proposed for estimating

the effects of anisotropic consolidation using the results of isotropically consolidated-undrained triaxial tests with pore water pressure measurements. The various simplified procedures are discussed in detail in Section 4 of this paper.

The undrained shear strength,  $\tau_{ff}$ , to be used in the second stage of the computations in Lowe and Karafiath's procedure is determined from the family of envelopes like those shown in Fig. 3.4. In order to determine the value of  $\tau_{ff}$  both the effective normal stress on the failure plane at consolidation,  $\bar{\sigma}_{fc}$ , and the effective principal stress ratio at consolidation,  $\bar{\sigma}_{1c}/\bar{\sigma}_{3c}$ , are determined. The effective normal stress on the failure plane is determined in the same manner as in the Corps of Engineers' procedure. That is, the total normal force on the base of each slice, computed from the first-stage stability computations, is divided by the area of the base of the slice and the pore water pressure is then subtracted. The effective principal stress ratio,  $K_c$ , is not known and, thus, cannot be determined as easily as the effective normal stress because only the stresses on the shear plane are calculated in limit equilibrium analyses. To calculate the effective principal stress ratio Lowe and Karafiath assumed that the directions of the principal stresses are the same before drawdown as they would be at failure. Thus, the effective principal stresses at consolidation act in the same direction with respect to the shear surface as they would act if failure would occur (Fig. 3.5). Knowing the effective normal stress ( $\bar{\sigma}_{fc}$ ) and shear stress ( $\tau_{fc}$ ) on the shear surface at consolidation, i.e., before drawdown, then enables the principal stresses to be calculated (Fig. 3.6). The principal stresses are given by the following:

$$\bar{\sigma}_{1c} = \bar{\sigma}_{fc} + \tau_{fc} \left( \tan \bar{\phi} + \frac{1}{\cos \bar{\phi}} \right) \quad 3.3$$

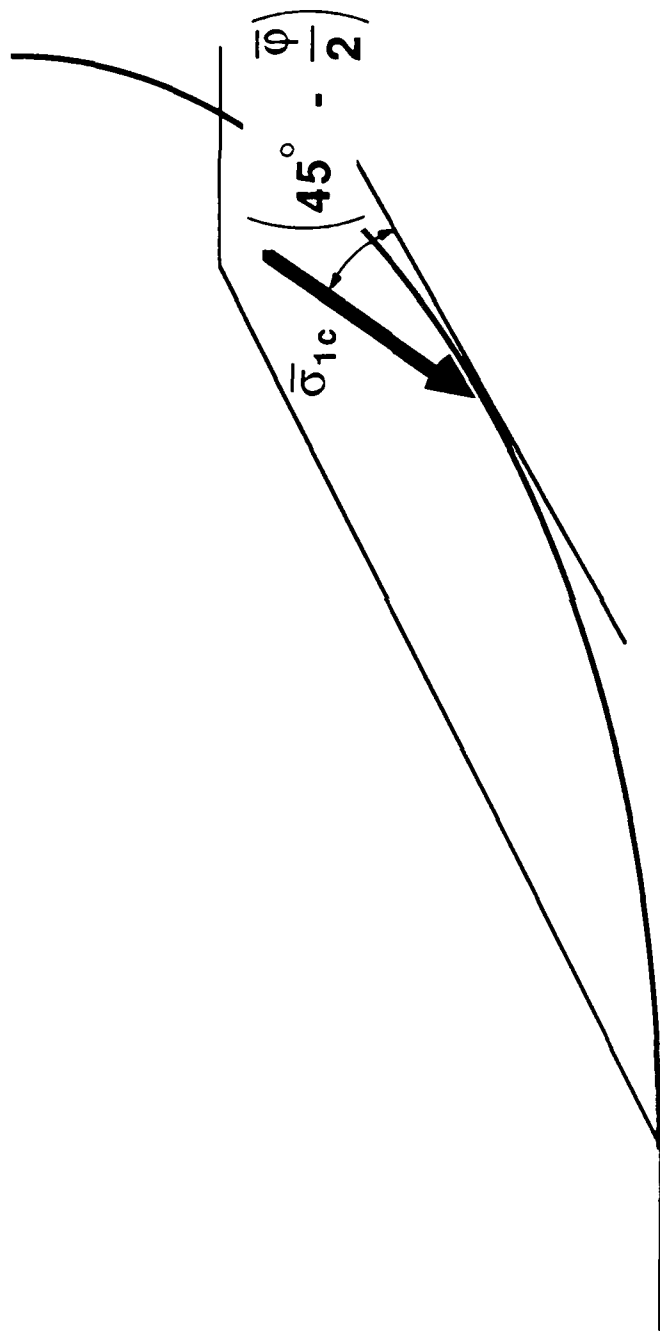


Figure 3.5 - Orientation of Major Principal Stress at Consolidation ( $\bar{\sigma}_{1c}$ ) Assumed in Lowe and Karafiath's Procedure

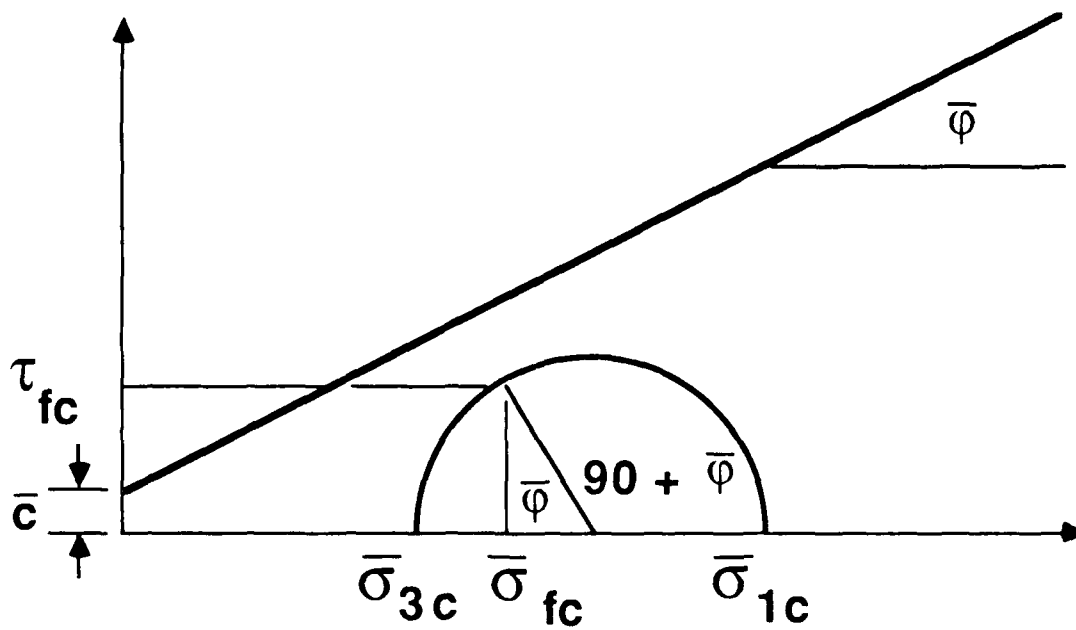
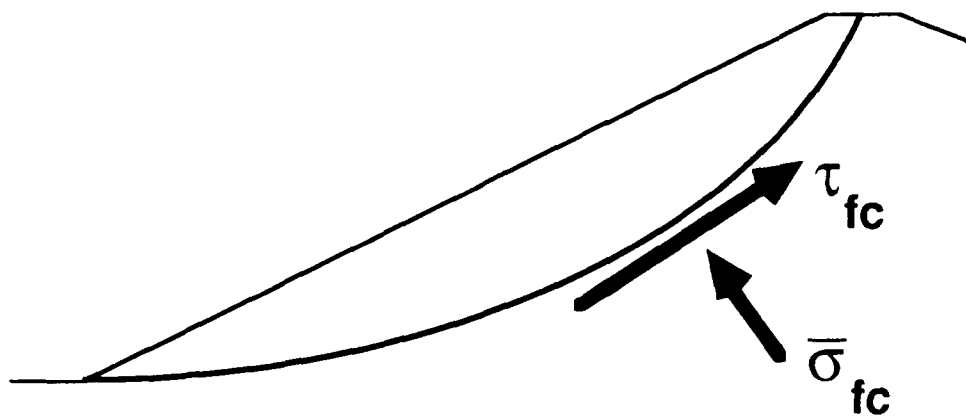


Figure 3.6 - Relationship between Stresses on the Shear Plane and the Principal Stresses at Consolidation for Low and Karafiath's Procedure

and,

$$\bar{\sigma}_{3c} = \bar{\sigma}_{fc} + \tau_{fc} \left( \tan \bar{\phi} - \frac{1}{\cos \bar{\phi}} \right) \quad 3.4$$

The shear stress,  $\tau_{fc}$ , is the shear stress on the shear plane at consolidation and is calculated from the first-stage stability computations by dividing the shear force on the base of each slice by the respective area<sup>2</sup>. Once the principal stresses have been calculated the effective principal stress ratio ( $K_c$ ) is computed and with the effective normal stress on the failure plane at consolidation ( $\bar{\sigma}_{fc}$ ) also known the undrained shear strength is determined from the family of shear strength envelopes. The undrained shear strength,  $\tau_{ff}$ , becomes the "cohesion" component of shear strength for the second-stage stability computations and  $\phi$  is set equal to zero ( $c = \tau_{ff}$ ,  $\phi = 0$ ). Once the shear strength is determined, the second-stage stability computations are fundamentally the same as those by any other two-stage analysis procedure, including the Corps of Engineers procedure.

Some difficulties may be encountered with Lowe and Karafiath's procedure for soils where an effective cohesion intercept ( $\bar{c}$ ) exists. In such cases, the maximum effective principal stress ratio associated with the consolidated-drained (effective stress) envelope is not a constant, but varies with the effective stress. As the effective stresses decrease and become small, the effective principal stress ratio at failure first approaches a value of infinity as  $\bar{\sigma}_{3c}$  approaches zero (Fig. 3.7a) and, then, the effective principal stress ratio becomes negative; the

---

<sup>2</sup>The reader is again referred to Wright (1986b) for the specific equations used to compute the shear force on the base of slices in the various limit equilibrium procedures employed in UTEXAS2.

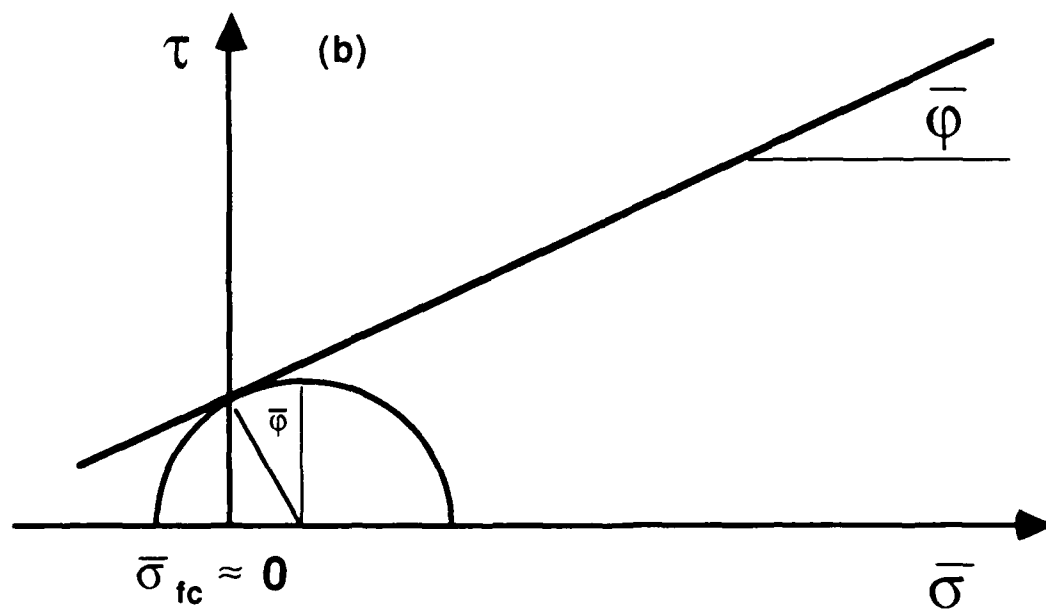
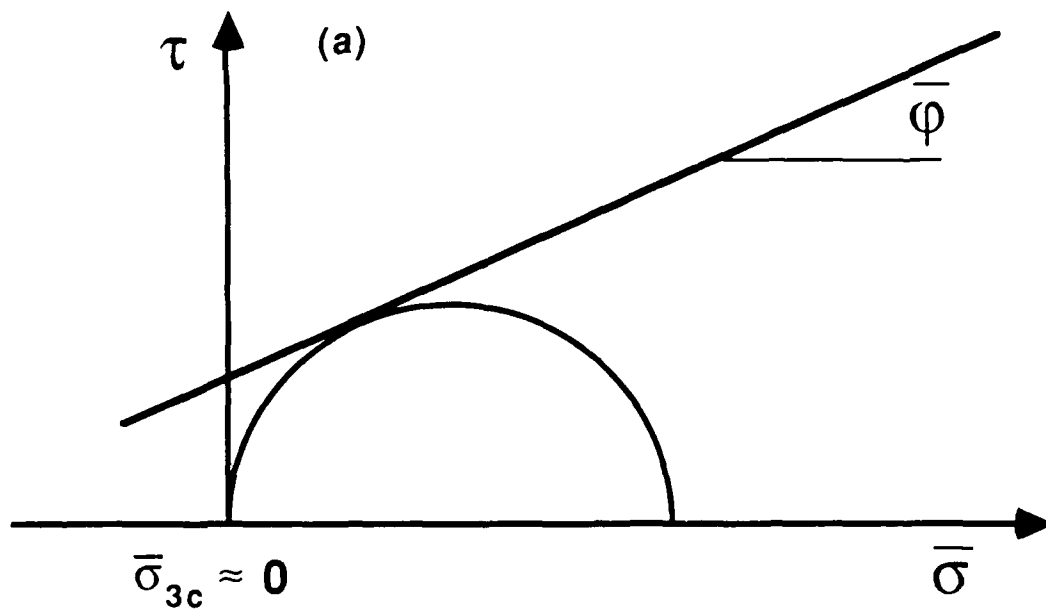


Figure 3.7 - Mohr's Circles for Stresses at Failure for  
 (a) the Minor Principal Stress Approaching Zero, and  
 (b) the Effective Stress on the Failure Plane Approaching Zero

effective principal stress ratio is clearly negative when  $\bar{\sigma}_{fc}$  reaches zero (Fig. 3.7b). Any attempt to interpolate shear strength values between strength envelopes corresponding to the maximum effective principal stress ratio ( $K_f$ ), and some lower effective principal stress ratio becomes complicated when the value of  $K_f$  becomes very large or negative. In addition to the problems associated with defining  $K_f$  for the failure envelope, either one or both of the effective principal stresses (at consolidation) which are calculated from Eqs. 3.3 and 3.4 using the stresses computed from the first-stage stability computations may also become negative. In order to avoid these difficulties several alternatives exist and one or more may be necessary to overcome these problems. First, low stresses and potentially negative values of the corresponding principal stresses calculated from the stability analyses may be at least partially eliminated by introducing a tension crack into the stability computations. Secondly, with regard to computing the effective principal stress ratio associated with the effective stress failure envelope, Wong, Duncan and Seed (1983), neglected the effective cohesion intercept and assumed a constant effective principal stress ratio at failure given by,

$$K_f = \frac{\sigma_{1f}}{\sigma_{3f}} = \tan^2(45 + \bar{\phi}/2) \quad 3.5$$

In addition the effective cohesion intercept ( $c$ ) may be neglected entirely in the stability computations, including the first-stage computations. This would both eliminate the possibility of negative values being computed for the stresses in the first-stage stability computations and the effective principal stress ratio associated with the effective stress failure envelope would be a constant and finite

quantity. None of the alternatives in Lowe and Karafiath's procedure is ideal nor have any been investigated in sufficient detail at the present time to warrant recommending one in preference to another. However, the effective cohesion intercept,  $\bar{c}$ , often has a very important effect on the computed factor of safety for small slopes and shallow slides, and the manner in which the effective cohesion is treated may have an important effect on the computed factors of safety for sudden drawdown.

#### DISCUSSION

Both two-stage procedures are conceptually similar. Both involve calculating the effective stresses before drawdown from a set of stability calculations for the steady seepage condition and, then, using the stresses to estimate undrained shear strengths at the time of drawdown. A second set of stability calculations is then performed using the estimated undrained shear strengths. The only major difference between the two approaches is in the procedures used to estimate the undrained shear strengths. In a broad sense, the Corps of Engineers' procedure represents a conservative, lower-bound approach to the one suggested by Lowe and Karafiath. However, the use of the R-type failure envelope in the Corps of Engineers' procedure warrants some further discussion.

R envelope versus  $\tau_{ff} - \bar{\sigma}_{fc}$  line. The R envelope is obtained by first constructing a series of "Mohr's" circles, where the minor principal stress represents the minor principal effective stress at the time of consolidation ( $\sigma_{3c}$ ), and the diameter of the circle represents the principal stress difference at the time of failure ( $\sigma_{1f} - \sigma_{3f}$ ) as shown in Fig. 3.8. The "Mohr's" circles and corresponding failure envelopes constructed using such circles are referred to in most textbooks and

much of the literature as "total stress" circles and envelopes, respectively. However, this nomenclature is not correct inasmuch as the minor principal stress is the effective stress at the time of consolidation, while the diameter of the circle represents values at failure. The stresses being used are not actually total stresses nor do they occur simultaneously; the stresses are not associated with a given state of stress. Circles like the ones plotted for the R envelope are only valid Mohr's circles when the stresses occur at the same instant. The circles would be a valid representation of the total stresses at failure provided that no back pressure is used in the laboratory test or no pore pressure exists in the field. This is seldom the case and, thus, the circles in general are invalid. For the remainder of this paper circles like the one shown in Fig. 3.8 will be referred to as "circles of stress," rather than Mohr's circles.

Although the circles of stress on which the R envelope is based have no fundamental basis, the envelope which is drawn tangent to the circles may possess close similarity to the line representing the relationship between  $\tau_{ff}$  and  $\bar{\sigma}_{fc}$  for the case of isotropic consolidation. The similarity can be illustrated by referring to Fig. 3.9. The circle of stress shown is the one normally constructed for obtaining the R envelope. Line A-A' is drawn tangent to the circle to represent an R envelope (Only one circle is shown for clarity, although several circles are required to draw the failure envelope). The stresses on the failure plane at consolidation,  $\sigma_{fc}$  (=  $\sigma_{3c}$  in the case of isotropic consolidation) and the shear stress on the failure plane at failure,  $\tau_{ff}$ , are also indicated in this figure. Finally the line B-B' is shown drawn through points with the coordinates  $\tau_{ff}$ ,  $\sigma_{fc}$ . It can be

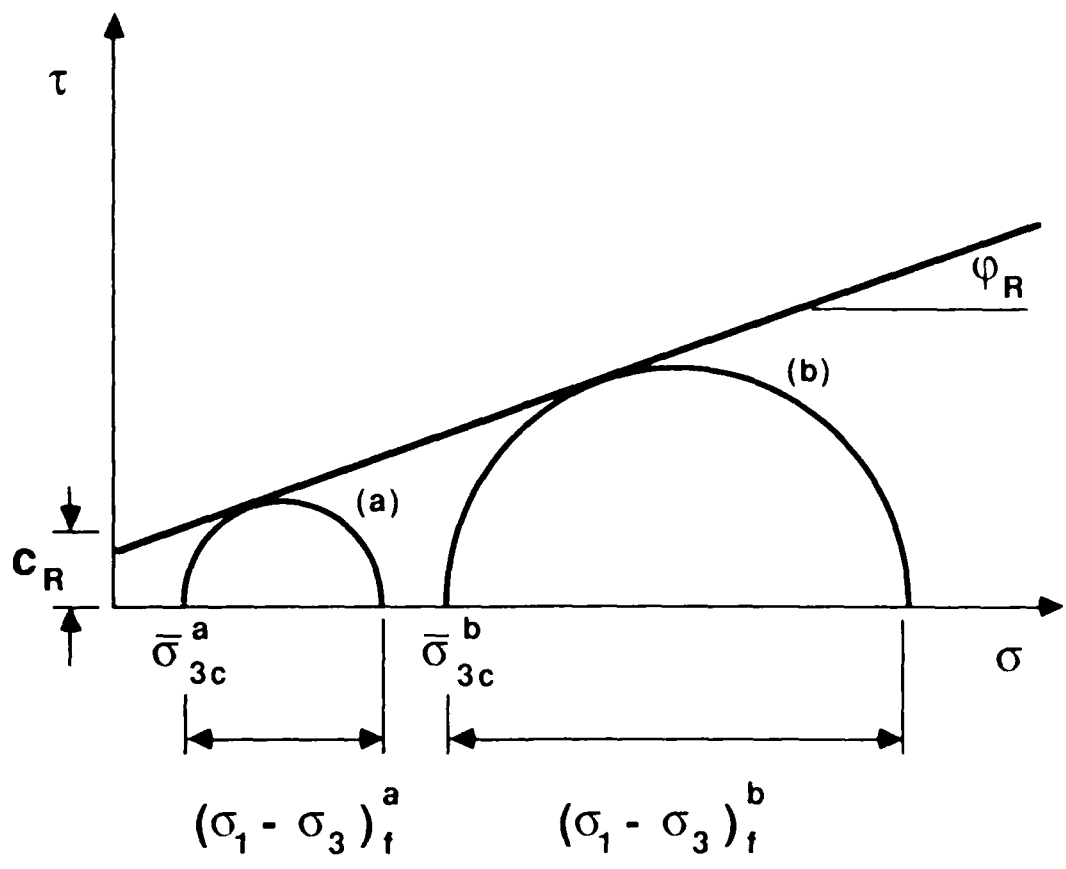


Figure 3.8 - Circles of Stress and the Corresponding R-Envelopes

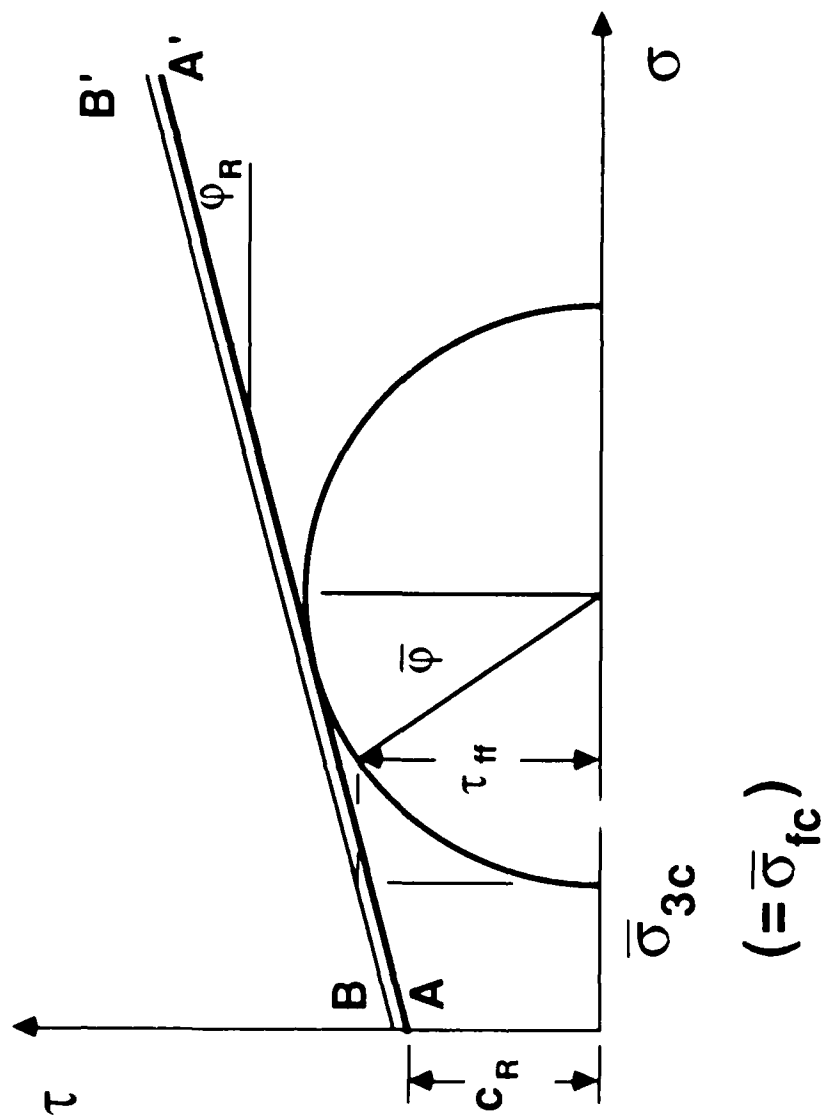


Figure 3. Relationship between the R-envelope and the Line Representing the Relationship between  $\tau_H$  and  $\tau_{fc}$  for Isotropic Consolidation

seen that the lines A-A' and B-B' are similar. In order to examine the degree to which the two lines are similar to one another a series of calculations were performed in which the slope and intercept values for the R envelope were compared with the corresponding values for the line representing the relationship between  $\tau_{ff}$  and  $\bar{c}_{fc}$ . The intercept ( $\tau_0$ ) and slope angle ( $\theta_T$ ) for the line representing the relationship between  $\tau_{ff}$  and  $\bar{c}_{fc}$  are related to the intercept and slope of the R envelope,  $c_R$  and  $\phi_R$ , respectively, and the value of the effective stress friction angle,  $\phi$ : The intercept,  $\tau_0$ , is given by,

$$\tau_0 \text{ (intercept)} = c_R N_\phi \cos \phi \quad 3.6$$

and the slope angle,  $\theta_T$ , is given by..

$$\theta_T \text{ (slope angle)} = \tan^{-1} \left[ \frac{1}{2} (N_\phi - 1) \cos \phi \right] \quad 3.7$$

where,

$$N_\phi = \tan^2 \left( 45 + \frac{\phi_R}{2} \right) \quad 3.8$$

Values of the intercept and slope of the  $\tau_{ff}-\bar{c}_{fc}$  line are shown for a relatively wide range in values of  $c_R$ ,  $\phi_R$  and  $\phi$  in Table 3.1. The percentage difference between the intercept of the  $\tau_{ff}-\bar{c}_{fc}$  line,  $\tau_0$ , and the "cohesion",  $c_R$ , for the R-envelope, and the corresponding differences in the slope angles,  $\theta_T$  and  $\phi_R$  for the two envelopes are also shown. The differences shown are independent of the cohesion value ( $c_R$ ) and become larger (and increasingly positive) as the difference between the friction angles,  $\phi_R$  and  $\phi$ , increases. Differences of almost 30 percent in magnitude may occur. The R envelope will yield lower strengths than the  $\tau_{ff}-\bar{c}_{fc}$  line for the majority of cases illustrated. However, there are at least some cases ( $\phi_R = 15$  degrees,  $\phi = 45$  degrees) where the R envelope may yield higher strengths. Accordingly, it is not entirely evident that the Corps of Engineers procedure which uses the R

TABLE 3.1

COMPARISON OF THE SLOPE AND INTERCEPT FOR THE  $\tau_{ff} - \bar{\sigma}_{fc}$  ENVELOPES  
WITH THE STRENGTH PARAMETERS FROM THE R ENVELOPE ( $c_R$  and  $\phi_R$ )

| $c_R$<br>(psf) | $\phi_R$<br>(degs) | $\bar{\phi}$<br>(degs) | $\tau_0$<br>(psf) | $\theta_\tau$<br>(degs) | $\frac{c_R - \tau_0}{\tau_0}$<br>(%) | $\frac{\phi_R - \theta_\tau}{\theta_\tau}$<br>(%) |
|----------------|--------------------|------------------------|-------------------|-------------------------|--------------------------------------|---|
| 50             | 10                 | 25                     | 54.0              | 10.8                    | -7.4                                 | -7.3  |
| 300            | 10                 | 25                     | 324.0             | 10.8                    | -7.4                                 | -7.3  |
| 700            | 10                 | 25                     | 756.1             | 10.8                    | -7.4                                 | -7.3  |
| 1000           | 10                 | 25                     | 1080.1            | 10.8                    | -7.4                                 | -7.3  |
| 3000           | 10                 | 25                     | 3240.3            | 10.8                    | -7.4                                 | -7.3  |
| 50             | 20                 | 25                     | 64.7              | 25.2                    | -22.7                                | -20.7   |
| 300            | 20                 | 25                     | 388.3             | 25.2                    | -22.7                                | -20.7   |
| 700            | 20                 | 25                     | 906.0             | 25.2                    | -22.7                                | -20.7   |
| 1000           | 20                 | 25                     | 1294.3            | 25.2                    | -22.7                                | -20.7   |
| 3000           | 20                 | 25                     | 3883.0            | 25.2                    | -22.7                                | -20.7   |
| 50             | 10                 | 35                     | 48.8              | 9.8                     | 2.4                                  | 2.4   |
| 300            | 10                 | 35                     | 292.9             | 9.8                     | 2.4                                  | 2.4   |
| 700            | 10                 | 35                     | 683.4             | 9.8                     | 2.4                                  | 2.4   |
| 1000           | 10                 | 35                     | 976.2             | 9.8                     | 2.4                                  | 2.4   |
| 3000           | 10                 | 35                     | 2928.7            | 9.8                     | 2.4                                  | 2.4   |
| 50             | 20                 | 35                     | 58.5              | 23.1                    | -14.5                                | -13.3   |
| 300            | 20                 | 35                     | 351.0             | 23.1                    | -14.5                                | -13.3   |
| 700            | 20                 | 35                     | 818.9             | 23.1                    | -14.5                                | -13.3   |
| 1000           | 20                 | 35                     | 1169.9            | 23.1                    | -14.5                                | -13.3   |
| 3000           | 20                 | 35                     | 3509.6            | 23.1                    | -14.5                                | -13.3   |
| 50             | 30                 | 35                     | 70.9              | 39.3                    | -29.5                                | -23.7   |
| 300            | 30                 | 35                     | 425.6             | 39.3                    | -29.5                                | -23.7   |
| 700            | 30                 | 35                     | 993.2             | 39.3                    | -29.5                                | -23.7   |
| 1000           | 30                 | 35                     | 1418.8            | 39.3                    | -29.5                                | -23.7   |
| 3000           | 30                 | 35                     | 4256.4            | 39.3                    | -29.5                                | -23.7   |
| 50             | 10                 | 45                     | 42.1              | 8.5                     | 18.7                                 | 18.3  |
| 300            | 10                 | 45                     | 252.8             | 8.5                     | 18.7                                 | 18.3  |
| 700            | 10                 | 45                     | 589.9             | 8.5                     | 18.7                                 | 18.3  |
| 1000           | 10                 | 45                     | 842.7             | 8.5                     | 18.7                                 | 18.3  |
| 3000           | 10                 | 45                     | 2528.1            | 8.5                     | 18.7                                 | 18.3  |
| 50             | 20                 | 45                     | 50.5              | 20.2                    | -1.0                                 | -0.9  |
| 300            | 20                 | 45                     | 303.0             | 20.2                    | -1.0                                 | -0.9  |
| 700            | 20                 | 45                     | 706.9             | 20.2                    | -1.0                                 | -0.9  |
| 1000           | 20                 | 45                     | 1009.9            | 20.2                    | -1.0                                 | -0.9  |
| 3000           | 20                 | 45                     | 3029.6            | 20.2                    | -1.0                                 | -0.9  |
| 50             | 30                 | 45                     | 61.2              | 35.3                    | -18.4                                | -14.9   |
| 300            | 30                 | 45                     | 367.4             | 35.3                    | -18.4                                | -14.9   |
| 700            | 30                 | 45                     | 857.3             | 35.3                    | -18.4                                | -14.9   |
| 1000           | 30                 | 45                     | 1224.7            | 35.3                    | -18.4                                | -14.9   |
| 3000           | 30                 | 45                     | 3674.2            | 35.3                    | -18.4                                | -14.9   |

envelope will always be more conservative than Lowe and Karafiath's procedure, which uses the more correct  $\tau_{ff}-\bar{\sigma}_{fc}$  line. The differences between the two procedures will depend on the values of  $\phi_R$  and  $\bar{\sigma}$  as well as on the effective principal stress ratio ( $K_c$ ) in the case of Lowe and Karafiath's procedure.

It is fortuitous that the R envelope and the line representing the relationship between  $\tau_{ff}$  and  $\bar{\sigma}_{fc}$  are as similar as they are over a broad range of values. This close similarity was recognized by Johnson (1974) and provided a portion of the the rationale for adoption of the R envelope in the Corps of Engineers' procedure. The numerical comparisons presented in Table 3.1 suggest that the R envelope should generally lead to conservative estimates of shear strength relative to the fundamentally more correct  $\tau_{ff}$  vs.  $\bar{\sigma}_{fc}$  relationship, although exceptions to this are also shown.

R envelope construction. At least two different criteria appear to be currently used in constructing the R envelope from a series of consolidated-undrained triaxial shear tests. The first criterion is the one utilized above and consists of drawing the failure envelope tangent to the circles of stress as illustrated previously in Fig. 3.8. The second criterion consists of constructing the envelope by drawing a line through points on the circle of stress corresponding to stresses on the failure plane as shown in Fig. 3.10. The Corps of Engineer's Stability Manual suggests that both approaches are used: Envelopes are drawn tangent to the circles of stress in the case of "undisturbed" soil and through points corresponding to stresses on the failure plane in the case of "compacted" soil. Wong, Duncan and Lee (1970) appear to have considered the R envelopes to be drawn through points on the failure plane.

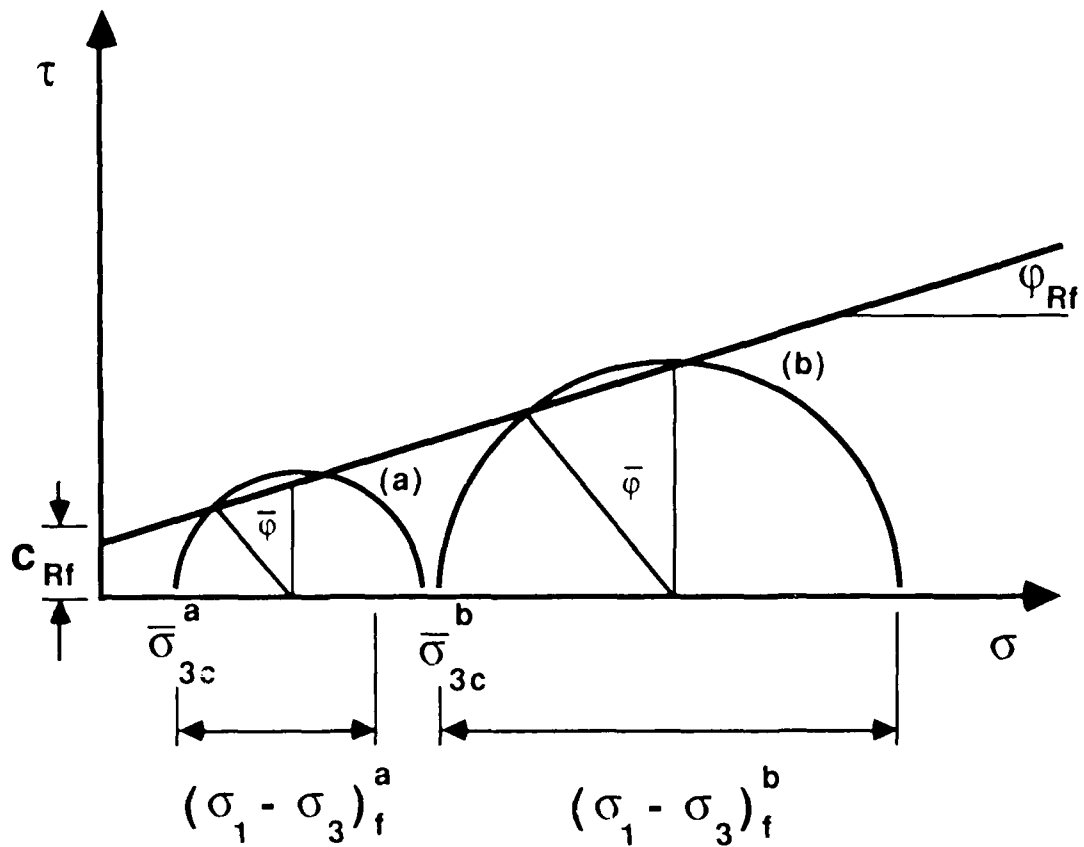


Figure 3.10 - R-Envelope Constructed through Points Corresponding to Stresses on the Failure Plane

stresses on the failure plane. Many textbooks show the R envelope (consolidated-undrained "total stress envelope") as apparently being drawn tangent to the circles of stress (e. g. Sowers, 1979; Holtz and Kovacs, 1981; Terzaghi and Peck, 1967). There does not appear to be any universally accepted procedure for constructing R envelopes and there probably never will be due to the rather arbitrary nature of the envelope.

The relationship between the intercepts and slopes of R envelopes drawn tangent to the circles of stress and drawn through points corresponding to the stresses on the failures plane can be derived theoretically. The relationship between the "cohesion" intercepts is given by,

$$c_{Rf} = c_R \frac{\cos \bar{\phi} \cos \phi_R}{1 - \sin \bar{\phi} \sin \phi_R} \quad 3.9$$

where,  $c_{Rf}$  represents the intercept of the envelope drawn through points corresponding to stresses on the failure plane,  $c_R$  and  $\phi_R$  represent the intercept and slope, respectively, of the envelope drawn tangent to the circles of stress, and  $\bar{\phi}$  is the effective stress friction angle. The relationship between the "friction angles" is given by,

$$\phi_{Rf} = \tan^{-1} \left[ \frac{\cos \bar{\phi} \sin \phi_R}{1 - \sin \bar{\phi} \sin \phi_R} \right] \quad 3.10$$

where,  $\phi_{Rf}$  represents the slope of the envelope drawn through points corresponding to stresses on the failure plane. Values of  $c_{Rf}$  and  $\phi_{Rf}$  are shown in Table 3.2 for a range in values of  $c_R$ ,  $\phi_R$  and  $\phi$ . The percentage differences between the two sets of intercepts ( $c_R$  and  $c_{Rf}$ ) and the two sets of slopes ( $\phi_R$  and  $\phi_{Rf}$ ) are also shown in this table. The differences, expressed as percentages are independent of the

TABLE 3.2

COMPARISON OF THE SHEAR STRENGTH PARAMETERS FOR R-ENVELOPES DRAWN TANGENT TO CIRCLES OF STRESS ( $c_R$ ,  $\phi_R$ ) AND R-ENVELOPES DRAWN THROUGH POINTS CORRESPONDING TO STRESSES ON THE FAILURE PLANE ( $c_{Rf}$ ,  $\phi_{Rf}$ )

| $c_R$ | $\phi_R$ | $\bar{\phi}$ | $c_{Rf}$ | $\phi_{Rf}$ | $\frac{c_{Rf} - c_R}{c_R}$ | $\frac{\phi_{Rf} - \phi_R}{\phi_R}$ |
|-------|----------|--------------|----------|-------------|----------------------------|-------------------------------------|
| (psf) | (degs)   | (degs)       | (psf)    | (degs)      | (%)                        | (%)                                 |
| 50    | 10       | 25           | 48.2     | 9.6         | -3.8                       | -3.7                                |
| 300   | 10       | 25           | 289.0    | 9.6         | -3.8                       | -3.7                                |
| 700   | 10       | 25           | 674.3    | 9.6         | -3.8                       | -3.7                                |
| 1000  | 10       | 25           | 963.2    | 9.6         | -3.8                       | -3.7                                |
| 3000  | 10       | 25           | 2889.7   | 9.6         | -3.8                       | -3.7                                |
| 50    | 20       | 25           | 49.8     | 19.9        | -0.4                       | -0.4                                |
| 300   | 20       | 25           | 298.7    | 19.9        | -0.4                       | -0.4                                |
| 700   | 20       | 25           | 696.9    | 19.9        | -0.4                       | -0.4                                |
| 1000  | 20       | 25           | 995.6    | 19.9        | -0.4                       | -0.4                                |
| 3000  | 20       | 25           | 2986.7   | 19.9        | -0.4                       | -0.4                                |
| 50    | 10       | 35           | 44.8     | 9.0         | -11.6                      | -11.4                               |
| 300   | 10       | 35           | 268.8    | 9.0         | -11.6                      | -11.4                               |
| 700   | 10       | 35           | 627.2    | 9.0         | -11.6                      | -11.4                               |
| 1000  | 10       | 35           | 895.9    | 9.0         | -11.6                      | -11.4                               |
| 3000  | 10       | 35           | 2687.8   | 9.0         | -11.6                      | -11.4                               |
| 50    | 20       | 35           | 47.9     | 19.2        | -4.4                       | -4.1                                |
| 300   | 20       | 35           | 287.3    | 19.2        | -4.4                       | -4.1                                |
| 700   | 20       | 35           | 670.3    | 19.2        | -4.4                       | -4.1                                |
| 1000  | 20       | 35           | 957.6    | 19.2        | -4.4                       | -4.1                                |
| 3000  | 20       | 35           | 2872.8   | 19.2        | -4.4                       | -4.1                                |
| 50    | 30       | 35           | 49.7     | 29.9        | -0.5                       | -0.4                                |
| 300   | 30       | 35           | 298.4    | 29.9        | -0.5                       | -0.4                                |
| 700   | 30       | 35           | 696.3    | 29.9        | -0.5                       | -0.4                                |
| 1000  | 30       | 35           | 994.7    | 29.9        | -0.5                       | -0.4                                |
| 3000  | 30       | 35           | 2984.0   | 29.9        | -0.5                       | -0.4                                |
| 50    | 10       | 45           | 39.7     | 8.0         | -26.0                      | -25.5                               |
| 300   | 10       | 45           | 238.2    | 8.0         | -26.0                      | -25.5                               |
| 700   | 10       | 45           | 555.7    | 8.0         | -26.0                      | -25.5                               |
| 1000  | 10       | 45           | 793.8    | 8.0         | -26.0                      | -25.5                               |
| 3000  | 10       | 45           | 2381.5   | 8.0         | -26.0                      | -25.5                               |
| 50    | 20       | 45           | 43.8     | 17.7        | -14.1                      | -13.0                               |
| 300   | 20       | 45           | 262.9    | 17.7        | -14.1                      | -13.0                               |
| 700   | 20       | 45           | 613.5    | 17.7        | -14.1                      | -13.0                               |
| 1000  | 20       | 45           | 876.4    | 17.7        | -14.1                      | -13.0                               |
| 3000  | 20       | 45           | 2629.3   | 17.7        | -14.1                      | -13.0                               |
| 50    | 30       | 45           | 47.4     | 28.7        | -5.6                       | -4.6                                |
| 300   | 30       | 45           | 284.2    | 28.7        | -5.6                       | -4.6                                |
| 700   | 30       | 45           | 663.1    | 28.7        | -5.6                       | -4.6                                |
| 1000  | 30       | 45           | 947.3    | 28.7        | -5.6                       | -4.6                                |
| 3000  | 30       | 45           | 2841.9   | 28.7        | -5.6                       | -4.6                                |

cohesion values and increase as the difference between the friction angle from the R envelope,  $\phi_R$ , and the effective stress envelope,  $\bar{\phi}$ , increase. Differences of over 25 percent are shown in the extreme case ( $\phi_R = 10$  degrees,  $\bar{\phi} = 45$  degrees).

Use of an R envelope which is drawn through points on the circles of stress corresponding to stresses on the failure plane appears to be unnecessarily conservative in instances when the envelope is to then be used to represent the relationship between  $\tau_{ff}$  and  $\bar{\sigma}_{fc}$ . The combined effect of constructing the R envelope through points representing stresses on the failure plane and using the envelope to express the relationship between  $\tau_{ff}$  and  $\bar{\sigma}_{fc}$  will be to underestimate the undrained shear strength in almost all cases. This underestimate coupled with the additional conservatism associated with the use of isotropic consolidation and an envelope representing a minimum of the R-S strengths appears to excessively compound conservatism.

## SECTION 4

### ESTIMATION OF ACU STRENGTH ENVELOPES FROM ICU TESTS

(Wright)

Lowe and Karafiath's (1960a) procedure employs a series of envelopes, each envelope corresponding to a particular effective principal stress ratio at consolidation,  $K_c (= \bar{\sigma}_{1c}/\bar{\sigma}_{3c})$ . Such envelopes may be obtained by performing several series of consolidated-undrained triaxial shear tests employing anisotropic stress for consolidation and with each series of tests being performed at a selected effective principal stress ratio. Testing of this type is laborious, expensive and often the scatter among results at different effective principal stress ratios leads to considerable uncertainty in the strength envelopes even after extensive testing has been completed. As an alternative several procedures have been proposed for estimating the ACU envelopes from the results of ICU triaxial shear tests. Wong, Duncan and Seed (1983) examined the available procedures for estimating the strength envelopes from the results of tests employing isotropic consolidation. They also compared the differences among the failure envelopes using data obtained from a series of tests performed on the soil from Hirfanli Dam and presented by Lowe and Karafiath (1960b).

The various procedures for estimating the undrained shear strength for anisotropic consolidation from the results of tests employing isotropic consolidation are briefly restated in this chapter. The appropriate equations used to estimate the failure envelopes for various values of the effective principal stress ratio for anisotropic consolidation are included. Most of these equations were originally

presented by Wong, Duncan and Seed (1983). In several cases they considered the effective cohesion,  $\bar{c}$ , to be zero; in other cases non-zero cohesion was accounted for. All of the equations presented herein for the various procedures have been derived for the case where an effective cohesion value may exist. The equations presented by Wong, Duncan and Seed also were all based on the assumption that the R envelope passes through points on the circles of stress corresponding to stresses on the failure plane rather than being tangent to the circles of stress. The convention used by Wong, Duncan and Seed has been retained for this section of the report to permit the work in this report to be compared to their earlier work.

Useful insight into the various procedures for estimating failure envelopes for anisotropic consolidation was gained during this study by examining the values of Skempton's pore pressure coefficient,  $A_f$ , which are implicit in each of the interpolation procedures. In general the lower the value of the pore pressure coefficient, the higher will be the value of the corresponding undrained shear strength. The appropriate equations for computing the pore pressure coefficients were derived in conjunction with the preparation of the present paper and are also presented in this section.

Comparisons were made among both the strength envelopes ( $\tau_{ff} - \bar{\sigma}_{fc}$ ) and pore pressure coefficients for the various procedures for several different soils. These comparisons are presented at the end of this section.

#### TAYLOR'S PROCEDURE

Taylor assumed that the effective stress paths for anisotropic consolidation are coincident with the effective stress paths for

isotropic consolidation for the portion of the loading which is undrained, i. e. after consolidation. Accordingly, the undrained shear strength obtained with isotropic consolidation will be identical to the undrained shear strength obtained for any specimen which is consolidated to an effective stress state existing at any stage in the ICU test.

$\tau_{ff}$  versus  $\bar{\sigma}_{fc}$  envelopes.

Points corresponding to the  $\tau_{ff}-\bar{\sigma}_{fc}$  line for a given anisotropic consolidation stress ratio,  $K_c$ , are obtained from the effective stress paths for specimens which were isotropically consolidated by identifying the points on the stress paths where the effective principal stress ratio ( $\bar{\sigma}_1/\bar{\sigma}_3$ ) is equal to the desired stress ratio ( $K_c$ ). The effective stresses corresponding to the selected point on the effective stress path ( $\bar{\sigma}_3, \bar{\sigma}_{fc}$ ) are then considered to represent the effective stress at consolidation for the selected anisotropic consolidation stress ratio; the shear strength corresponding to the selected stress path from the isotropically consolidated specimen is then considered to also be the shear strength for the anisotropically consolidated specimen.

Taylor's procedure formally requires that the actual stress path be used to estimate the strength envelopes. However, if the effective stress path is assumed to be linear ( $\bar{A}$  is constant during shear) the envelopes for anisotropic consolidation can be estimated directly from the R envelope and effective stress shear strength parameters,  $\bar{c}$  and  $\bar{\phi}$ . To estimate the failure envelopes for a linear stress path, the effective minor principal stress at consolidation corresponding to the equivalent test with isotropic consolidation must first be found. The equivalent isotropic consolidation pressure will be termed,  $\bar{\sigma}_{3CI}$ , and can be computed by solving the following equation:

$$\bar{\sigma}_{3cI} = \bar{\sigma}_{3c} + \frac{d_1 + \frac{d_2}{\bar{\sigma}_{3cI} + d_3} [\bar{\sigma}_{3cI} (K_c - 1)]}{1 + (K_c - 1)d_1 + \frac{(K_c - 1)d_2}{\bar{\sigma}_{3cI} + d_3}} \quad 4.1$$

where,  $\bar{\sigma}_{3c}$  is the effective consolidation pressure for an anisotropically consolidated specimen and,

$$d_1 = \frac{1}{2} \cos \bar{\phi} (\cot \phi_{Rf} - \cot \bar{\phi}) \quad 4.2$$

$$d_2 = \frac{1}{2} (\bar{c} \cot \bar{\phi} - c_{Rf} \cot \phi_{Rf}) (\cos \bar{\phi} \cot \phi_{Rf} + \sin \bar{\phi} - 1) \quad 4.3$$

$$d_3 = c_{Rf} \cot \phi_{Rf} \quad 4.4$$

The undrained shear strength,  $\tau_{ff}$ , is then computed from the following equation:

$$\tau_{ff} = \frac{\bar{\sigma}_{3cI} \tan \phi_{Rf} + c_{Rf}}{1 - (1 - \sin \bar{\phi}) \tan \phi_{Rf} / \cos \bar{\phi}} \quad 4.5$$

where  $\bar{\sigma}_{3cI}$  is determined by solving Eq. 4.1.

#### Pore Pressure Coefficients, $\bar{A}_f$ .

Once the equivalent effective minor principal stress,  $\bar{\sigma}_{3cI}$ , is calculated for any values of  $\bar{\sigma}_{3c}$  (or  $\bar{\sigma}_{fc}$ ) and  $K_c$  as described above, the corresponding pore pressure coefficient can be calculated from the following equation, which is obtained for isotropic consolidation:

$$A_f = d_1 + \frac{d_2}{\bar{\sigma}_{3cI} + d_3} \quad 4.6$$

The equivalent consolidation pressure,  $\bar{\sigma}_{3cI}$ , is, again, obtained from the solution to Eq. 4.1.

#### LOWE AND KARAFIATH'S PROCEDURE

Lowe and Karafiath expressed the pore water pressures at failure by an equation of the form,

$$\Delta u_f = \psi_1 (\Delta \sigma_{1f} - \Delta \sigma_{3f}) + \psi_2$$

where " $\psi_1$ " and " $\psi_2$ " are pore pressure coefficients<sup>1</sup>. The pore pressure coefficients are determined from ICU tests and are related to the R strength parameters ( $c_{Rf}$  and  $\phi_{Rf}$ ) as follows,

$$\psi_1 = \frac{1}{2} \cos \bar{\phi} (\cot \phi_{Rf} - \cot \bar{\phi}) \quad 4.7$$

$$\psi_2 = - (c_{Rf} \cot \phi_{Rf} - \bar{c} \cot \bar{\phi}) \quad 4.8$$

Lowe and Karafiath assumed that the pore pressure coefficients " $\psi_1$ " and " $\psi_2$ " are the same for isotropic and anisotropic consolidation.

$\tau_{ff}$  versus  $\bar{\sigma}_{fc}$  envelopes.

The relationship between the undrained shear strength and the effective stress on the failure plane at consolidation is given by,

$$\tau_{ff} = \frac{\frac{2\bar{\sigma}_{fc}}{[(K_c + 1) - (K_c - 1)\sin \bar{\phi}] + \bar{c}[(1 + e_1) \cot \bar{\phi}] - e_2}{(1 + e_1) \cot \bar{\phi} + \tan \bar{\phi} - \frac{1}{\cos \bar{\phi}}}} \quad 4.9$$

where,

$$e_1 = \frac{\frac{N_{\bar{\phi}} - K_c}{1 + \sin \bar{\phi}} \psi_1}{1 + (K_c - 1)\psi_1} \quad 4.10$$

$$e_2 = \frac{\bar{c}[\cos \bar{\phi} \frac{N_{\bar{\phi}} - K_c}{1 + \sin \bar{\phi}} + 2 N_{\bar{\phi}}] \psi_1 + \psi_2}{1 + (K_c - 1)\psi_1} \quad 4.11$$

and,

$$N_{\bar{\phi}} = \tan^2(45 + \frac{\bar{\phi}}{2}) \quad 4.12$$

---

<sup>1</sup>Lowe and Karafiath originally used the designation,  $A_f$ , for  $\psi_1$ . However, the designation  $\psi_1$  has been adopted for this paper to avoid confusion with Skempton's pore pressure coefficient,  $A$ ,  $\bar{A}$ ,  $\bar{A}_f$ , etc. The parameter,  $\psi_1$ , is not equivalent to any of Skempton's pore pressure coefficients.

### Pore Pressure Coefficients, $A_f$ .

Pore pressures coefficients are calculated by first calculating the pore pressure at failure from the following equation:

$$\Delta u_f = \frac{(\bar{\sigma}_{3c} N_{\bar{\phi}} + 2\bar{c}\sqrt{N_{\bar{\phi}}} - K_c \bar{\sigma}_{3c}) \psi_1 + \psi_2}{1 - (1 - N_{\bar{\phi}}) \psi_1} \quad 4.13$$

The corresponding difference in the principal stress changes,  $\Delta\sigma_{1f} - \Delta\sigma_{3f}$ , is computed from the following equation:

$$\Delta\sigma_{1f} - \Delta\sigma_{3f} = (\bar{\sigma}_{3c} - \Delta u_f)(N_{\bar{\phi}} - 1) + 2\bar{c}\sqrt{N_{\bar{\phi}}} - \bar{\sigma}_{3c}(K_c - 1) \quad 4.14$$

The pore pressure coefficient is then obtained by dividing the change in pore pressure at failure by the difference in the principal stress changes as,

$$A_f = \frac{\Delta u_f}{\Delta\sigma_{1f} - \Delta\sigma_{3f}} \quad 4.15$$

### MODIFIED KARAFIATH PROCEDURE

This procedure was suggested by Wong, Duncan and Seed. They assumed that the relationship between Skempton's pore pressure coefficient  $A_f$  and the effective stress on the failure plane at consolidation,  $\bar{\sigma}_{fc}$ , was independent of the effective principal stress ratio at consolidation ( $K_c$ ). Accordingly, the relationship between the pore pressure coefficient and  $\bar{\sigma}_{fc}$  was uniquely defined and could be calculated from the results of tests performed on isotropically consolidated specimens.

### $\tau_{ff}$ versus $\bar{\sigma}_{fc}$ envelopes.

The following equation has been derived, expressing the relationship between the undrained shear strength,  $\tau_{ff}$ , and the effective stress on the failure plane at consolidation,  $\bar{\sigma}_{fc}$ :

$$\tau_{ff} = \frac{2\bar{\sigma}_{fc} \left[ \frac{[(K_c + 1) - (K_c - 1)\sin\bar{\phi}] + \bar{c}\cot\bar{\phi}(1 + \alpha_1) - \alpha_2}{(1 + \alpha_1)\cot\bar{\phi} + \tan\bar{\phi} - \frac{1}{\cos\bar{\phi}}} \right]}{(1 + \alpha_1)\cot\bar{\phi} + \tan\bar{\phi} - \frac{1}{\cos\bar{\phi}}} \quad 4.16$$

where,

$$\alpha_1 = \frac{A(N_\phi - K_C)}{(1 + \sin\bar{\phi})[1 + A(K_C - 1)]} \quad 4.17$$

$$\alpha_2 = \frac{A\bar{c}N_\phi [(1 - \sin\bar{\phi})K_C + 1 + \sin\bar{\phi}]}{(1 + \sin\bar{\phi})[1 + A(K_C - 1)]} \quad 4.18$$

and  $N_\phi$  is given by Eq. 4.12.

#### Pore Pressure Coefficients, $\bar{A}_f$ .

For isotropically consolidated specimens the pore pressure coefficient at failure is expressed in terms of the effective consolidation pressure,  $\bar{\sigma}_{3C}$ , the strength parameters from the R envelope,  $c_{Rf}$  and  $\phi_{Rf}$ , and the effective stress friction angle,  $\phi$ , by

$$\bar{A}_f = d_1 + \frac{d_2}{\bar{\sigma}_{3C} + d_3} \quad 4.19$$

where,  $d_1$ ,  $d_2$  and  $d_3$  are give by Eqs. 4.2, 4.3 and 4.4, respectively. Inasmuch as Eq. 4.19 is written for the case of isotropic consolidation, the consolidation pressure,  $\bar{\sigma}_{3C}$ , is also equal to the effective normal stress on the failure plane at consolidation. In the case of anisotropic consolidation Eq. 4.19 is rewritten by replacing the effective stress,  $\bar{\sigma}_{3C}$ , by the effective normal stress on the failure plane at consolidation,  $\bar{\sigma}_{fC}$ . Thus, the expression for  $\bar{A}_f$  now becomes,

$$\bar{A}_f = d_1 + \frac{d_2}{\bar{\sigma}_{fC} + d_3} \quad 4.20$$

The effective normal stress on the failure plane at consolidation in Eq. 4.20 can be expressed in terms of the effective minor principal stress at consolidation ( $\bar{\sigma}_{fC}$ ) and the effective principal stress ratio at consolidation by,

$$\bar{\sigma}_{fc} = \sigma_{3c} \left[ \frac{K_c + 1}{2} - \frac{K_c - 1}{2} \sin \phi \right] \quad 4.21$$

Thus, Eq. 4.20 can be used to calculate  $A_f$  for any values of  $\sigma_{3c}$  and  $K_c$ .

#### EXTENSION OF NOORANY AND SEED'S STUDY

This approach was first suggested by Wong, Duncan and Seed, based on earlier work of Noorany and Seed. The procedure is based on the assumption that the relationship between the pore water pressure coefficient  $A_f$  and the effective normal stress on the failure plane at consolidation is the same for isotropic and anisotropic consolidation. Accordingly, the assumptions employed in this approach are identical to those used in the Modified Khattab procedure: only the form of the algebraic equations used to compute various quantities are different.

#### $\tau_{ff}$ versus $\bar{\sigma}_{fc}$ envelopes.

The undrained shear strength is computed from:

$$\tau_{ff} = \frac{2\bar{\sigma}_{fc} \cos \phi \sin \phi [1 + A_f(K_c - 1)] + c \cos^2 \phi}{[(K_c + 1) - (K_c - 1) \sin \phi] + 1 + (2A_f - 1) \sin \phi} \quad 4.22$$

where, the pore pressure coefficient,  $A_f$ , is obtained from,

$$A_f = \frac{\cos \phi [1 - \cot(\phi) + \frac{1}{2} \tan^2 \phi_{Rf}] (\bar{\sigma}_{fc} \sin \phi + c \cos \phi) - (1 - \sin \phi)_{Rf}}{c_{Rf} + \frac{1}{2} \tan^2 \phi_{Rf}} \quad 4.23$$

Equations 4.22 and 4.23 represent extensions to the equations presented by Wong, Duncan and Seed to include an effective cohesion,  $c$ . The undrained shear strength computed from Eq. 4.22 is identical to the undrained shear strength computed from Eq. 4.16 although the two equations appear to be somewhat different.

### Pore Pressure Coefficients, $A_f$ .

The pore pressure coefficient at failure is computed from Eq. 4.23, which was given above. The pore pressure coefficients computed from Eqs. 4.20 and 4.23 are identical, although the equations are, again, somewhat different in algebraic form.

#### EXTENSION OF H. BENJAMIN'S STUDY

This procedure was also suggested by Wong, Duncan and Seed, and is based on earlier work by Benjamin (1975). The procedure is based on the assumption that the ratio of the undrained shear strength ( $s_u$ ) to effective major principal stress at consolidation ( $\bar{\sigma}_{1c}$ ) is the same for isotropic and anisotropic consolidation.

### $\tau_{ff}$ versus $\bar{\sigma}_{fc}$ envelopes.

The undrained shear strength is related to the effective stress on the failure plane at consolidation by the equation.

$$\tau_{ff} = \frac{c_{Rf} + \sigma_{fc} \frac{2 K_c \tan \bar{\phi}_{Rf}}{[(K_c + 1) - (K_c - 1) \sin \bar{\phi}]}}{[1 - \cot(45 + \frac{\bar{\phi}}{2}) \tan \phi_{Rf}]} \quad 4.24$$

### Pore Pressure Coefficients, $A_f$ .

The pore pressure coefficient,  $A_f$ , is computed by first computing the change in pore pressure at failure from the following equation:

$$\Delta u_f = \bar{\sigma}_{3c} \left( 1 - \frac{2}{\sigma_{3c} (N_\phi - 1)} + \left[ \frac{\tau_{ff}}{\cos \bar{\phi}} + \bar{c} v N_\phi \right] \right) \quad 4.25$$

The corresponding difference in the principal stress changes,  $\Delta \sigma_{1f} - \Delta \sigma_{3f}$ , is computed using the following equation:

$$\Delta \sigma_{1f} - \Delta \sigma_{3f} = \sigma_{3c} \left[ \frac{2 \tau_{ff} / \sigma_{3c}}{\cos \bar{\phi}} - (K_c - 1) \right] \quad 4.26$$

Finally, the pore pressure coefficient is computed by dividing the change in pore pressure at failure by the difference in the principal stress changes as,

$$A_f = \frac{\Delta u_f}{\Delta \sigma_{1f} - \Delta \sigma_{3f}} \quad 4.27$$

#### LINEAR INTERPOLATION PROCEDURE

The linear interpolation procedure consists of interpolating linearly between the  $\tau_{ff}-\bar{\sigma}_{fc}$  lines for isotropic consolidation ( $K_c = 1.0$ ) and for anisotropic consolidation with  $K_c = K_f$ . The envelope corresponding to anisotropic consolidation with  $K_c = K_f$ , is identical to the effective stress failure envelope determined from consolidated-drained shear tests and can be determined either from consolidated-drained tests or isotropically consolidated-undrained shear tests with pore pressure measurements.

#### $\tau_{ff}$ versus $\bar{\sigma}_{fc}$ envelopes.

Lines corresponding to intermediate consolidation stress ratios between unity and the value at failure are obtained by linearly interpolating between the lines of  $\tau_{ff}$  versus  $\bar{\sigma}_{fc}$  obtained for isotropic consolidation ( $K_c = 1.0$ ) and for the maximum permissible effective principal stress ratio, i. e. the value,  $K_f$ , at failure in a consolidated-drained shear test. The line representing the relationship between  $\tau_{ff}$  and  $\bar{\sigma}_{fc}$  for isotropic consolidation is represented by the equation,

$$\tau_{ff} = \frac{c + \bar{\sigma}_{fc} \tan \phi_{Rf}}{1 - (1 - \sin \phi) \tan \phi_{Rf} / \cos \phi} \quad 4.28$$

The line representing the relationship between  $\tau_{ff}$  and  $\bar{\sigma}_{fc}$  for anisotropic consolidation is simply the effective stress failure envelope, i. e.

$$\tau_{ff} = \bar{c} + \bar{\sigma}_{fc} \tan \bar{\phi} \quad 4.29$$

The maximum effective principal stress ratio for the effective stress failure envelope is related to the effective stress shear strength parameters and the effective normal stress on the failure plane at failure,  $\bar{\sigma}_{fc}$  (or at consolidation since  $\bar{\sigma}_{fc} = \bar{\sigma}_{ff}$ ) by the expression,

$$K_f = \tan^2(45 + \frac{\bar{\phi}}{2}) + \frac{[(K_c + 1) - (K_c - 1)\sin\bar{\phi}] \bar{c}}{\bar{\sigma}_{fc}} \tan(45 + \frac{\bar{\phi}}{2}) \quad 4.30$$

Thus, if the effective stress cohesion value,  $\bar{c}$ , is not zero, the maximum value of the effective principal stress ratio ( $K_f$ ) actually varies with the effective normal stress on the failure plane. This complicates linear interpolation in that a value of  $K_f$  must be calculated each time an interpolation is performed depending on the value of the effective normal stress on the failure plane. Duncan Wong and Seed avoided this problem in at least one instance where the effective cohesion was not zero by ignoring the cohesion and computing the effective principal stress ratio at failure from the expression,

$$K_f = \tan^2(45 + \frac{\bar{\phi}}{2}) \quad 4.31$$

By neglecting the cohesion value in computing  $K_f$  a slightly conservative estimate is made of the shear strength in the linear interpolation.

#### Pore Pressure Coefficients, $A_f$ .

Pore pressure coefficients are calculated by first determining the pore pressure at failure from the following:

$$\Delta u_f = \sigma_{3c} - \frac{2\tau_{ff}}{\cos\bar{\phi}} - \frac{2\bar{c}N_{\bar{\phi}}}{(N_{\bar{\phi}} - 1)}$$

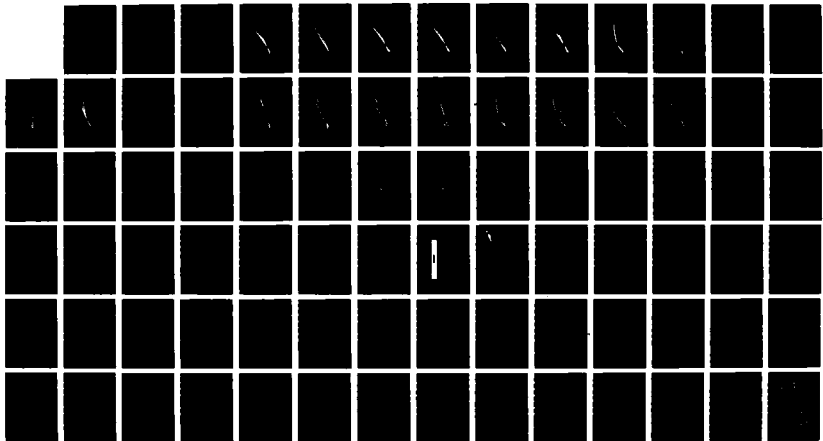
AD-R187 248

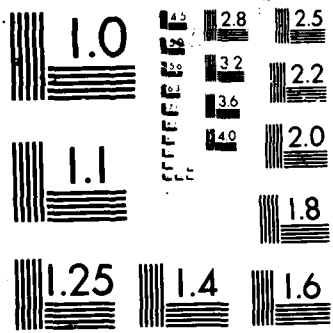
AN EXAMINATION OF SLOPE STABILITY COMPUTATION  
PROCEDURES FOR SUDDEN DRAIN. (U) ARMY ENGINEER  
WATERWAYS EXPERIMENT STATION VICKSBURG MS GEOTE.  
S G WRIGHT ET AL. SEP 87 WES/MP/QL-87-25 F/G 8/18

2/2

UNCLASSIFIED

ML





where  $\tau_{ff}$  is computed by linear interpolation and corresponds to the value of  $\bar{\sigma}_{3c}$  in this equation. (Note: the relationship between  $\bar{\sigma}_{3c}$  and  $\bar{\sigma}_{fc}$  in Eq. 4.32 is given by Eq. 4.21). The difference in the principal stress changes is computed from,

$$\Delta\sigma_{1f} - \Delta\sigma_{3f} = \frac{2\tau_{ff}}{\cos\phi} - \bar{\sigma}_{3c}(K_c - 1) \quad 4.33$$

Finally, the pore pressure coefficient,  $\bar{A}_f$ , is computed from,

$$A_f = \frac{\Delta u_f}{\Delta\sigma_{1f} - \Delta\sigma_{3f}} \quad 4.34$$

#### COMPARISON OF PROCEDURES

Undrained strength envelopes in the form of lines representing the relationship between  $\tau_{ff}$  and  $\bar{\sigma}_{fc}$  were computed using the equations presented above for several different soils. The corresponding relationships between the pore pressure coefficient,  $\bar{A}_f$  and  $\bar{\sigma}_{fc}$  were also computed and compared.

##### Pilarcitos Dam Soil

Wong, Duncan and Seed presented shear strength envelopes for sandy clay material from the upstream slope of Pilarcitos Dam. The shear strength envelopes (R and S) for this soil were curved and several sets of strength parameters were reported, depending on the range in stress over which the failure envelopes were drawn. For low stresses (0-10 psi) the following values were reported:

##### Effective stress envelope:

$$\bar{c} = 0, \bar{\phi} = 45 \text{ degrees}$$

##### R envelope:

$$c_{Rf} = 60 \text{ psf}, \phi_{Rf} = 23 \text{ degrees}$$

The first set of comparative calculations was performed using these data from Wong, Duncan and Seed.

$\tau_{ff}$  versus  $\bar{\sigma}_{fc}$  envelopes. Envelopes for anisotropic consolidation stress ratios,  $K_c$ , of 1, 2, 3, 4, 5, and 5.83 ( $= K_f$ ) are shown in Figs. 4.1 through 4.6, for Taylor's procedure, Lowe and Karafiath's procedure, the Modified Karafiath procedure, the Extension of Noorany and Seed, the Extension of Benjamin, and the linear interpolation procedure, respectively.

$\bar{A}_f$  versus  $\bar{\sigma}_{fc}$ . The variations in the pore pressures coefficients,  $\bar{A}_f$ , with the effective normal stress on the failure plane at consolidation are shown in Figs. 4.7 through 4.12, for Taylor's procedures, Lowe and Karafiath's procedure, the Modified Karafiath procedure, the Extension of Noorany and Seed, the Extension of Benjamin, and the linear interpolation procedures, respectively. The relationships are again shown for consolidation stress ratios of 1, 2, 3, 4, 5 and 5.83.

#### Other soils.

Variations in  $\tau_{ff}$  and  $\bar{A}_f$  with  $\bar{\sigma}_{fc}$  were also calculated for three additional sets (Set Nos. 2, 3 and 4) of soil properties. Data for Set No. 2 were obtained from Wong, Duncan and Seed and were based on data for a brown sandy clay from a dam site in Rio Blanco, Colorado. Data for Set No. 3 represent the values obtained from the Pilarcitos Dam referred to above for a range in stress from 0 to 100 psi. The final set, Set No. 4, of data were estimated based on data for Hirfanli Dam presented by Lowe and Karafiath (1960b). Data for the three additional sets as well as the set used previously are summarized in Table 4.1.

Taylor's procedure - Material property set 1

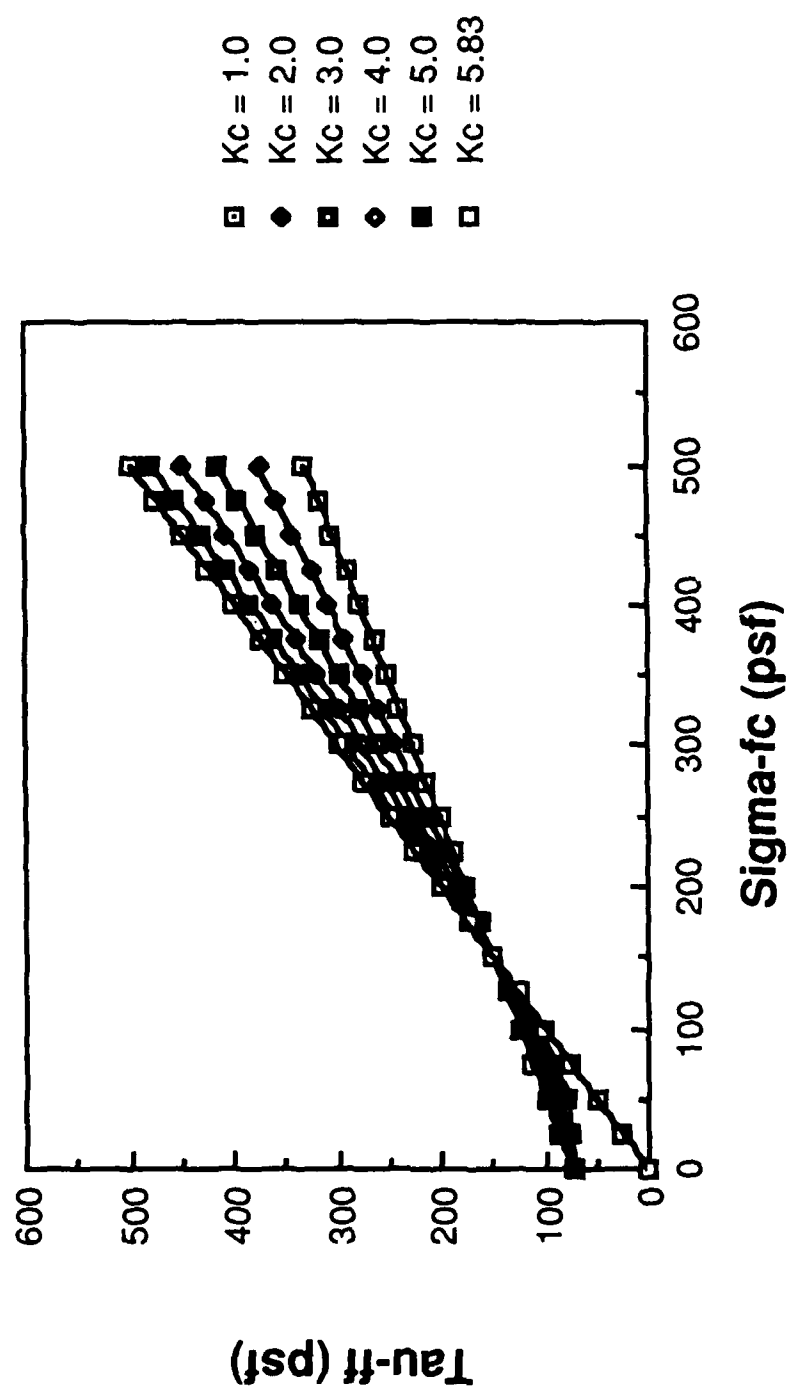


Figure 4.1 - Shear Strength Envelopes ( $\tau_{ff}$  vs.  $\sigma_{ff}$ ) for Various Effective Principal Consolidation Stress Ratios ( $K_c$ ) Estimated from Strength Parameters for Isotropic Consolidation Using Taylor's Procedure

Low & Karafiath's procedure - Material property set 1

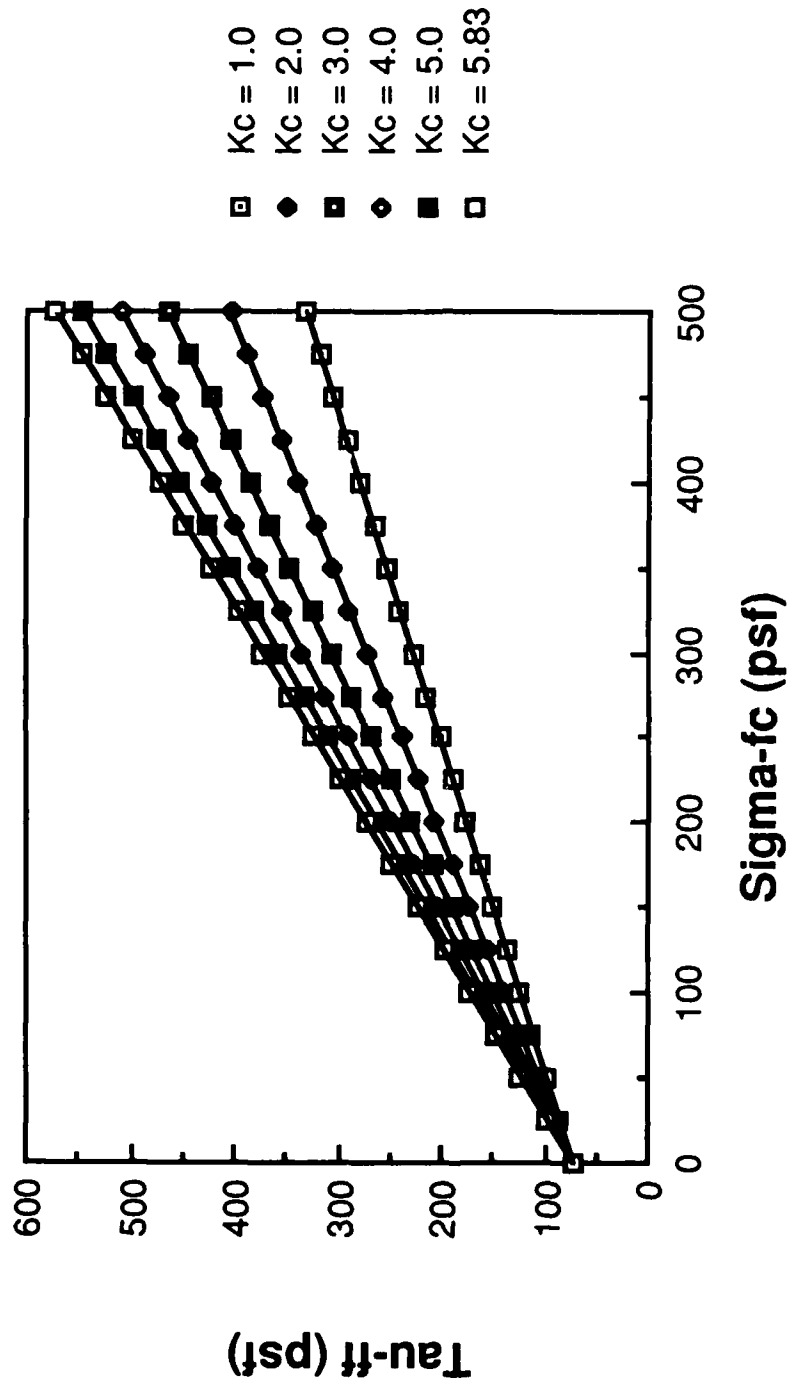


Figure 4.2 - Shear Strength Envelopes ( $\tau_{ff}$  vs.  $\bar{\sigma}_{fc}$ ) for Various Effective Principal Consolidation Stress Ratios ( $K_c$ ) Estimated from Strength Parameters for Isotropic Consolidation Using Lowe and Karafiath's Procedure

Modified Karafiath Procedure - Material property set 1

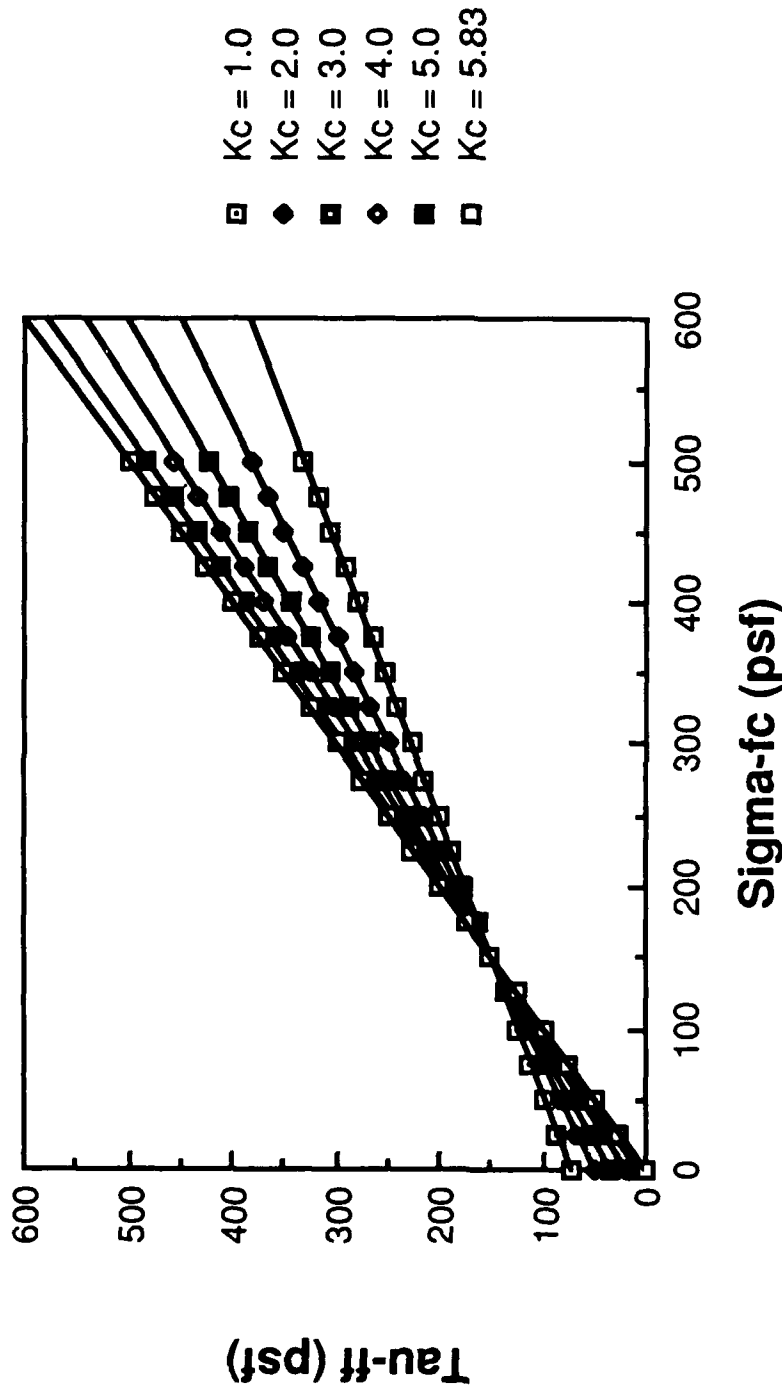


Figure 4.3 - Shear Strength Envelopes ( $\tau_{ff}$  vs.  $\bar{\sigma}_{fc}$ ) for Various Effective Principal Consolidation Stress Ratios ( $K_c$ ) Estimated from Strength Parameters for Isotropic Consolidation Using the Modified form of L6we and Karafiath's Procedure

**Extension of Noorany and Seed - Material property set 1**

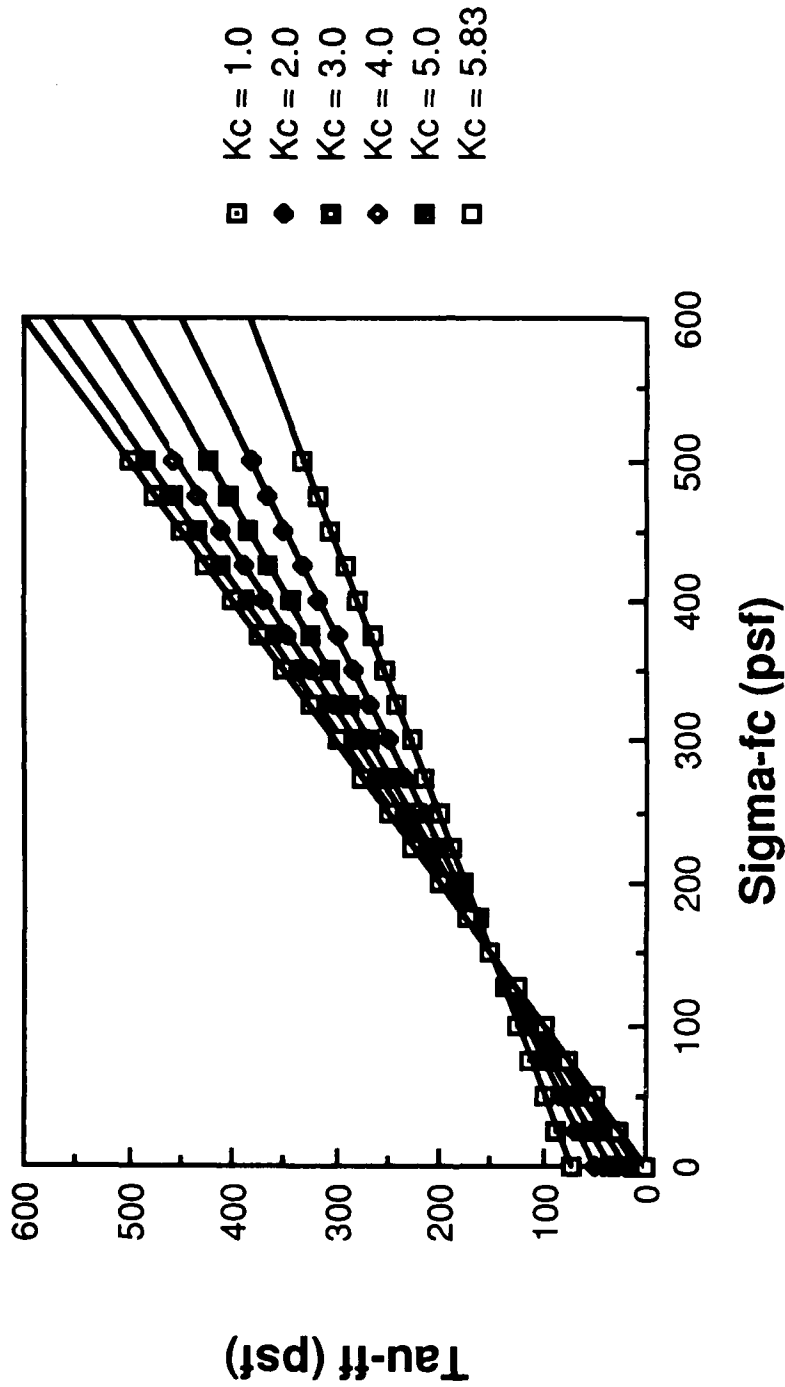


Figure 4.4 - Shear Strength Envelopes ( $\tau_{ff}$  vs.  $\bar{\sigma}_{fc}$ ) for Various Effective Principal Consolidation Stress Ratios ( $K_c$ ) Estimated from Strength Parameters for Isotropic Consolidation Using the Extension of Noorany and Seed's Procedure

Extension of Benjamin's Study - Material property set 1

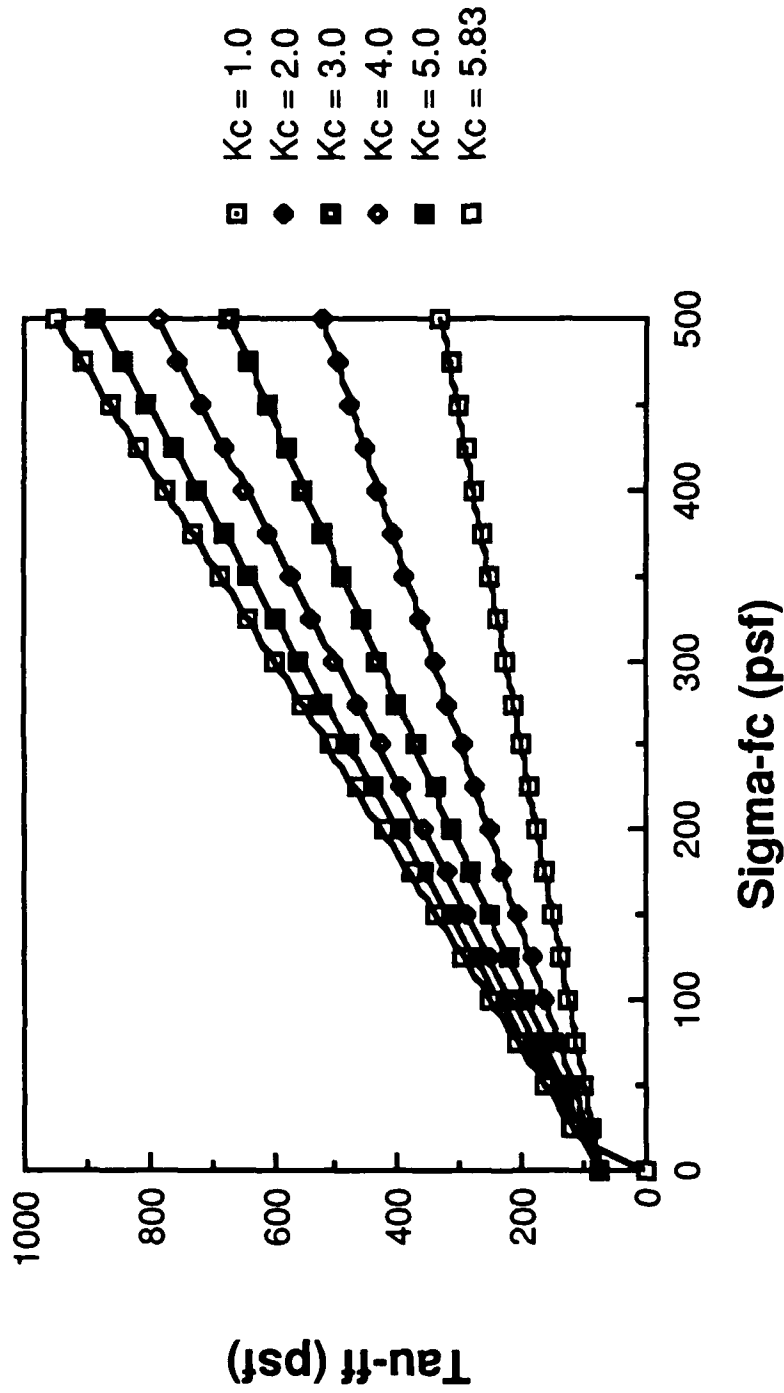


Figure 4.5 - Shear Strength Envelopes ( $\tau_{ff}$  vs.  $\bar{\sigma}_{fc}$ ) for Various Effective Principal Consolidation Stress Ratios ( $K_c$ ) Estimated from Strength Parameters for Isotropic Consolidation Using the Extension of Benjamin's Study

### Linear Interpolation - Material property set 1

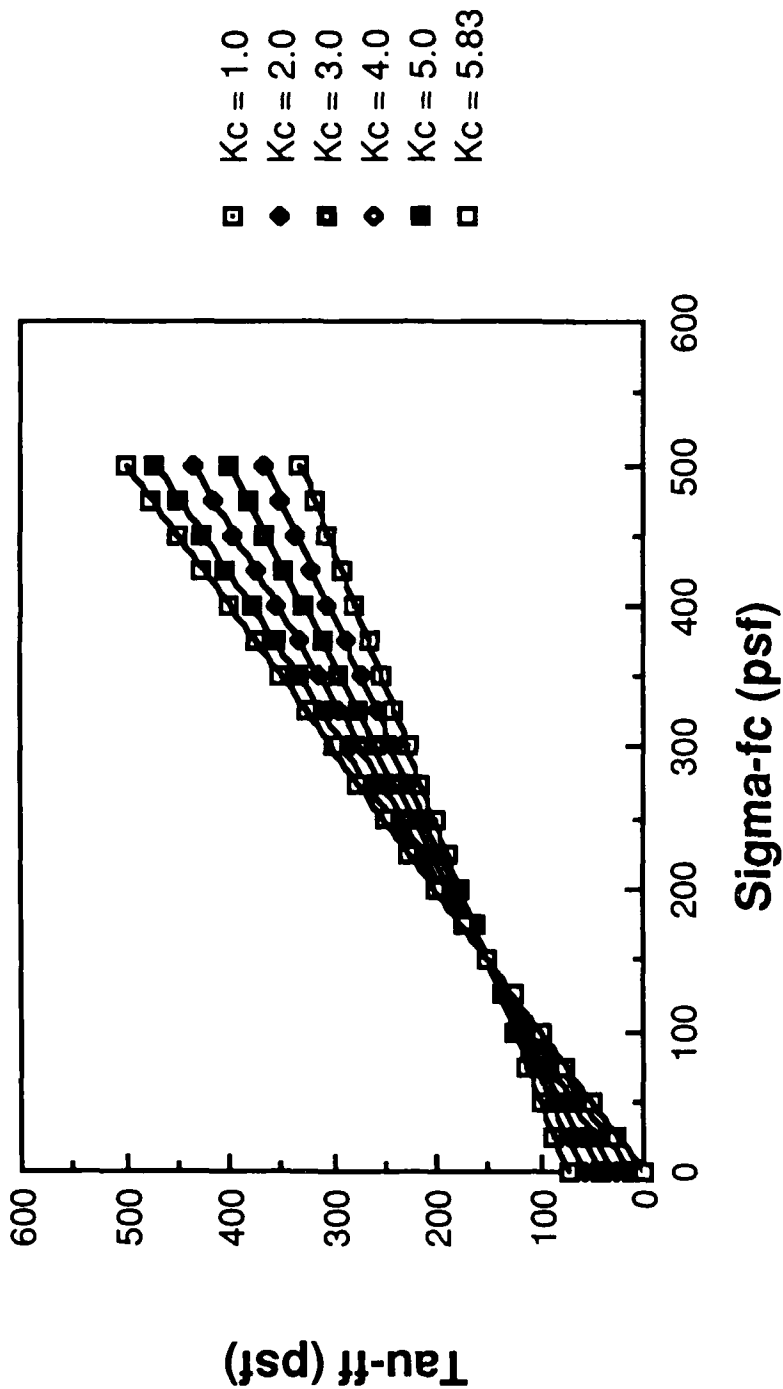


Figure 4.6 - Shear Strength Envelopes ( $\tau_{ff}$  vs.  $\sigma_{fc}$ ) for Various Effective Principal Consolidation Stress Ratios ( $K_c$ ) Estimated from Strength Parameters for Isotropic Consolidation Using Linear Interpolation

### Taylor's Procedure - Material property set 1

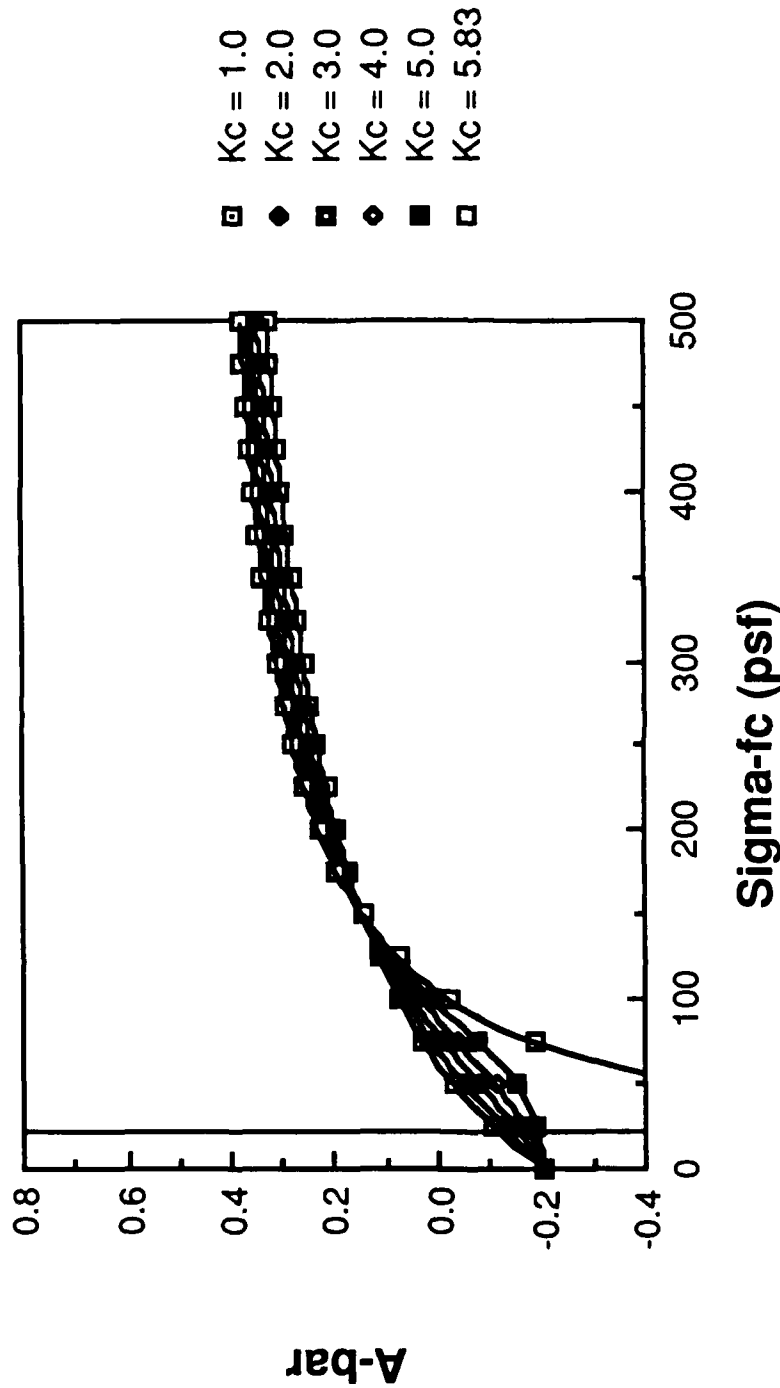


Figure 4.7 - Variation in the Pore Pressure Coefficient,  $\bar{A}_f$ , with Effective Normal Stress on the Failure Plane at Consolidation,  $\sigma_{fc}$ , for Various Effective Principal Consolidation Stress Ratios ( $K_c$ ) Estimated from Strength Parameters for Isotropic Consolidation Using Taylor's Procedure

**Low and Karafiath's Procedure - Material property set 1**

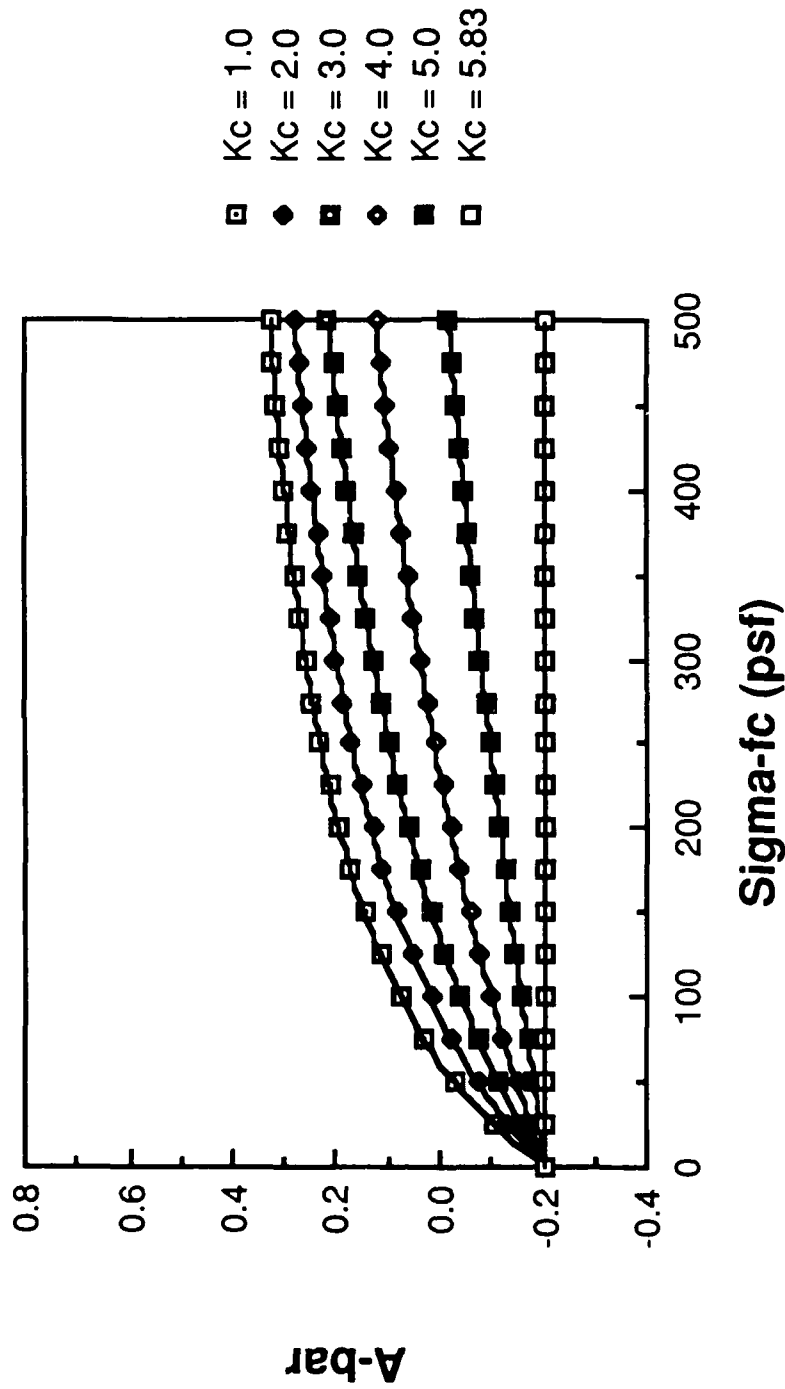


Figure 4.8 - Variation in the Pore Pressure Coefficient,  $\bar{A}_f$ , with Effective Normal Stress on the Failure Plane at Consolidation,  $\bar{\sigma}_{fc}$ , for Various Effective Principal Consolidation Stress Ratios ( $K_c$ ) Estimated from Strength Parameters for Isotropic Consolidation Using Low and Karafiath's Procedure

Modified Karafiath Procedure - Material property set 1

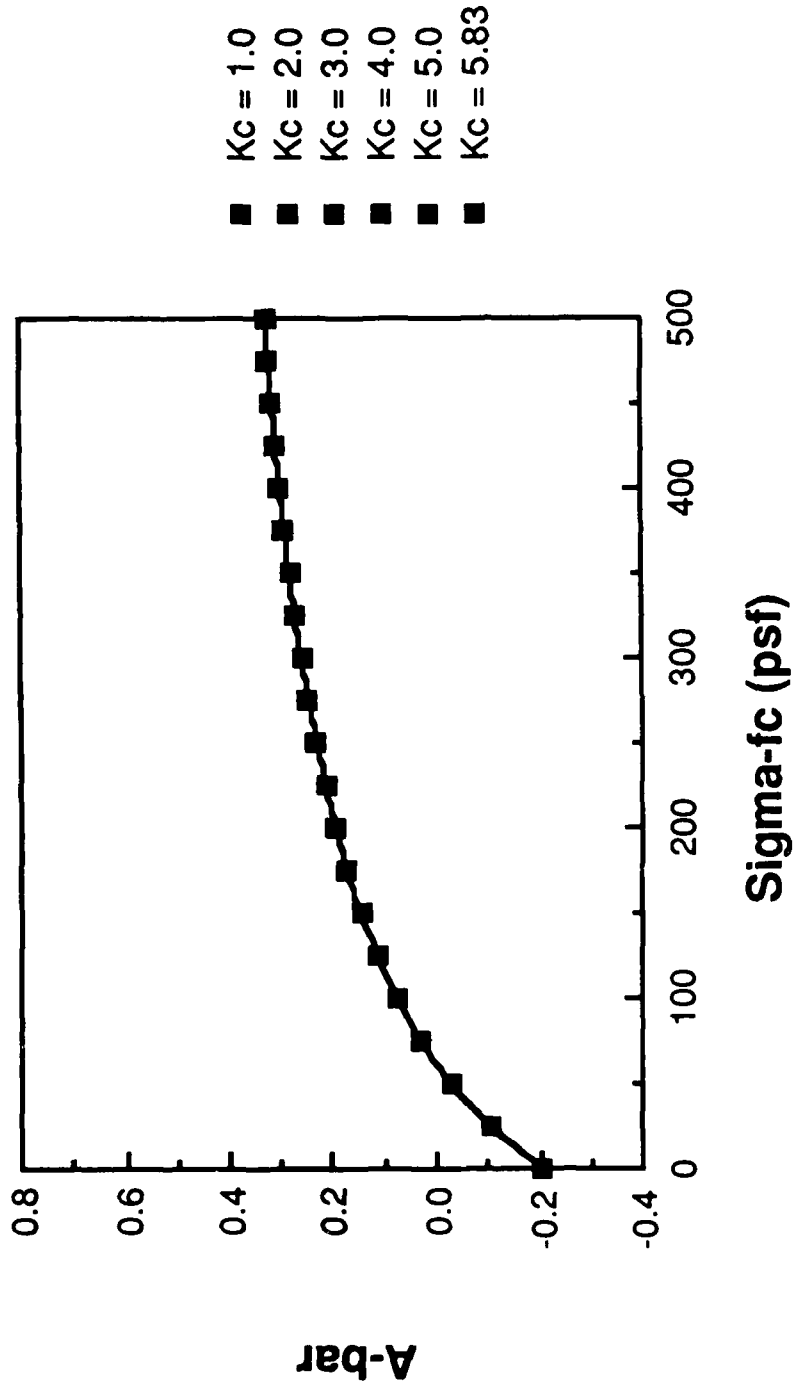


Figure 4.9 - Variation in the Pore Pressure Coefficient,  $\bar{A}_p$ , with Effective Normal Stress on the Failure Plane at Consolidation,  $\sigma_{fc}$ , for Various Effective Principal Consolidation Stress Ratios ( $K_c$ ) Estimated from Strength Parameters for Isotropic Consolidation Using the Modified Form of Lowe and Karafiath's Procedure

**Extension of Noorany and Seed - Material property set 1**

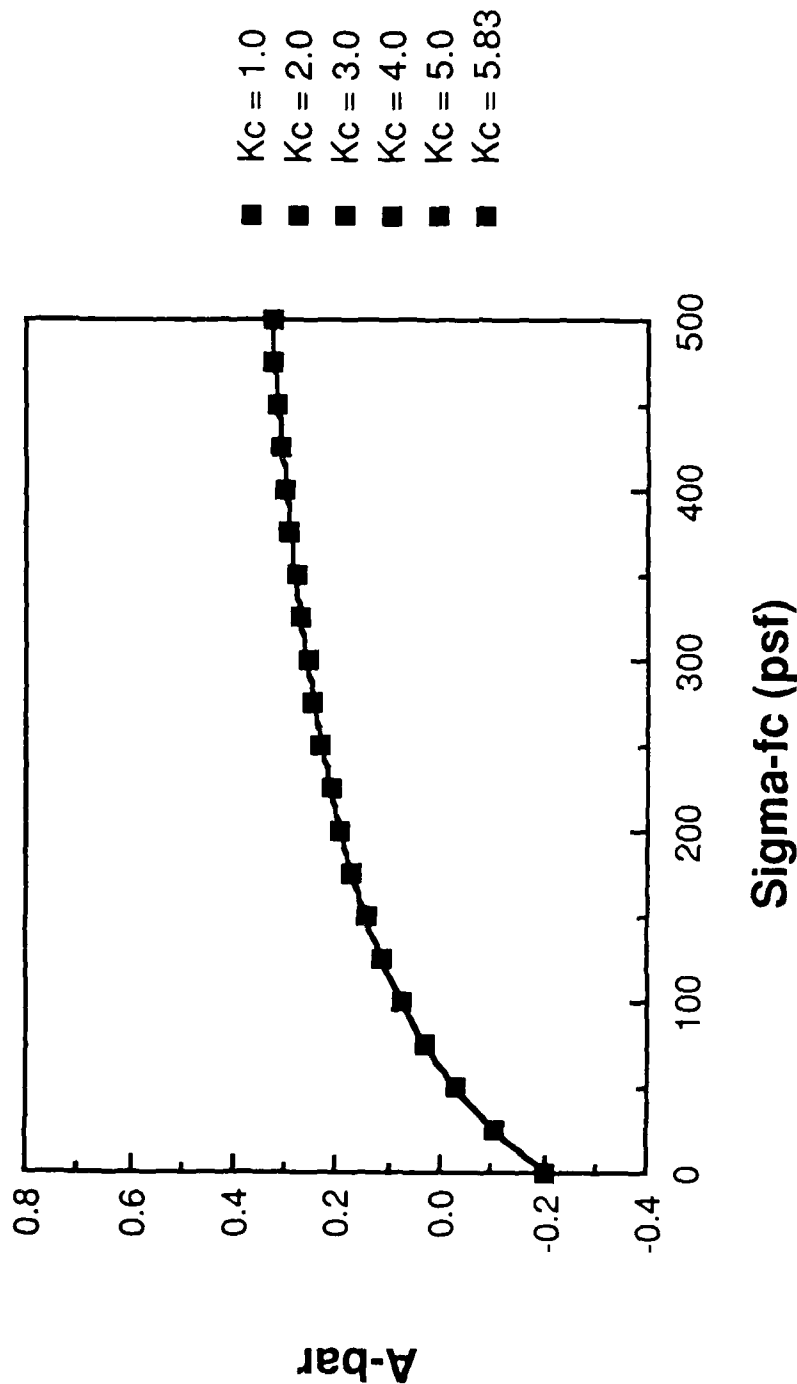


Figure 4.10 - Variation in the Pore Pressure Coefficient,  $\bar{A}_f$ , with Effective Normal Stress on the Failure Plane at Consolidation,  $\sigma_{fc}$ , for Various Effective Principal Consolidation Stress Ratios (K) Estimated from Strength Parameters for Isotropic Consolidation Using the Extension of Noorany and Seed's Procedure

### Extension of Benjamin's Study - Material property set 1

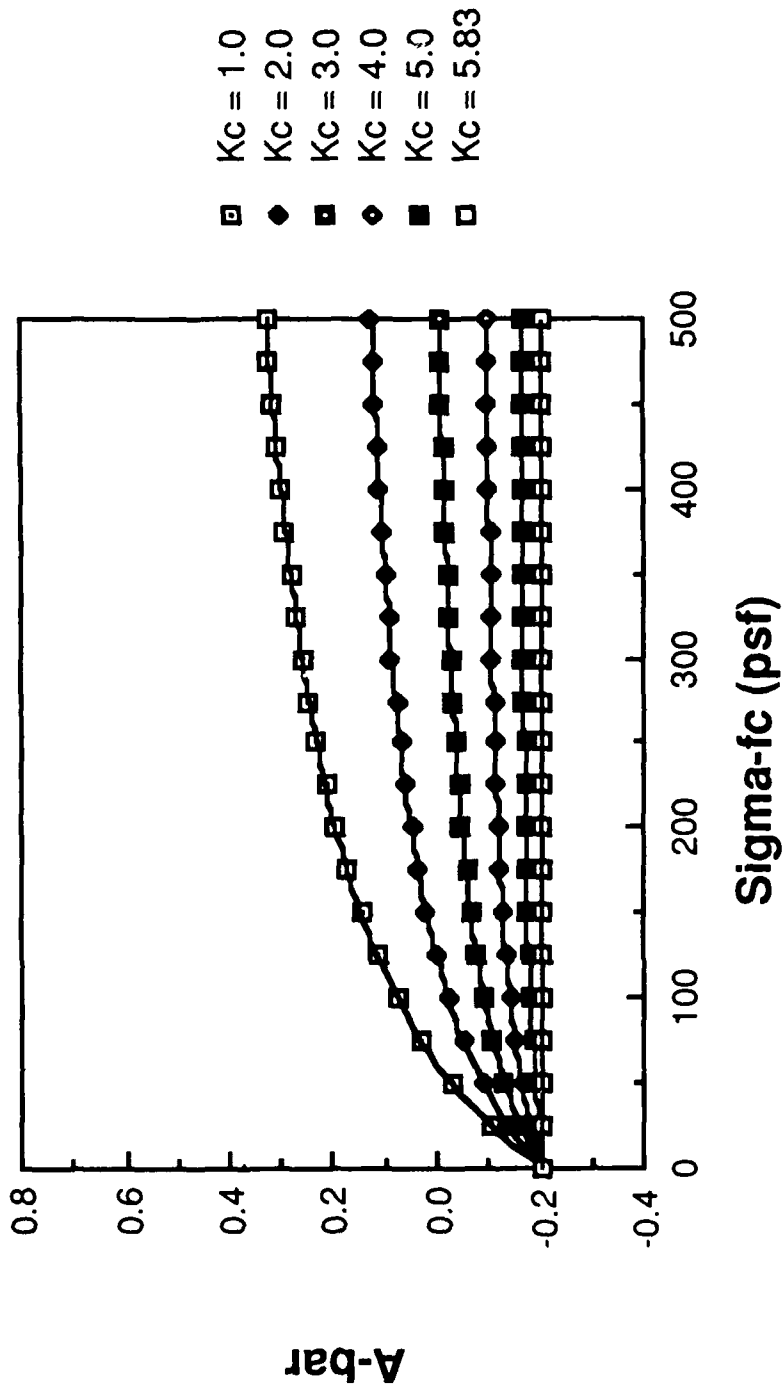


Figure 4.11 - Variation in the Pore Pressure Coefficient,  $\bar{A}_f$ , with Effective Normal Stress on the Failure Plane at Consolidation,  $\sigma_{fc}$ , for Various Effective Principal Consolidation Stress Ratios ( $K_c$ ) Estimated from Strength Parameters for Isotropic Consolidation Using the Extension of Benjamin's Study

Linear Interpolation - Material property set 1

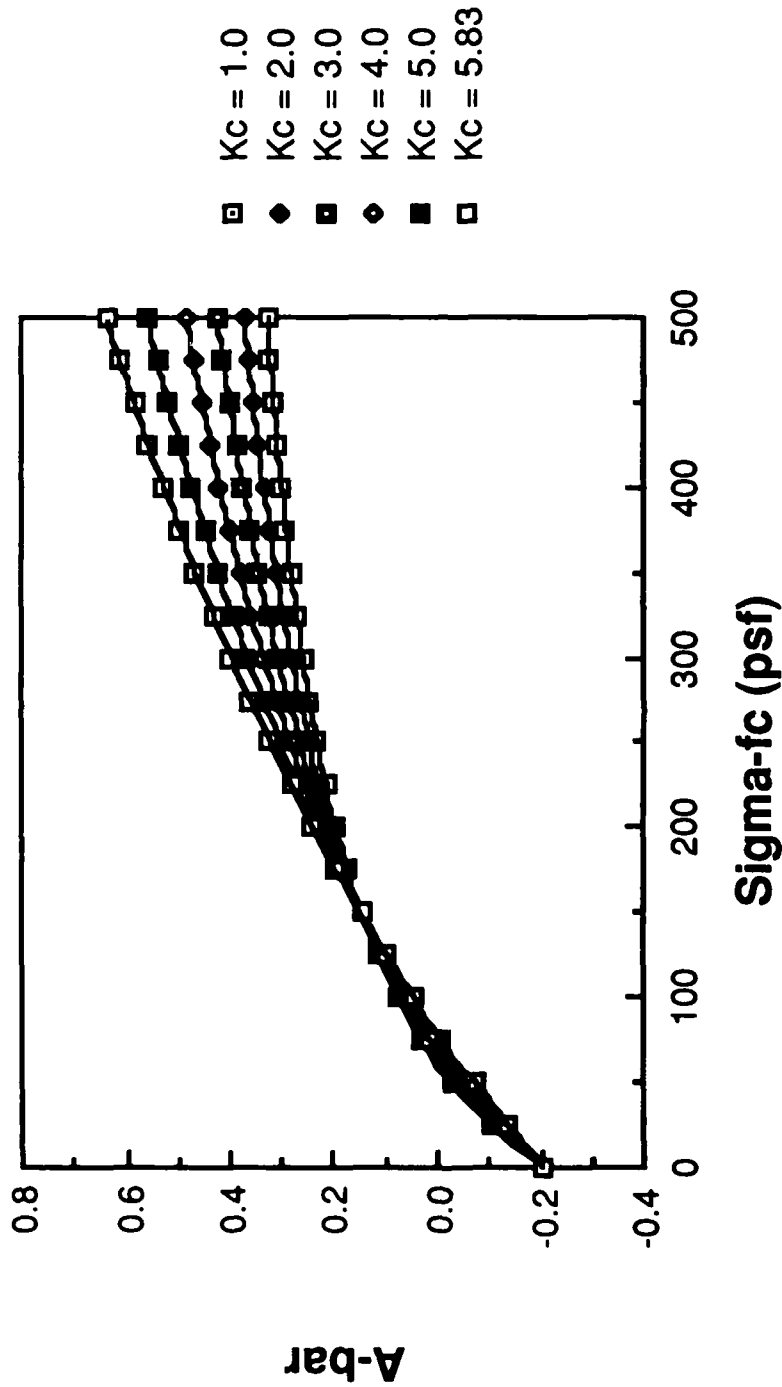


Figure 4.12 - Variation in the Pore Pressure Coefficient,  $\bar{A}_f$ , with Effective Normal Stress on the Failure Plane at Consolidation,  $\bar{\sigma}_{fc}$ , for Various Effective Principal Consolidation Stress Ratios ( $K_c$ ) Estimated from Strength Parameters for Isotropic Consolidation Using Linear Interpolation

TABLE 4.1

SUMMARY OF FOUR SETS OF SOIL PROPERTIES USED TO  
COMPARE PROCEDURES FOR ESTIMATING SHEAR STRENGTH  
ENVELOPES FOR ANISOTROPIC CONSOLIDATION

| Property Set | $c_R$<br>(psf) | $\phi_R$<br>(degs) | $\bar{c}$<br>(psf) | $\bar{\phi}$<br>(degs) | $K_c$ |
|--------------|----------------|--------------------|--------------------|------------------------|-------|
| 1            | 60             | 23                 | 0                  | 45                     | 3.41  |
| 2            | 700            | 15                 | 200                | 31                     | 2.06  |
| 3            | 300            | 15.5               | 0                  | 34                     | 2.27  |
| 4            | 1400           | 22.5               | 0                  | 35                     | 2.35  |

Values of undrained shear strength and pore pressure coefficients were computed for each of the sets of soil properties for a single anisotropic consolidation stress ratio. The stress ratio was computed as the average of the value at failure ( $K_f$ ) and unity, i. e.

$$K_c = \frac{K_f + 1}{2} \quad 4.35$$

The stress ratio ( $K_c$ ) is shown in Table 4.1 for each set of data. The effective stresses,  $\bar{\sigma}_{fc}$ , used for computations with each set of data ranged from zero to values approximately two-to-three times the effective stress at the point where the R and S envelopes intersect. This range was judged to be the range of principal interest and was selected accordingly.

$\tau_{ff}$  versus  $\bar{\sigma}_{fc}$  envelopes. Envelopes are shown in Figs. 4.13 through 4.16, for soil property Sets 1 through 4, respectively. For each set of properties envelopes are shown for the six procedures discussed: Taylor's procedures, Lowe and Karafiath's procedure, the Modified Karafiath procedure, the Extension of Noorany and Seed, the Extension of Benjamin, and the linear interpolation procedures.

$\bar{A}_f$  versus  $\bar{\sigma}_{fc}$ . Corresponding variations in the pore pressure coefficients,  $\bar{A}_f$ , with the effective normal stress on the failure plane at consolidation are shown in Figs. 4.17 through 4.20, for the four sets of soil properties.

#### Discussion.

Several consistent patterns exist in the failure envelopes shown in Figs. 4.13 through 4.16. Lowe and Karafiath's procedure and the extension of Benjamin's work appear to consistently overestimate the shear strength relative to what is found by the other procedures.

### Material Property Set 1

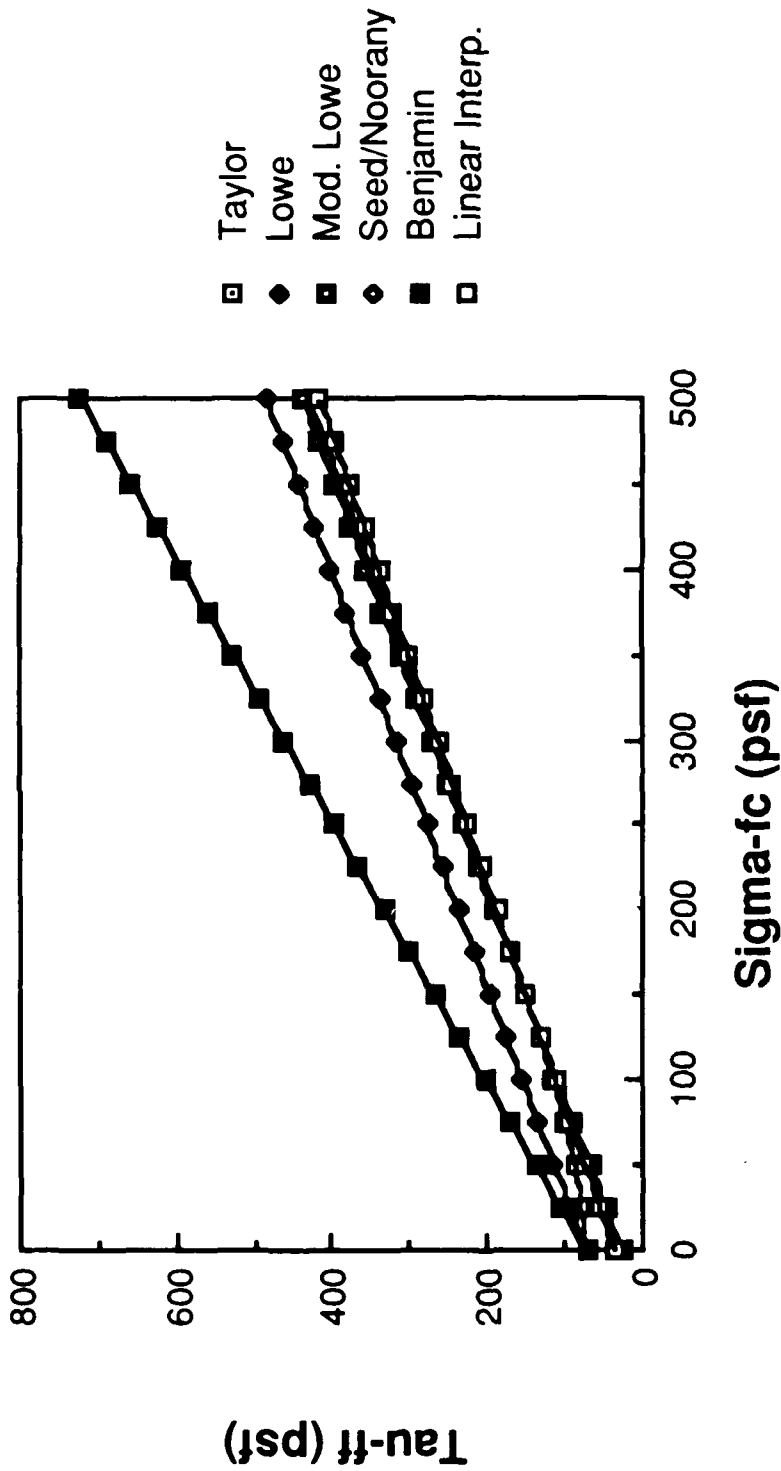


Figure 4.13 - Shear Strength Envelopes ( $\tau_{ff}$  vs.  $\sigma_{fc}$ ) for an Effective Principal Consolidation Stress Ratio ( $K_c$ ) of 3.42 Estimated from Strength Parameters for Isotropic Consolidation Using Several Procedures: Material Property Set No. 1

### Material Property Set 2

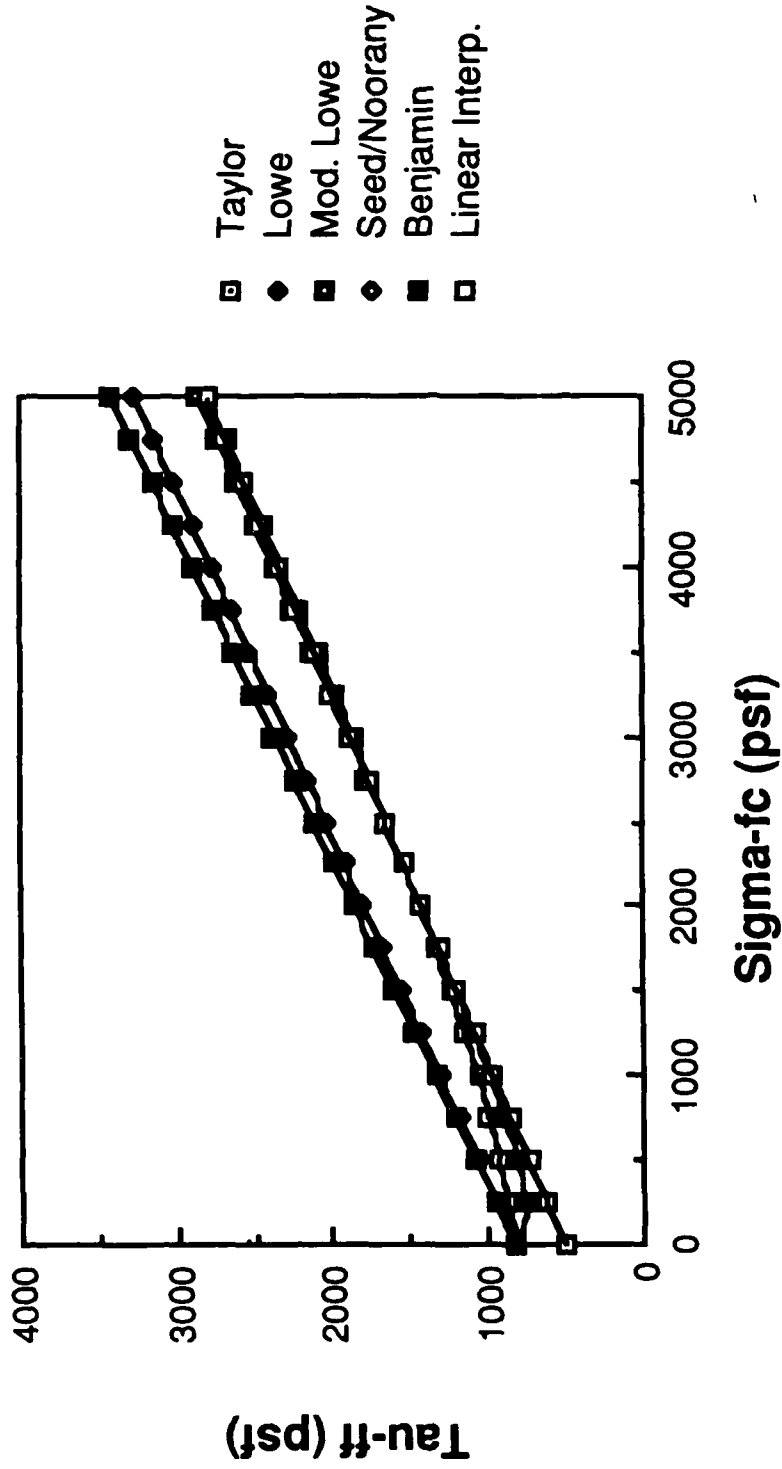


Figure 4.14 - Shear Strength Envelopes ( $\tau_{ff}$  vs.  $\bar{\sigma}_{fc}$ ) for an Effective Principal Consolidation Stress Ratio ( $K_c$ ) of 2.06 Estimated from Strength Parameters for Isotropic Consolidation Using Several Procedures: Material Property Set No. 2

### Material Property Set 3

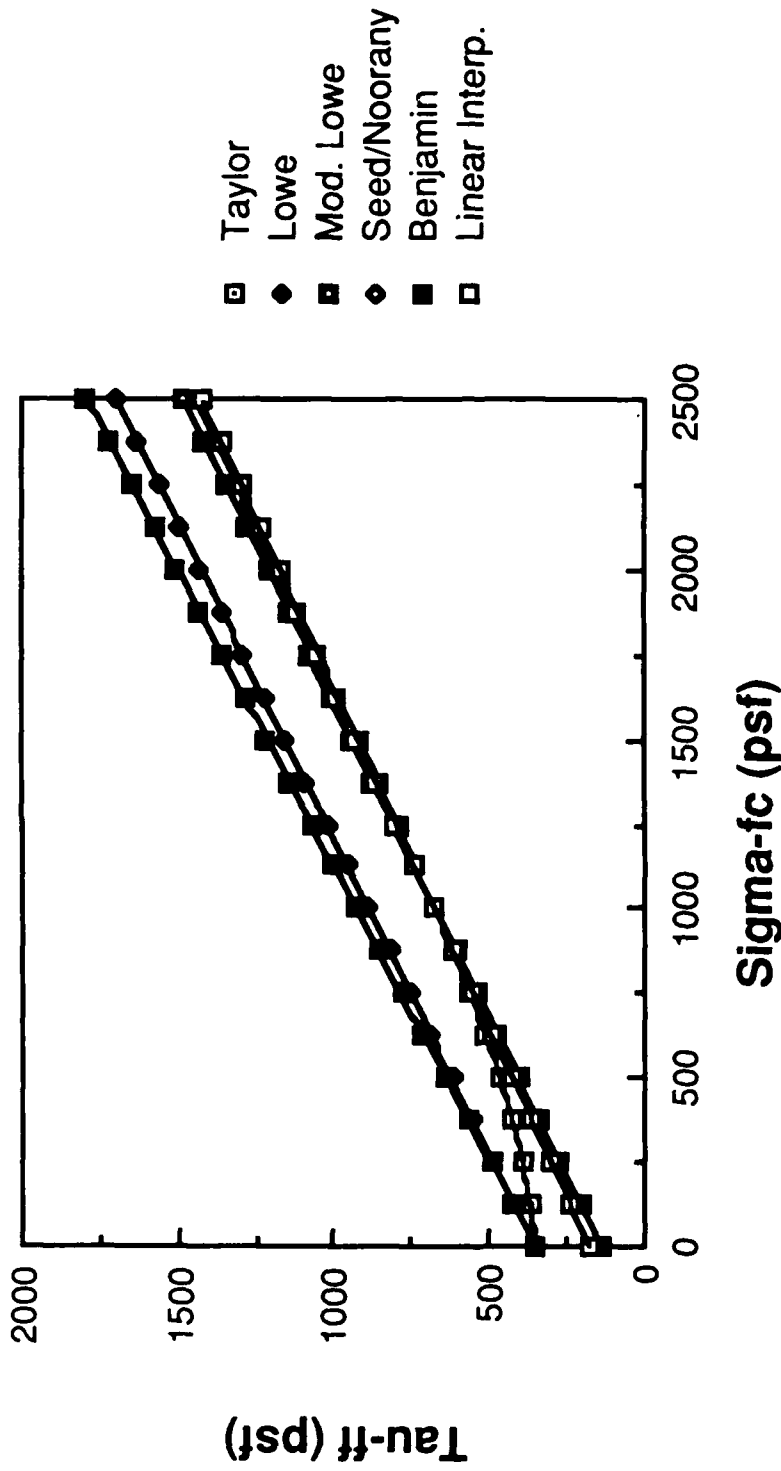


Figure 4.15 - Shear Strength Envelopes ( $\tau_{ff}$  vs.  $\bar{\sigma}$ ) for an Effective Principal Consolidation Stress Ratio ( $K_c$ ) of 2.27 Estimated from Strength Parameters for Isotropic Consolidation Using Several Procedures: Material Property Set No. 3

### Material Property Set 4

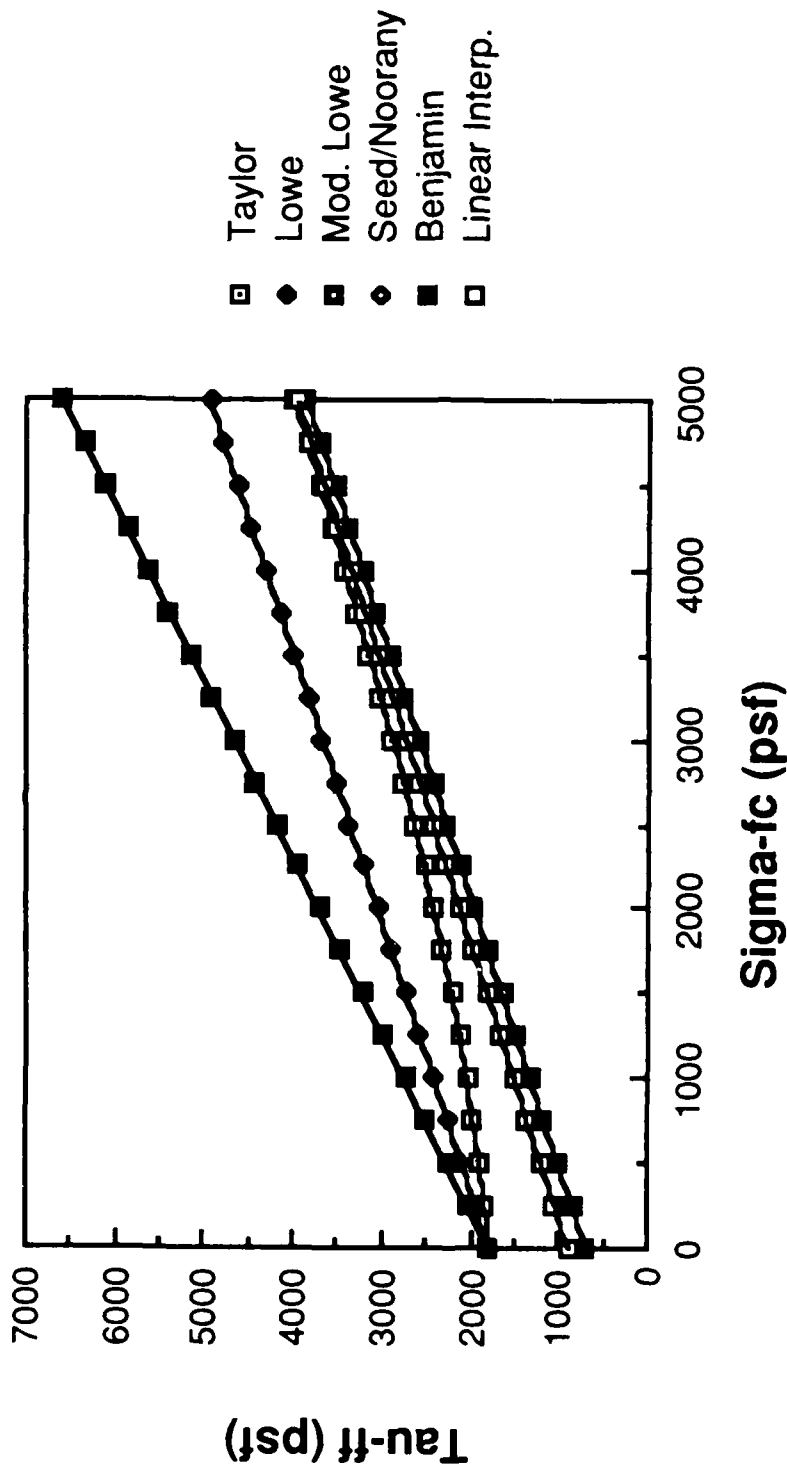


Figure 4.16 - Shear Strength Envelopes ( $\tau_{ff}$  vs.  $\sigma_{fc}$ ) for an Effective Principal Consolidation Stress Ratio ( $K_c$ ) of 2.35 Estimated from Strength Parameters for Isotropic Consolidation Using Several Procedures: Material Property Set No. 4

### Material Property Set 1

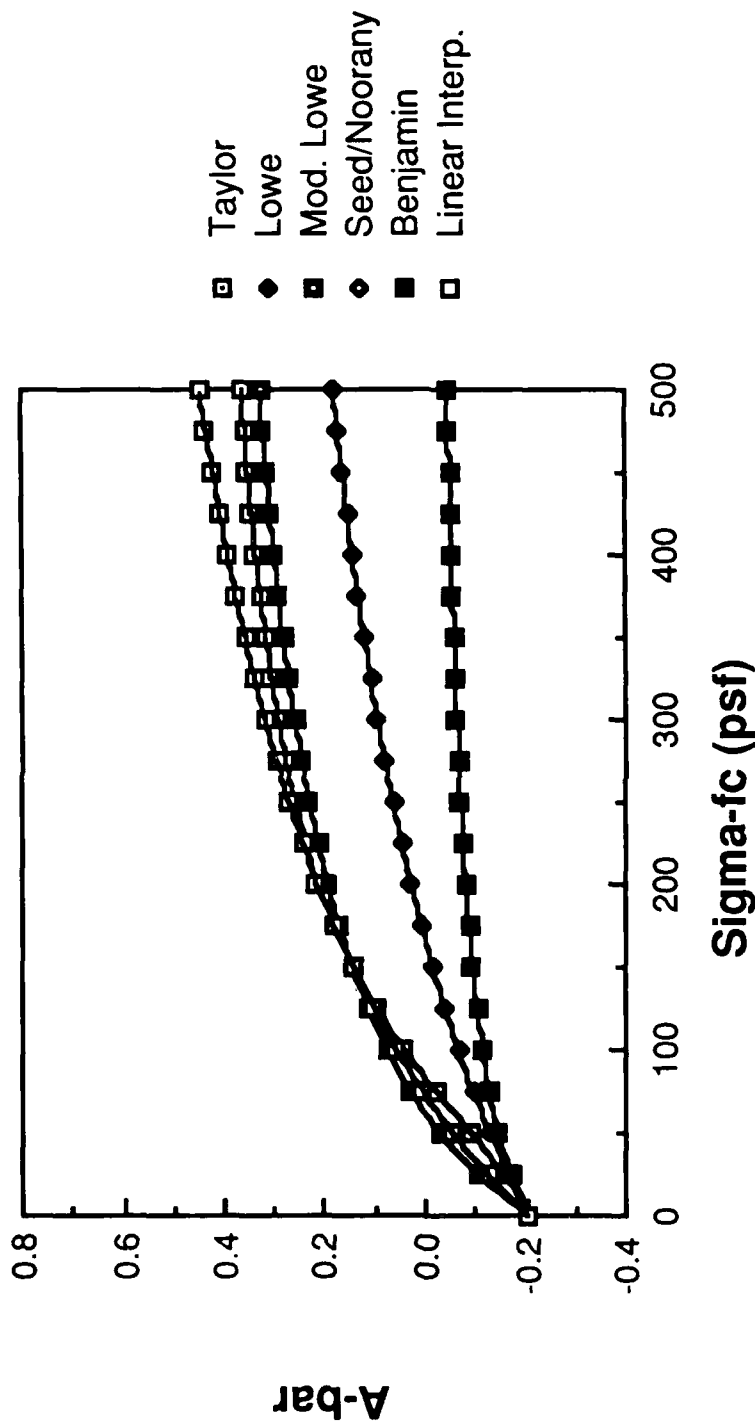


Figure 4.17 - Variation in the Pore Pressure Coefficient,  $\bar{A}_f$ , with Effective Normal Stress on the Failure Plane at Consolidation,  $\sigma_{fc}$ , for an Effective Principal Consolidation Stress Ratio ( $K_C$ ) of 3.42 Estimated from Strength Parameters for Isotropic Consolidation Using Several Procedures: Material Property Set No. 1

### Material Property Set 2

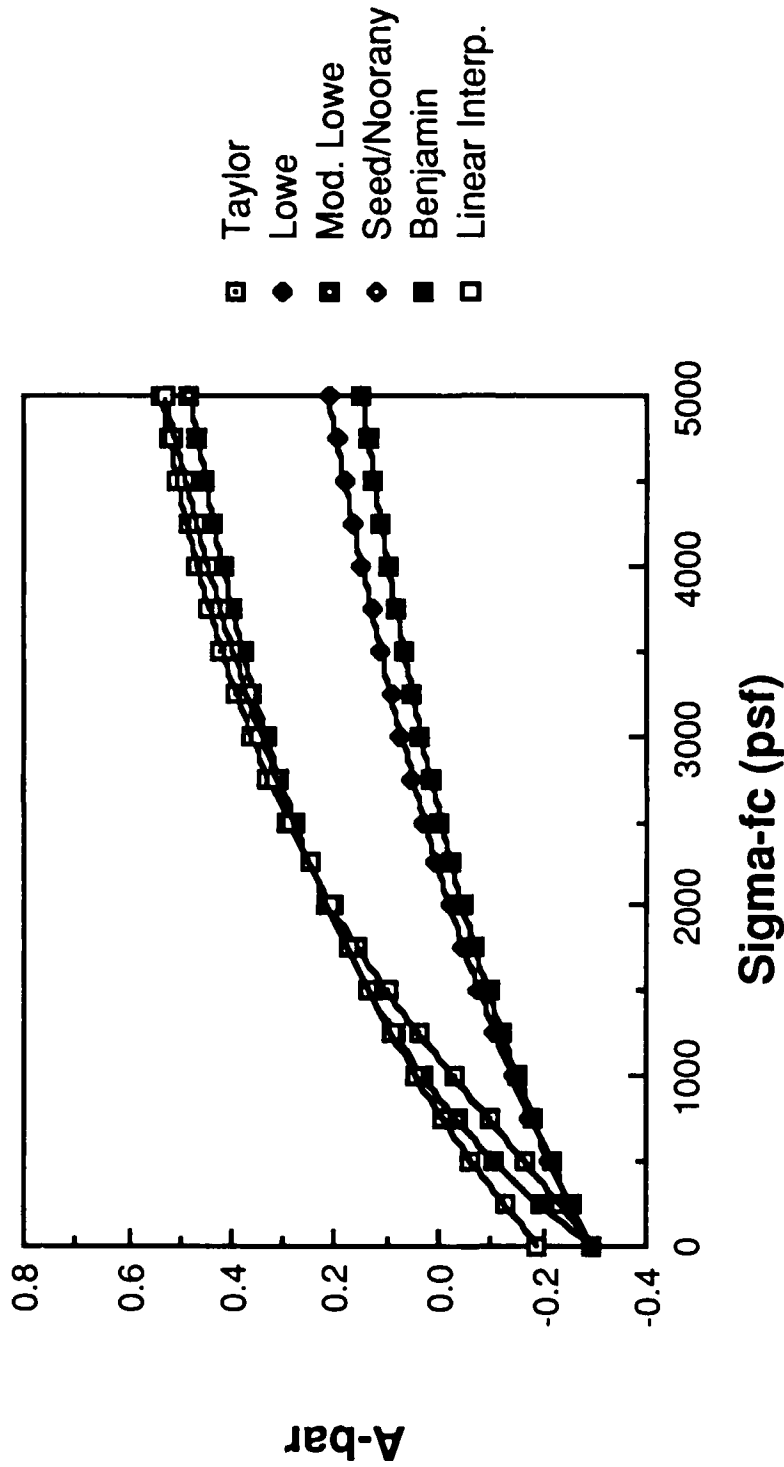


Figure 4.18 - Variation in the Pore Pressure Coefficient,  $\bar{A}_f$ , with Effective Normal Stress on the Failure Plane at Consolidation,  $\sigma_{fc}$ , for an Effective Principal Consolidation Stress Ratio ( $K_c$ ) of 2.06 Estimated from Strength Parameters for Isotropic Consolidation Using Several Procedures: Material Property Set No. 2

### Material Property Set 3

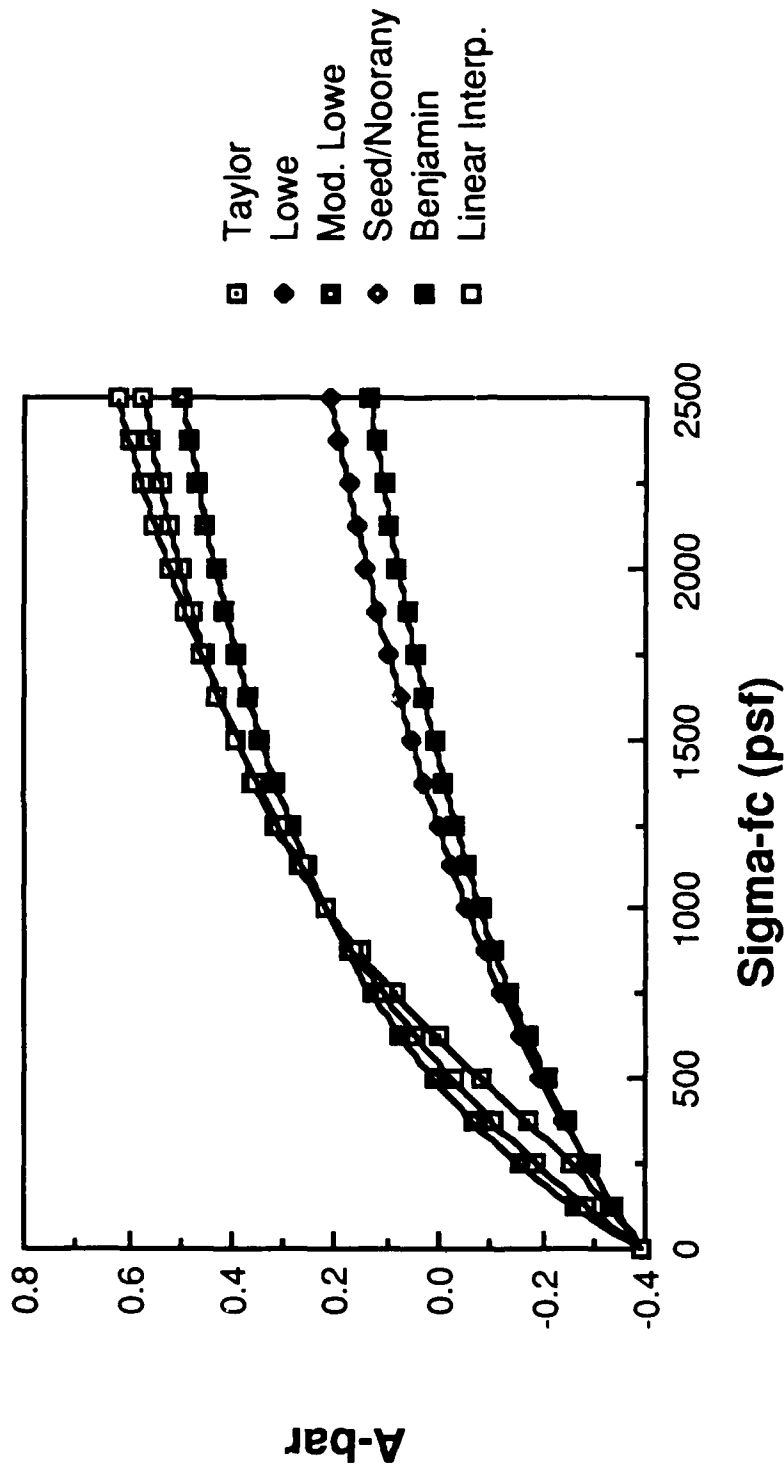


Figure 4.19 - Variation in the Pore Pressure Coefficient,  $\bar{A}_f$ , with Effective Normal Stress on the Failure Plane at Consolidation,  $\sigma_{fc}$ , for an Effective Principal Consolidation Stress Ratio ( $K_c$ ) of 2.27 Estimated from Strength Parameters for Isotropic Consolidation Using Several Procedures: Material Property Set No. 3

### Material Property Set 4

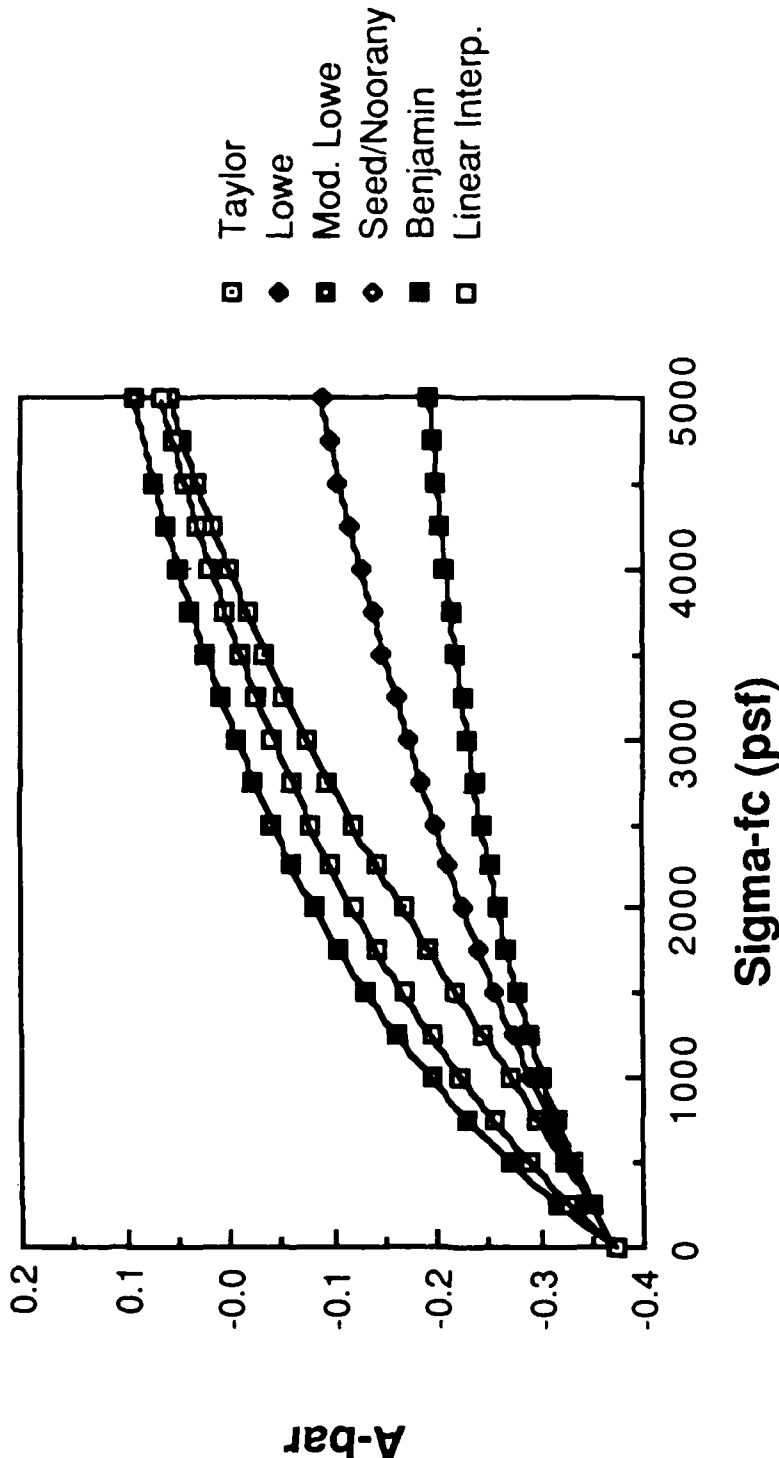


Figure 4.20 - Variation in the Pore Pressure Coefficient,  $\bar{A}_f$ , with Effective Normal Stress on the Failure Plane at Consolidation,  $\sigma_{fc}$ , for an Effective Principal Consolidation Stress Ratio ( $K_c$ ) of 2.35 Estimated from Strength Parameters for Isotropic Consolidation Using Several Procedures: Material Property Set No. 4

Taylor's procedure suggests higher strength at low effective stress as compared to the Modified Karafiath procedure, the Extension of Noorany and Seed, and the linear interpolation procedures. However, the higher strength estimated using Taylor's procedure in the cases illustrated may result from the assumption of a linear stress path. The assumption of a linear stress path was made for the present study to simplify the calculations and because in most cases actual effective stress path data were not readily available. Wong, Duncan and Seed did not observe the higher strengths at low effective stresses with Taylor's procedure when they used actual effective stress paths for the soil (from Hirfanli Dam) which they examined. Taylor's procedure, the Modified Karafiath procedure, the Extension of Noorany and Seed, and the linear interpolation procedures all produced essentially identical envelopes at the higher stresses for all four sets of soil properties considered. This is substantially in agreement with the findings of Wong, Duncan and Seed for the soil from Hirfanli Dam.

The pore pressure coefficients shown in Figs. 4.17 through 4.20 also show patterns similar to those observed for the failure envelopes. As expected, Lowe and Karafiath's procedure and the Extension of Benjamin produce lower pore pressure coefficients, which is consistent with the higher strengths produced by these procedures. The pore pressure coefficients calculated using Taylor's procedure, the Modified Karafiath procedure, the Extension of Noorany and Seed, and the linear interpolation procedures are all similar. The deviations observed in the failure envelopes with Taylor's procedure at low stresses are much less obvious when the pore pressure coefficients are examined and reflect the

sensitivity of the shear strength to small differences in pore pressure coefficient at low stress.

Comparison of the strength envelopes and pore pressure coefficients with measured values for tests where anisotropic consolidation is used would be very helpful in establishing the validity of the various procedures. There are probably sufficient data already in the literature to permit at least some such comparisons to be made; however, additional testing would also be useful. Laboratory tests where anisotropic consolidation is employed typically show sufficient scatter to make it difficult to differentiate between results for one effective principal stress ratio and another. The existence of such scatter probably justifies such approximate procedures as those discussed in this section. However, in order to verify the procedures much more accurate data are required than are often obtained in routine testing. The additional effort required to develop such information is needed to verify the approximate procedures.

Regardless of the validity of the various procedures for estimating the effects of anisotropic consolidation, the results for even the case of isotropic consolidation illustrate the significant variation in the pore pressure coefficient,  $\bar{A}_f$ , with consolidation pressure. Procedures, like Bishop's and Morgenstern's effective stress procedure, which are based on the assumption of a constant value for the pore pressure coefficient, clearly must be considered as approximate procedures. The data for all four soils considered show that the pore pressure coefficient is actually negative at low stresses and increases to positive values as the confining pressure increases. Although Bishop's and Morgenstern's procedure employs conservative, positive values, and,

thus, could be considered "safe", the possibility exists that the procedure is excessively conservative in at least some cases.

## SECTION 5

### AN ALTERNATE APPROACH FOR SUDDEN DRAWDOWN

(Wright)

The effective stress approach first suggested by Bishop (1954) and later employed by Morgenstern (1963) is attractive for several fundamental reasons: First, the procedure is based on effective stresses. Accordingly, the shear strength parameters are based on effective stresses and can be obtained from test results obtained employing either consolidated-drained procedures or consolidated-undrained procedures with pore pressure measurements. The effective stress shear strength parameters are generally much less sensitive to effects of sample disturbance and compaction conditions (dry density, water content, compaction method, etc.), than the strength parameters for either the R-envelope or  $\tau_{ff}$  versus  $\bar{\sigma}_{fc}$  relationships. Secondly, Bishop's and Morgenstern's procedure is based on the use of pore water pressures which have a rational fundamental basis and, at least conceptually, reflect the tendency of soil to change volume and develop changes in pore water pressures during undrained shear. Most of the other procedures for estimating pore water pressures do not reflect the fact that pore water pressures may change due to induced shear stresses during drawdown.

The principal limitations of Bishop's and Morgenstern's procedure result from the assumptions which are made to make the procedure simple. First, a single value of unity is adopted for the pore pressure parameter,  $B$ . This implies either that  $A$  and the ratio of the total principal stress changes  $\Delta\sigma_1/\Delta\sigma_3$  are both constant and independent of

soil type, or these two quantities vary in such a way that B is equal to unity. The second limitation of Bishop's and Morgenstern's procedure is associated with the assumption that the major principal stress change is equal to the change in vertical stress at the surface of the slope. As discussed earlier in Section 2 this assumption is clearly not valid near the face of the slope.

In order to eliminate some of the limitations imposed by the assumptions in Bishop's and Morgenstern's procedure ( $B = 1.0$ ,  $\Delta\sigma_1 = \Delta\sigma_v$ ) and to investigate the significance of these assumptions an alternate procedure has been established and used as part of the current study. The alternate procedure employs the finite element method to calculate the change in stress in the slope due to drawdown. The changes in stress are then used with appropriate values for the pore pressure coefficients (A and B) to compute the changes in pore water pressure caused by the drawdown. Finally, the changes in pore water pressure are added to the pore water pressures before drawdown to arrive at final values of pore water pressures after drawdown.

#### VALIDITY OF SKEMPTON'S PORE PRESSURE EQUATION

A fundamental hypothesis of Bishop's and Morgenstern's procedure, as well as the alternative procedure described herein, is that Skempton's (1954) equation and pore pressure coefficients are valid for computing changes in pore water pressures due to sudden drawdown. Before proceeding further with the discussion of the alternative procedure it is appropriate to first examine the validity of Skempton's equation. Skempton's equation can be written as,

$$\Delta u = B\Delta\sigma_3 + A(\Delta\sigma_1 - \Delta\sigma_3) \quad 5.1$$

where,  $\Delta u$  is the change in pore water pressure,  $\Delta\sigma_1$  and  $\Delta\sigma_3$ , are the major and minor principal stress changes, respectively, and  $\bar{A}$  and  $B$  are pore pressure coefficients. Equation 5.1 is based on the assumption that the change in pore water pressure is independent of changes in the intermediate principal stress,  $\Delta\sigma_2$ . Henkel (1960) and others (e. g. Perloff and Baron, 1976) have proposed that changes in pore water pressure are affected by changes in the intermediate principal stress. To account for the effects of the intermediate change in principal stress the following equation for changes in pore water pressure has been proposed:

$$\Delta u = \frac{\Delta\sigma_1 + \Delta\sigma_2 + \Delta\sigma_3}{3} + a\sqrt{(\Delta\sigma_1 - \Delta\sigma_2)^2 + (\Delta\sigma_2 - \Delta\sigma_3)^2 + (\Delta\sigma_3 - \Delta\sigma_1)^2} \quad 5.2$$

where  $\Delta\sigma_1$ ,  $\Delta\sigma_2$  and  $\Delta\sigma_3$  represent the major, intermediate and minor principal stress changes, respectively<sup>1</sup>.

Equations 5.1 and 5.2 are fundamentally different equations and different values will be predicted for changes in pore pressure depending on the loading path<sup>2</sup>. For example, if the pore pressure coefficients ( $\bar{A}$  and  $a$ ) are determined from tests with one loading path, e.g. triaxial compression, and then used in the respective equations (5.1 and 5.2) to predict the pore pressure changes for a different loading path, e. g. triaxial extension or some form of plane strain

---

<sup>1</sup>Equation 5.2 is written in the form for a saturated soil; a different form is required for partly saturated soils.

<sup>2</sup>In this case "loading" path includes the orientation of the principal stresses at consolidation, the orientation of the principal stress changes, the intermediate principal stress, and the deformation conditions (plane strain, triaxial, etc.)

deformation, different pore pressures will be predicted, depending on which of the two equations is used. The problem of predicting pore pressures and establishing the validity of Eqs. 5.1 or 5.2 is complicated by the fact that the pore pressure coefficients themselves may vary with the loading path due to inherent material anisotropy. For example, Duncan and Seed (1966) reported values of  $\bar{A}_f$  of 1.12 for plane strain tests in which the principal stress at failure was vertical and 0.70 for plane strain tests in which the major principal stress at failure was horizontal. Such variations in the pore pressure coefficients themselves make it very difficult to verify that either Eq. 5.1 or 5.2 is fundamentally more correct. However, in the present case where the interest lies in predicting pore water pressures due to sudden drawdown the problem is somewhat simpler: The purpose of using either Eq. 5.1 or 5.2 and the associated pore pressure coefficients is to estimate changes in pore pressure using a single value for the pore pressure coefficient,  $\bar{A}$  or  $a$ , regardless of the orientation of the principal stress changes. Accordingly, the most suitable equation (5.1 or 5.2) is the one which produces a pore pressure coefficient that is relatively independent of the loading path. The pore pressure coefficient which is the more unique in value for different loading paths reflects the more valid pore pressure coefficient for the present purposes.

Van Saun (1985) examined values of the pore pressure coefficients ( $\bar{A}$  and  $a$ ) measured for different loading paths from laboratory test data for approximately 20 soils. In each case both triaxial compression and extension tests were performed on specimens at comparable consolidation pressures and overconsolidation ratios. The soils for which data were

examined encompassed undisturbed specimens, compacted specimens and specimens reconstituted and consolidated from a slurry. Specimens ranged from normally consolidated to specimens with overconsolidation ratios of 24. Effective consolidation pressures ( $\bar{\sigma}_{1c}$ ) ranged from 5 to 120 psi. The values of Skempton's pore pressure coefficient,  $\bar{A}$ , based on these test data for triaxial extension tests are plotted versus the corresponding values for the compression tests in Fig. 5.1. A line is drawn to represent the line of equality for the two sets (compression, extension) of test values. A similar plot for the other pore pressure coefficient ( $a$ ) is shown in Fig. 5.2. The actual values shown in Fig. 5.2 have been multiplied by the square root of 2; in the case of triaxial shear where two of the principal stress changes are always equal Eq. 5.2 becomes:

$$\Delta u = \Delta \sigma_a + a\sqrt{2}(\Delta \sigma_1 - \Delta \sigma_3) \quad 5.3$$

where,

$$\Delta \sigma_a = \frac{1}{3}(\Delta \sigma_1 + \Delta \sigma_2 + \Delta \sigma_3) \quad 5.4$$

The quantity  $a\sqrt{2}$ , thus appears as a coefficient analogous to the coefficient  $\bar{A}$  in Eq. 5.1.

Examination of the data presented in Figs. 5.1 and 5.2 reveals that neither  $\bar{A}$  nor  $a$  are unique for compression and extension nor does one set of coefficients appear to be more unique than the other. However, at the same time both coefficients are reasonably similar for the two loading paths (triaxial compression, triaxial extension) represented by the data in Figs. 5.1 and 5.2. The average difference between the pore pressure coefficient  $\bar{A}_f$  for compression and extension tests is 0.16; the higher values generally being measured in extension tests. The average difference between the quantity  $a\sqrt{2}$  for compression and extension tests

# Skempton's Pore Pressure Coefficients

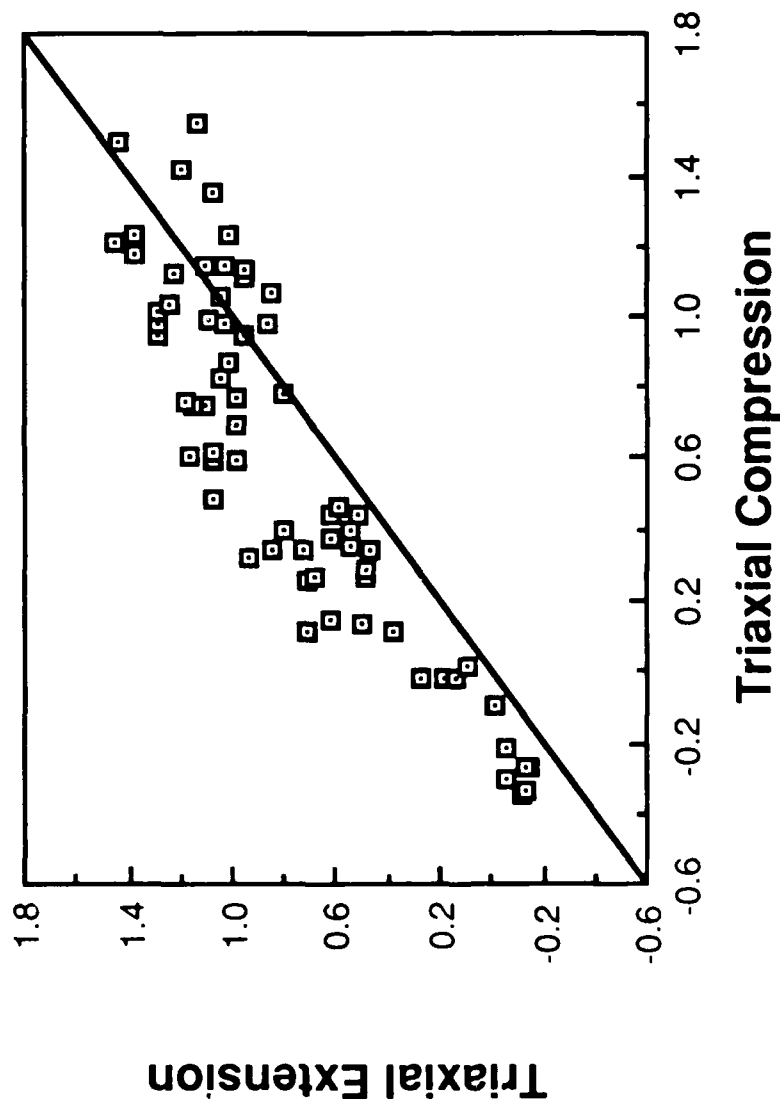


Figure 5.1 - Comparison of Skempton's Pore Pressure Coefficient,  $\bar{A}_f$ , from Triaxial Compression and Triaxial Extension Tests (After Van Saun, 1985)

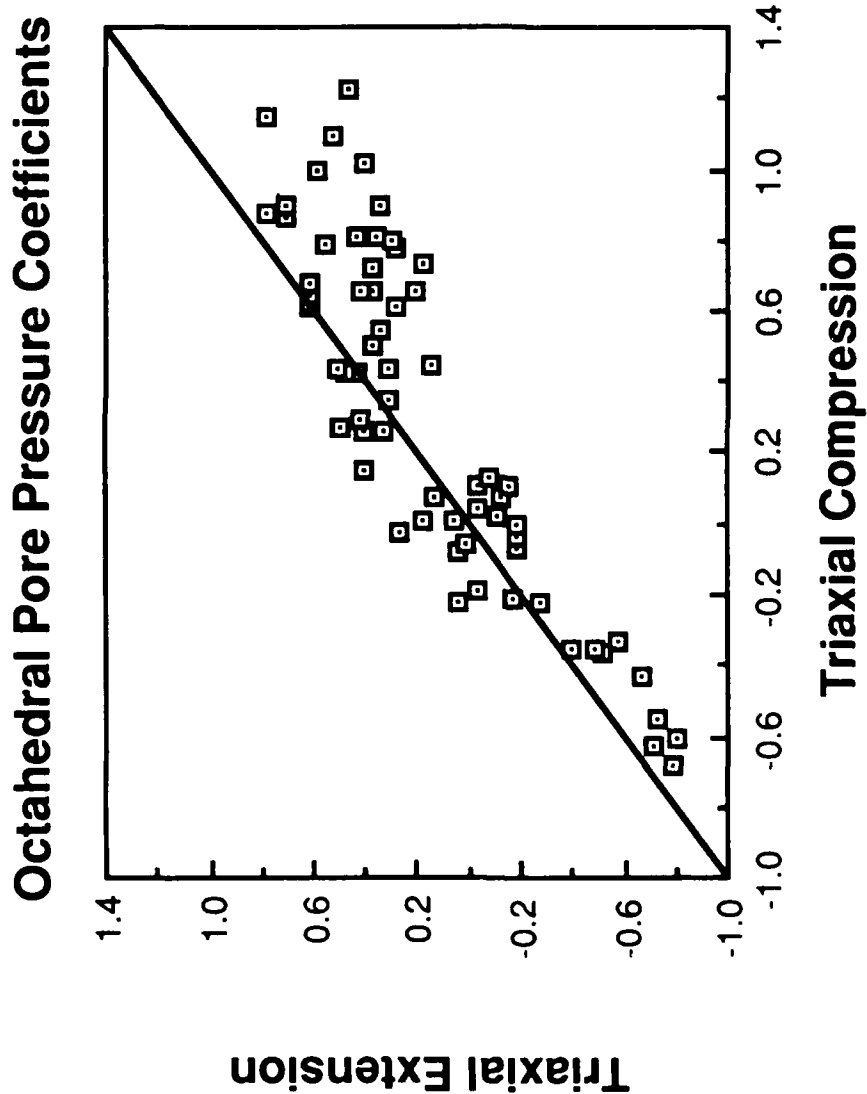


Figure 5.2 - Comparison of Henkel's Pore Pressure Coefficient,  $a/\sqrt{2}$ , from Triaxial Compression and Triaxial Extension Tests (After Van Saun, 1985)

is 0.17; the higher values generally being measured in compression tests. For practical purposes and based on the data summarized in Figs. 5.1 and 5.2, Eqs. 5.1 and 5.2 and their associated pore pressure coefficients appear to be equally suited for use in predicting pore water pressure due to sudden drawdown.

Although it would have been useful to examine similar types of data to those presented in Figs. 5.1 and 5.2 for the case of plane strain, such data are very limited and usually the intermediate principal stress is not known. The intermediate principal stress would have to be estimated to calculate the pore pressure coefficient,  $a$ , from Eq. 5.2.

Skempton's equation (Eq. 5.1) was selected for computing changes in pore pressure in the present study because of the apparently wider use of and experience with the equation and the past history of use of Skempton's pore pressure coefficients for sudden drawdown. The data shown in Figs. 5.1 and 5.2 suggest that Eq. 5.2 and the pore pressure coefficient,  $a$ , also could have been used with probably equal validity.

#### FINITE ELEMENT COMPUTATIONS

In the alternative procedure developed herein the change in stress due to drawdown is computed first by applying loads (stresses) at the face of the slope to represent the changes in stress caused by lowering the adjacent water level. Changes in stress are applied as "tensile" stresses acting away from the face of the slope to represent the unloading (Fig. 5.3). For the present study all computations were performed assuming linear elasticity and using a constant value for the soil modulus (Young's modulus). The actual value of modulus was immaterial inasmuch as only stresses were of interest; computed

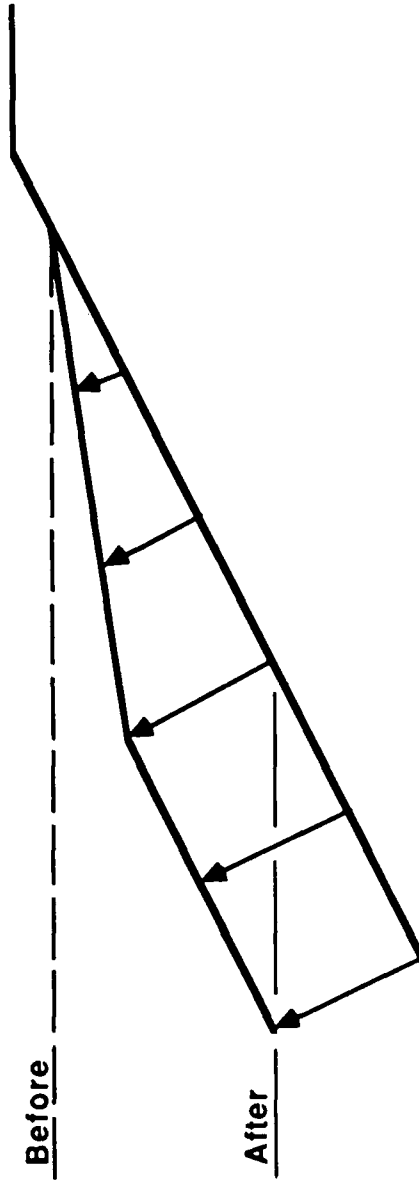


Figure 5.3 - Stresses Representing "Unloading" of Slope Face Due to Sudden Drawdown

displacements were ignored. Poisson's ratio was assumed to be 0.49 to approximate undrained loading (zero volume change).

A finite element computer program employing the "QM5" isoparametric quadrilateral element developed by Doherty, Wilson and Taylor (1969) was used to compute the changes in stress. Changes in stress were calculated at the centroids of each element and, accordingly the pore pressures which were subsequently calculated were calculated at the centroids of each element.

#### PORE PRESSURE COEFFICIENTS

Pore pressure coefficients were assumed to vary within the slope, depending on the effective stresses which existed just prior to drawdown. Pore pressure coefficients were computed at points corresponding to the location of the centroid of each of the finite elements which were used to compute changes in stress. Pore pressure coefficients were computed using Taylor's procedure which was described in Section 4 of this paper. A linear effective stress path was assumed. Thus, the pore pressure coefficient,  $\bar{A}$ , could be related to the strength parameters from the R envelope ( $c_R$  and  $\phi_R$ ), the effective stress friction angle,  $\bar{\phi}$ , and the state of stress (e. g.  $\bar{\sigma}_{3C}$  and  $K_C$ ). For purposes of computing pore pressure coefficients the strength parameters associated with the R envelope were considered to be those for an R envelope which is drawn tangent to the circles of stress, rather than through the points corresponding to stresses on the failure plane. Accordingly, the equations and procedures used to compute the pore pressure coefficient were different from those presented in Section 4 for Taylor's procedure, which were based on an envelope drawn through points corresponding to stresses on the failure plane.

To compute the pore pressure coefficient  $\bar{A}_f$  for a given effective principal stress ratio at consolidation ( $K_c$ ) and effective minor principal stress ( $\bar{\sigma}_{3c}$ ) an equivalent effective minor principal stress,  $\bar{\sigma}_{3cI}$ , for the corresponding stress path for isotropic consolidation is found first. The equivalent effective minor principal stress is determined by solving the following equation:

$$\bar{\sigma}_{3cI} = \bar{\sigma}_{3c} + \frac{\bar{\sigma}_{3cI}d_1 + d_2}{\bar{\sigma}_{3cI}d_3 + d_4} \frac{\bar{\sigma}_{3cI}(K_c - 1)}{1 + (K_c - 1) \frac{\bar{\sigma}_{3cI}d_1 + d_2}{\bar{\sigma}_{3cI}d_3 + d_4}} \quad 5.5$$

where,

$$d_1 = N_{\phi} - N_{\phi} \quad 5.6$$

$$d_2 = 2(\bar{c} N_{\phi} - c_R N_{\phi}) \quad 5.7$$

$$d_3 = (N_{\phi} - 1)(N_{\phi} - 1) \quad 5.8$$

$$d_4 = (N_{\phi} - 1) 2c_R N_{\phi} \quad 5.9$$

and,

$$N_{\phi} = \tan^2(45 + \frac{\phi}{2}) \quad 5.10$$

$$N_{\phi} = \tan^2(45 + \frac{\phi_R}{2}) \quad 5.11$$

Once the equivalent effective minor principal stress is calculated, the corresponding pore pressure coefficient is calculated from the following equation, which is obtained for isotropic consolidation:

$$A_f = \frac{\bar{\sigma}_{3cI}d_1 + d_2}{\bar{\sigma}_{3cI}d_3 + d_4} \quad 5.12$$

The minor principal stress ( $\sigma_{3c}$ ) and the effective principal stress ratio for consolidation ( $K_c$ ), which are used to compute the pore pressure coefficients, were estimated for the present study as follows: The effective vertical stress was calculated first assuming no head losses in the upstream slope; total unit weights were used above the

initial (pre-drawdown) water level and submerged unit weights were used below the water level. The effective vertical stress was assumed to be the major principal stress. The effective minor principal stress was calculated assuming that the effective principal stress ratio at consolidation was equal to the average of the value of the effective principal stress ratio at failure ( $K_f$ ) and a value of unity, i. e.

$$\bar{\sigma}_{3c} = \frac{\bar{\sigma}_v}{K_c} \quad 5.13$$

where,  $\bar{\sigma}_v$  represents the effective vertical stress and,

$$K_c = \frac{(1 + K_f)}{2} \quad 5.14$$

#### PORE PRESSURE COMPUTATIONS

Once the changes in stress and the pore pressure coefficients were determined for the center of each element, changes in pore water pressure were calculated from Skempton's equation:

$$\Delta u = B\Delta\sigma_3 + A(\Delta\sigma_1 - \Delta\sigma_3) \quad 5.15$$

where  $\Delta\sigma_1$  and  $\Delta\sigma_3$  are principal stress changes calculated by the finite element method,  $A$  represents the pore pressure coefficient determined in the manner described above, and  $B$  was assumed to be equal to unity (assuming a saturated soil). The initial pore water pressures,  $u_0$ , before drawdown were calculated assuming a horizontal water surface in the slope with no head losses. Thus,

$$u_0 = \gamma_w z_w \quad 5.16$$

where  $z_w$  is the distance from the free water surface to the centroid of the element. Finally, the pore pressures after drawdown,  $u_1$ , were calculated from,

$$u_1 = u_0 + \Delta u \quad 5.17$$

## STABILITY COMPUTATIONS

Stability computations were performed using the pore pressures at the centroids of each finite element to interpolate values along the shear surface. The computer program, UTEXAS2, was used for the computations and includes provisions for automatically performing the required interpolation (Wright, 1986a). Thus, once pore pressures were determined at the centroids of the finite elements all additional computations were performed using the existing computer program for slope stability analyses.

### SUMMARY

The finite element based procedure described in this section includes several potential improvements over previous procedures. The procedure accounts for the variation in the pore pressure coefficient,  $A$ , with effective consolidation pressures and employs rational procedures for estimating the changes in total stress in the slope caused by drawdown. A number of assumptions are also made in the procedure:

1. The soil is linearly elastic and has a constant modulus.
2. Poisson's ratio is constant and equal to 0.49.
3. Skempton's pore pressure coefficients are valid for computing changes in pore water pressure.
4. The major principal stress before drawdown is equal to the effective vertical overburden pressure ( $\gamma z, \gamma'z$ ).
5. The effective principal stress ratio for consolidation (before drawdown) is exactly midway between a value of unity and the value at failure (Eq. 5.14).

6. Taylor's procedure is valid for estimating the undrained shear strengths and corresponding pore pressure coefficients for anisotropic consolidation using results from tests with isotropic consolidation.

7. There is no head loss before drawdown; the pore pressures are governed by a horizontal piezometric surface at the adjacent free water level.

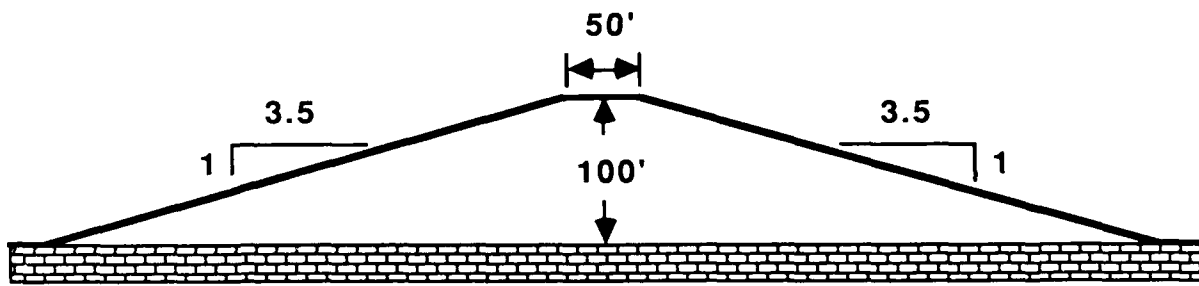
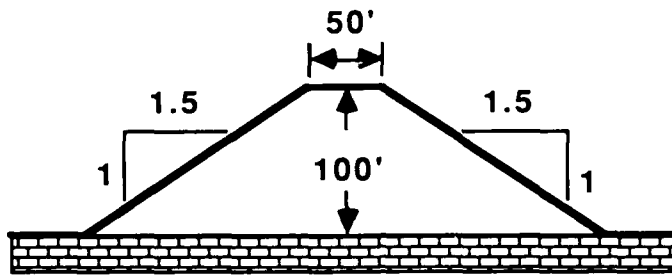
A number of parametric studies were performed using the finite element-based procedure for comparison with the results obtained by other procedures. The results obtained with this procedure are compared with the results from other procedures in the next section of this paper.

SECTION 6  
COMPARATIVE EXAMPLES AND CALCULATIONS  
(Wright)

Three series of example problems were selected for comparative studies employing the various procedures described in the preceding sections of this paper. The first series of examples was selected and used for comparison of the effective stress procedures. This series was entirely hypothetical and selected for comparative purposes only. The second series of examples was based on the Pilarcitos Dam. Pilarcitos Dam experienced a slide due to sudden drawdown and, thus, the actual factor of safety could be assumed to be close to unity. The third series of examples was selected and used to examine both the effective stress analysis procedures and the two-stage analysis procedures. The third series of examples is also hypothetical, although the strength properties are based on actual data from embankment dams.

EFFECTIVE STRESS PROCEDURES

The first series of examples selected for effective stress calculations are identical to a series of examples examined by Wong, Duncan and Seed (1983). A slope height of 100 feet and side slopes of 1.5:1 (horizontal:vertical) and 3.5:1 were used. The water level before drawdown was assumed to be at the crest of the slope; drawdown levels (L) of 35, 70 and 100 percent of the initial water level (H) were considered. Effective stress shear strength parameters were selected to correspond to values of the dimensionless parameter,  $\lambda_{c\phi}$  ( $= \gamma H \tan \phi / \bar{c}$ ) of 5, 10 and 50. Pertinent data for these examples are shown in Fig. 6.1



| <u>Cohesion, <math>\bar{c}</math></u> | <u>Friction Angle, <math>\bar{\phi}</math></u> | <u>Unit Weight, <math>\gamma</math></u> | <u><math>\lambda_{c\phi}</math></u> |
|---------------------------------------|--|---|-------------------------------------|
| 1500 psf                              | 30 degrees                                     | 125 pcf                                 | 5                                   |
| 750 psf                               | 30 degrees                                     | 125 pcf                                 | 10                                  |
| 150 psf                               | 30 degrees                                     | 125 pcf                                 | 50                                  |

Figure 6.1 - Parameters Used in First Series of Comparative Analyses Employing Effective Stress Procedures

Two effective stress procedures were used. The first was Bishop's and Morgenstern's procedure. In this case pore water pressures were represented by a piezometric line coincident with the face of the slope above the reservoir level, and coincident with the reservoir surface below the reservoir level (Fig. 6.2); the reservoir level represents the reservoir level after drawdown. The second effective stress procedure was based on pore water pressures obtained by solving the governing differential equation for steady-state seepage (Eq. 2.27). A finite element procedure was used to obtain the solution. The finite element procedure consisted of first locating the phreatic surface for steady seepage before drawdown using Neuman and Witherspoon's (1970) procedure where the finite element mesh is successively adjusted until the boundary conditions along the free surface (zero pressure; no flow) are satisfied (Fig. 6.3a). Once the free surface was located, the boundary conditions along the free surface were set to zero pressure and the heads along the upstream slope were set equal to the values after drawdown (Fig. 6.3b). New heads and pore water pressures were then computed. The new heads were used to calculate the pore water pressures after drawdown. This approach is essentially identical to the approaches Cedergren (1948, 1967) used with flow nets and Desai (1972, 1977) employed with the finite element method. However, in the present case drawdown was assumed to be instantaneous and, thus, partial drainage was not considered.

Factors of safety were calculated using the computer program, UTEXAS2 (Wright, 1986a), and assuming circular shear surfaces. The factors of safety are summarized in Table 6.1. The ratio of the factor of safety computed using pore pressures derived from the steady-state

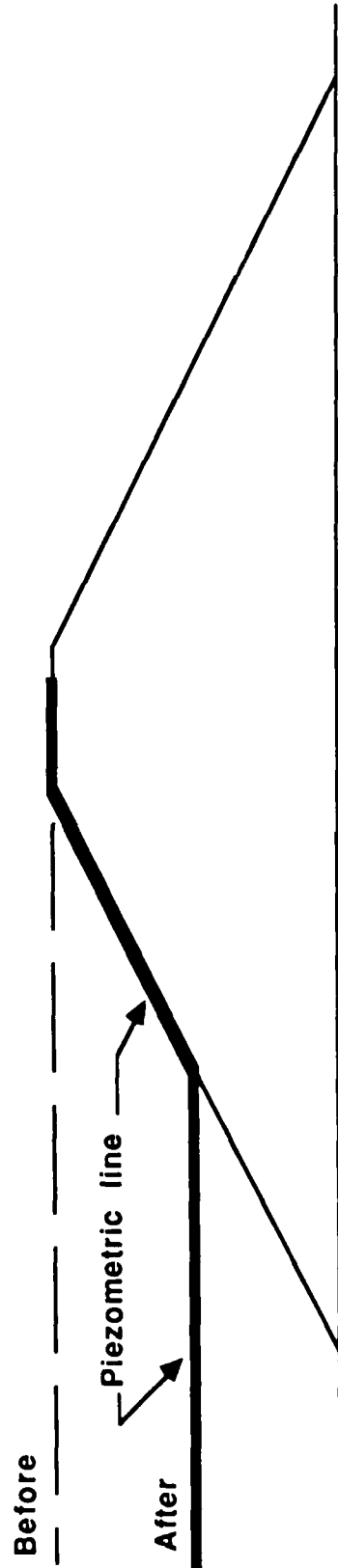
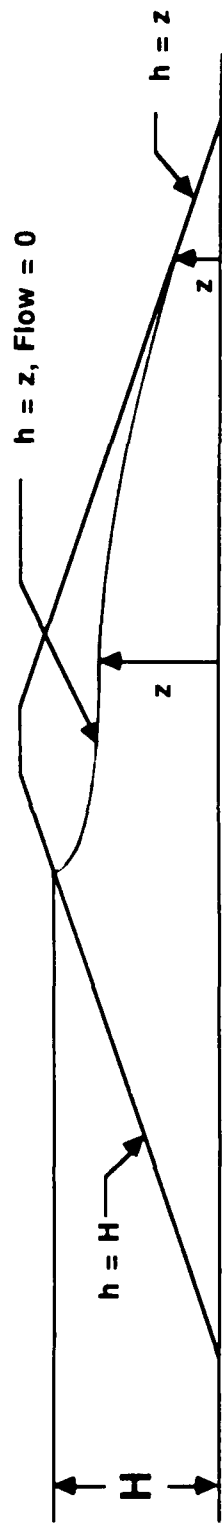


Figure 6.2 - Piezometric Line Used to Represent Pore Water Pressures  
by Bishop's and Morgenstern's Procedure

### (a) Before Drawdown



### (b) After Drawdown

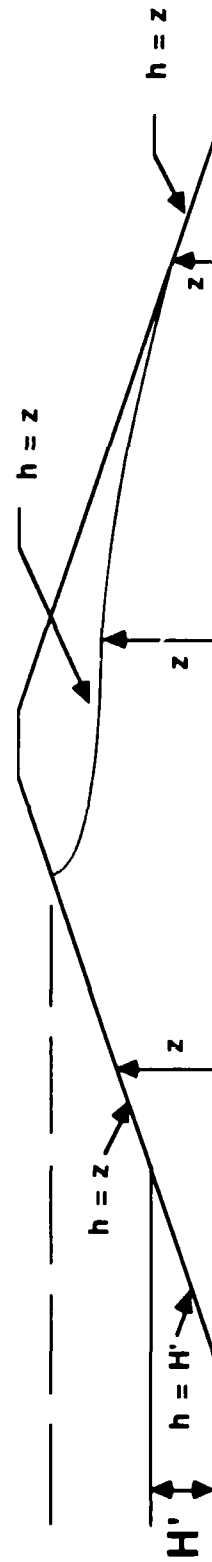


Figure 6.3 - Schematic Illustration of Pre-Drawdown and Post-Drawdown Boundary Conditions Used for Finite Element Solution of Steady-State Flow Equations

seepage solution to the factor of safety computed using pore pressures obtained by Bishop's and Morgenstern's procedure is also shown in this table. In all cases the factors of safety computed using the pore water pressures from the steady-state flow solution are higher than those computed using Bishop's and Morgenstern's approach. The differences between the factors of safety computed by the two approaches generally decrease as the slope angle decreases (slope ratio increases) and as the value of  $\lambda_{c\phi}$  decreases. The largest difference is approximately 29 percent (1.5:1 slope,  $\lambda_{c\phi} = 50$ ), while the smallest difference is only approximately 4 percent (3.5:1 slope,  $\lambda_{c\phi} = 5$ ). These differences are remarkably small considering the very different bases of the two approaches.

The differences between factors of safety computed using pore pressures obtained by Bishop's and Morgenstern's procedure and the steady-state flow solution may in some cases be much larger than those summarized in Table 6.1. In the preceding calculations the slope was assumed to be homogeneous and to rest on an impervious foundation as shown in Fig. 6.4a. If instead the slope rests on a pervious foundation, a significant downward flow would have been predicted with an attendant significant reduction in pore water pressures (Fig. 6.4b). Adams (1982) showed a similar effect may even occur for an impervious foundation in the case of sloping core dams. He showed that for the Lokvarka Dam (Fig. 6.5) the flow is predominately vertically downward except at the base of the core. This resulted in nearly horizontal equipotential lines throughout most of the core (Fig. 6.6). Such horizontal equipotential lines correspond to zero pore water pressure. Consequently, the factors of safety computed in this case (Lokvarka Dam) using pore pressures

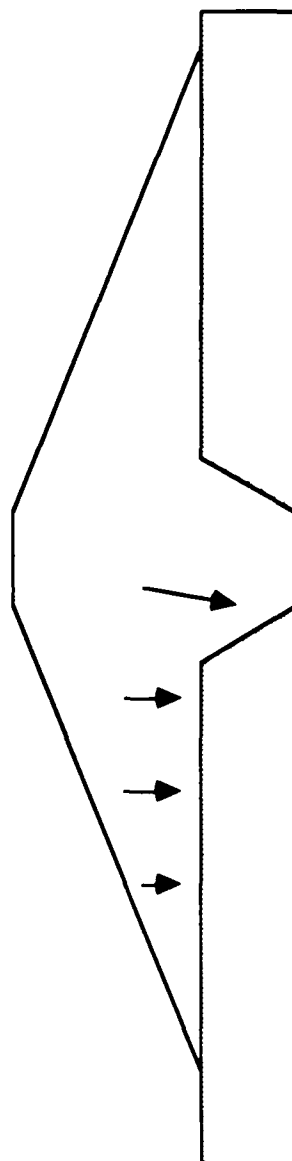
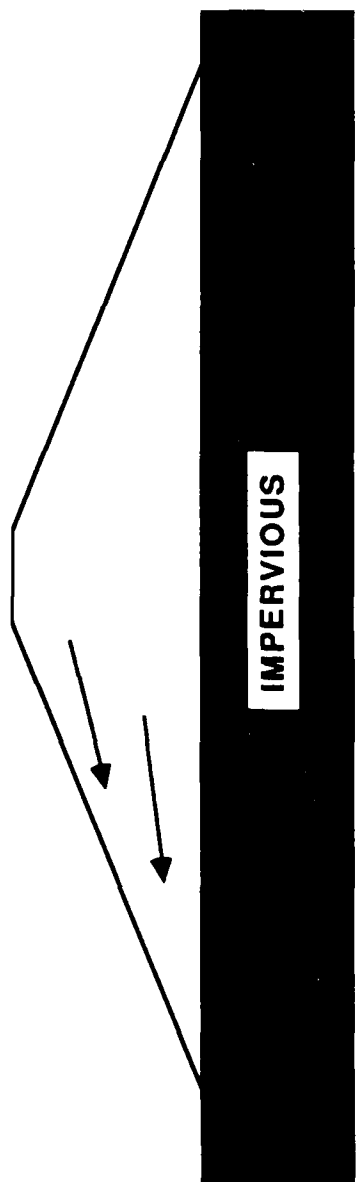


Figure 6.4 - Flow Paths for Drainage of Upstream Slope for  
 (a) Embankment on Impervious Foundation, and  
 (b) Embankment on Relatively Pervious Foundation

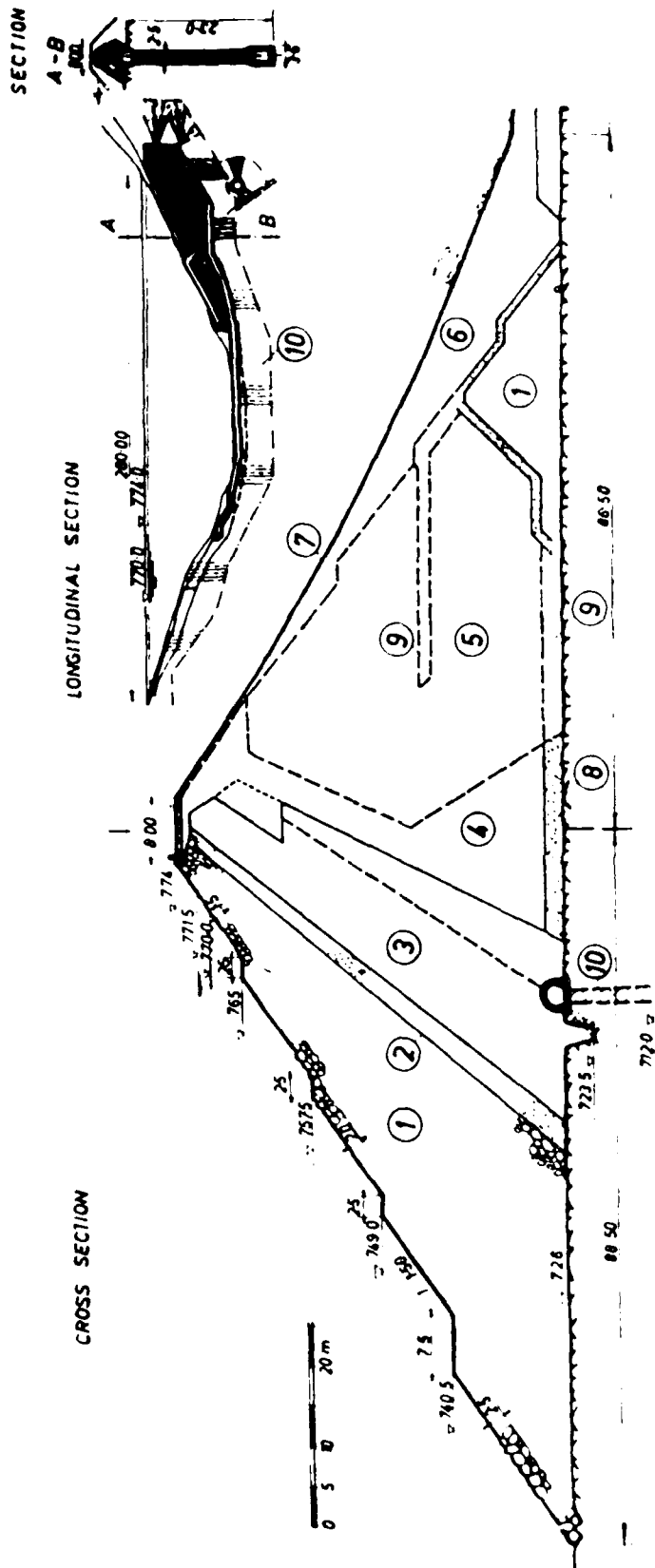


Fig. 2 Cross-section

|   |                        |
|---|------------------------|
| 1 Rock fill                               | 181,000 m <sup>3</sup> |
| 2 Transition filter                       | 29,000 ..              |
| 3 Clay core                               | 93,000 ..              |
| 4 Decomposed schist                       | 323,000 ..             |
| 5 Selected schist                         | 47,000 ..              |
| 6 Quarry waste                            |                        |
| Total 673,000 m <sup>3</sup>              |                        |
| 7 Planted downstream slope                |                        |
| 8 Drainage blanket                        |                        |
| 9 Drainage layers                         |                        |
| 10 Grouting curtain, 5200 m of bore holes |                        |

Section transversale

|   |                        |
|---|------------------------|
| 1 Entrochement  | 181,000 m <sup>3</sup> |
| 2 Filtrés de transition                                 | 29,000 ..              |
| 3 Noyau étanche   | 93,000 ..              |
| 4 Schiste décomposé                                     | 323,000 ..             |
| 5 Schiste sélectionné                                   | 47,000 ..              |
| 6 Tout venant   |                        |
| Total 673,000 m <sup>3</sup>                            |                        |
| 7 Talus (Parment) aval planté                           |                        |
| 8 Base filtrante  |                        |
| 9 Drainages   |                        |
| 10 Injections d'étanchement, au total 5200 m de forages |                        |

Figure 6.5 - Cross-Section of Lokvarka Dam (From Nonveiller, 1957)

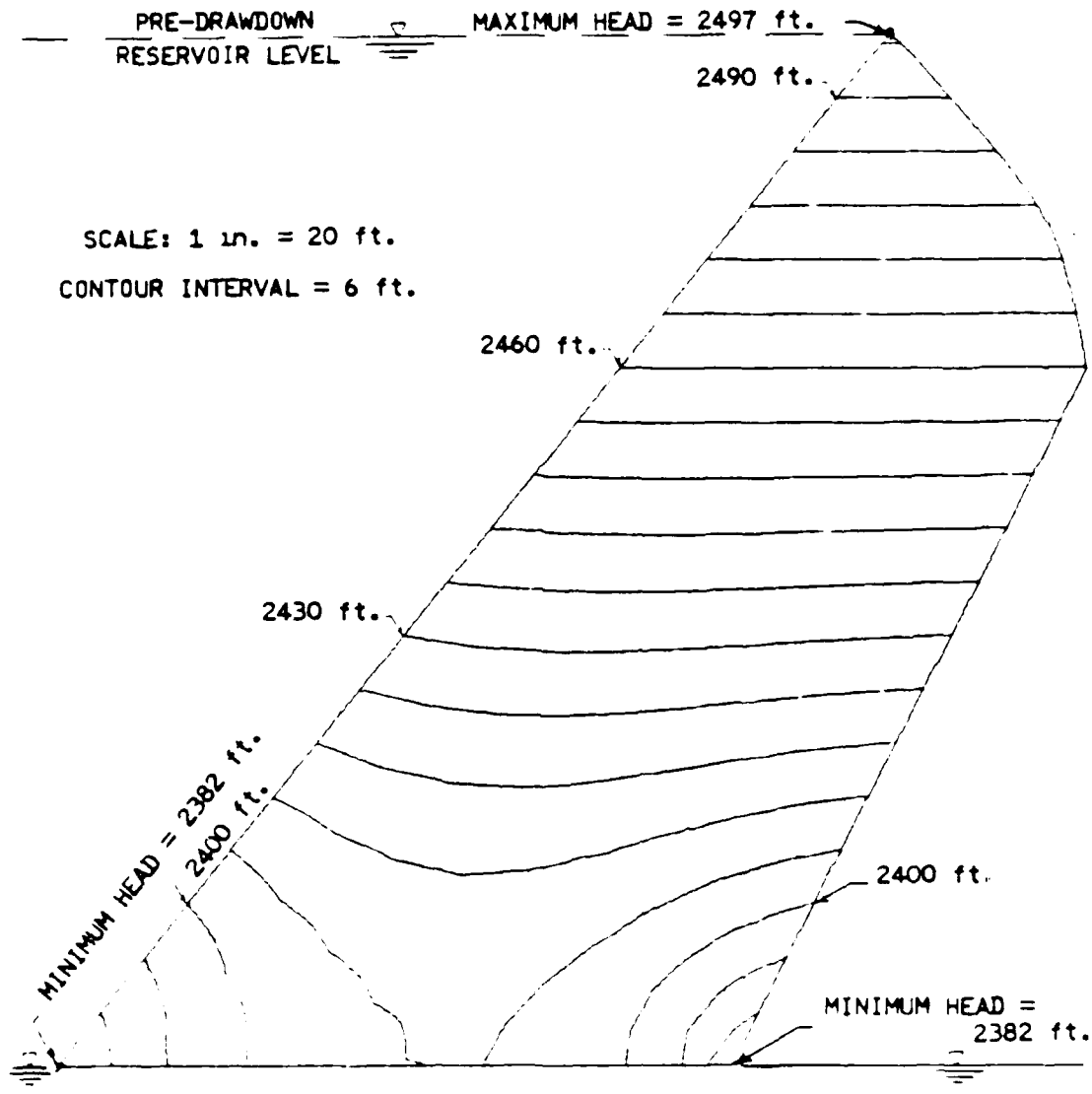


Figure 6.6 - Equipotential Lines From Solution of Steady-State Flow Equations for Lokvarka Dam Core After Full, Instantaneous, Drawdown (From Adams, 1982)

TABLE 6.1

SUMMARY OF FACTORS OF SAFETY CALCULATED BY EFFECTIVE STRESS  
METHODS FOR SELECTED EXAMPLES

| Slope<br>Ratio | $\lambda_{c\phi}$ | Drawdown<br>(percent) | F(Bishop/<br>Morgenstern) | F(Steady<br>Seepage) | <u>F(Steady Seepage)</u> |
|----------------|-------------------|-----------------------|---------------------------|----------------------|--------------------------|
|                |                   |                       |                           |                      | F(Bishop/Morgenstern)    |
| 1.5:1          | 5                 | 35                    | 2.014                     | 2.232                | 1.108                    |
| 1.5:1          | 10                | 35                    | 1.408                     | 1.584                | 1.125                    |
| 1.5:1          | 50                | 35                    | 0.715                     | 0.895                | 1.252                    |
| 1.5:1          | 5                 | 70                    | 1.522                     | 1.732                | 1.138                    |
| 1.5:1          | 10                | 70                    | 1.037                     | 1.213                | 1.170                    |
| 1.5:1          | 50                | 70                    | 0.544                     | 0.685                | 1.259                    |
| 1.5:1          | 5                 | 100                   | 1.397                     | 1.610                | 1.152                    |
| 1.5:1          | 10                | 100                   | 0.933                     | 1.116                | 1.196                    |
| 1.5:1          | 50                | 100                   | 0.484                     | 0.620                | 1.281                    |
| 3.5:1          | 5                 | 35                    | 3.395                     | 3.525                | 1.038                    |
| 3.5:1          | 10                | 35                    | 2.508                     | 2.630                | 1.049                    |
| 3.5:1          | 50                | 35                    | 1.457                     | -                    | -                        |
| 3.5:1          | 5                 | 70                    | 2.617                     | 2.720                | 1.039                    |
| 3.5:1          | 10                | 70                    | 1.918                     | 2.003                | 1.044                    |
| 3.5:1          | 50                | 70                    | 1.261                     | 1.327                | 1.052                    |
| 3.5:1          | 5                 | 100                   | 2.551                     | 2.659                | 1.042                    |
| 3.5:1          | 10                | 100                   | 1.842                     | 1.928                | 1.047                    |
| 3.5:1          | 50                | 100                   | 1.200                     | 1.253                | 1.044                    |

based on the steady-state flow equation would be expected to be much higher than those based on Bishop's and Morgenstern's procedure. Bishop's and Morgenstern's procedure is equivalent to assuming that the flow is horizontal toward the face of the slope and, thus, the equipotential lines are vertical.

#### ANALYSES FOR PILARCITOS DAM

Pilarcitos Dam was examined previously by Wong, Duncan and Seed (1983). They provide the following description:

"Pilarcitos Dam is a homogeneous rolled earthfill embankment. The crest of the dam is about 78 feet above the upstream toe. The upstream toe has a gradient of 2-1/2 to 1 for the lower 58 ft. (i. e. to El. 678), and a 3 to 1 slope from this point to the crest (El. 698). The water level was lowered from El. 692 to El. 657 between October 7 and November 19, 1969, at which time a drawdown slide occurred."

A cross-section of the embankment is shown in Fig. 6.7. The embankment was considered to have a total unit weight of 135 pcf. Effective stress shear strength parameters for the fill were:  $\bar{c} = 0$ ,  $\bar{\phi} = 45$  degrees. Strength parameters for the R envelope were given as:  $c_R = 60$  psf,  $\phi_R = 23$  degrees. Although the information was not given, the R envelope was assumed to have been constructed to be tangent to the circles of stress, i.e.  $c = c_R$ , rather than  $c_{Rf}$ , and  $\phi = \phi_R$ , rather than  $\phi_{Rf}$ .

Factors of safety were computed for the Pilarcitos Dam using the following procedures:

1. Bishop's and Morgenstern's procedure.
2. The effective stress procedure described in Section 5: Stresses caused by drawdown were calculated by the finite element method and

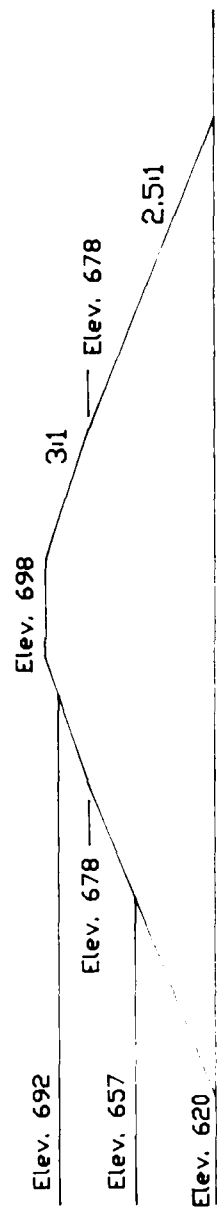


Figure 6.7 - Idealized Cross-Section Used for Analyses of Pilarcitos Dam

pore water pressure coefficients were used to compute the corresponding changes in pore pressure. This procedure is designated as the "Finite Element - A" procedure.

3. The Corps of Engineer's two-stage analysis procedure employing the bilinear (composite R-S) strength envelope.
4. Lowe and Karafiath's procedure; linear interpolation was used, as described in Section 4, to estimate the strength envelopes for values of  $K_c$  between unity and the value at failure ( $K_f$ ).
5. A two-stage analysis procedure employing a single  $\tau_{ff}$  versus  $\bar{\sigma}_{fc}$  relationship based on an effective principal stress ratio of 2 for consolidation. The single envelope was estimated using linear interpolation.

The fifth procedure employing a single envelope to describe the relationship between  $\tau_{ff}$  and  $\bar{\sigma}_{fc}$  was suggested by Wong, Duncan and Seed (1983) as an approximate way of accounting for the effects of anisotropic consolidation and as an alternative to Lowe and Karafiath's more rigorous approach. Wong, Duncan and Seed found the approach produced reasonable results and, accordingly, the procedure was examined as part of the current studies.

Values of the factors of safety are summarized in Table 6.2. The critical shear surface (circle) for Bishop's and Morgenstern's procedure was very shallow, corresponding essentially to a plane coincident with the face of the slope. The corresponding critical circles for the remaining four procedures listed above are shown in respective order in Figs. 6.8 through 6.11. The factors of safety computed by all five procedures were within approximately 15 percent of unity, which would in most cases be considered sufficiently close to unity to indicate

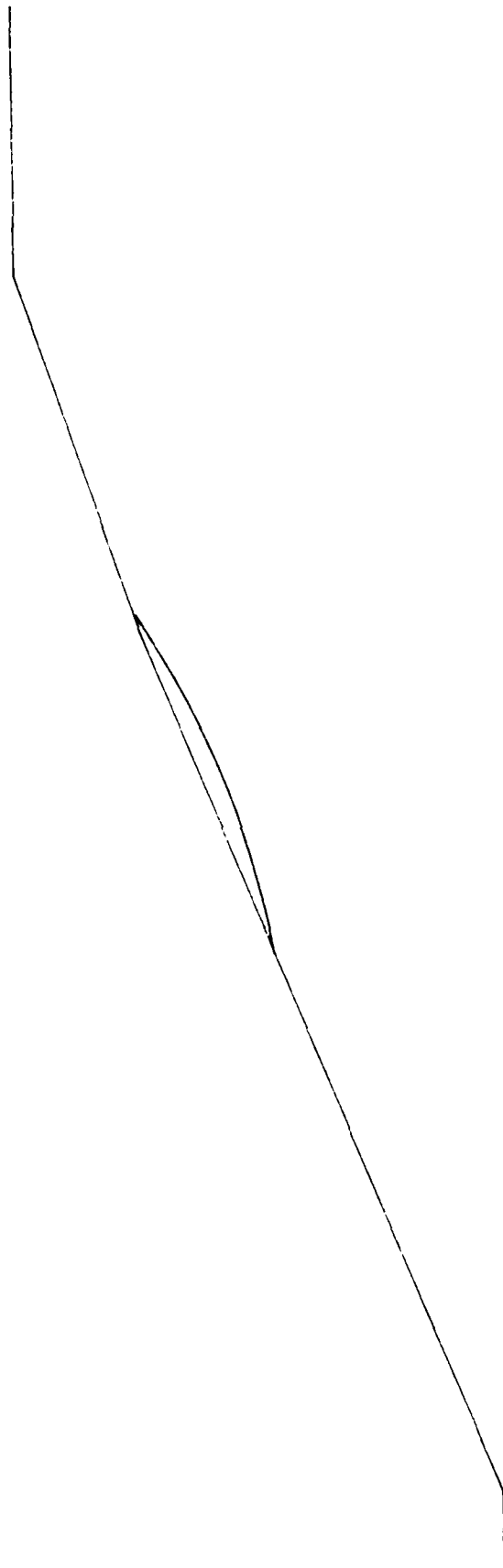


Figure 6.8 - Critical Shear Surface for Pilarcitos Dam Based on Effective Stress Analyses with Pore Pressures Calculated Using Stresses from Finite Element Computations and Pore Pressure Coefficients Estimated from the R-Envelope Using Taylor's Procedure

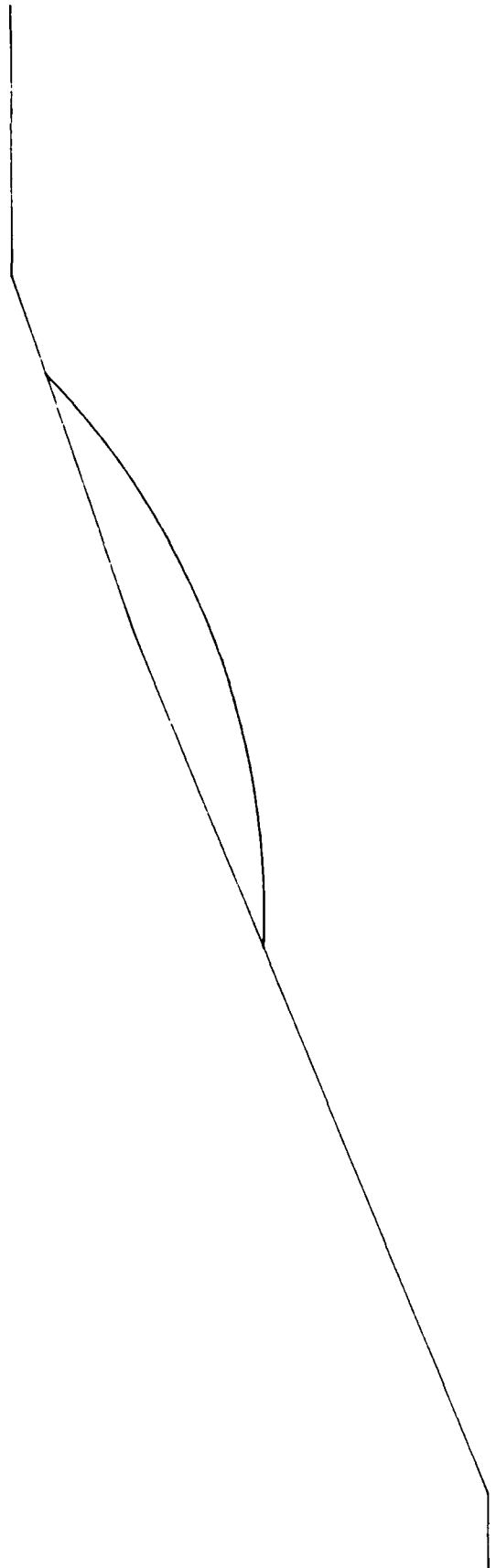


Figure 6.9 - Critical Shear Surface for Pilarcitos Dam Based on the Corps of Engineers' Procedure

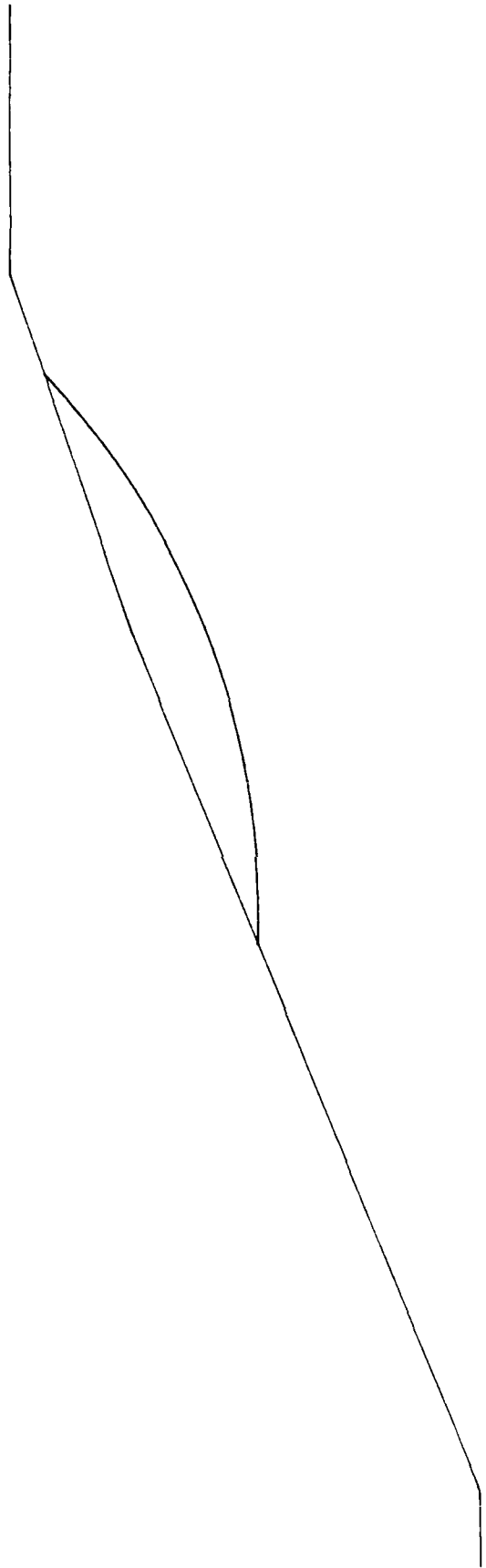


Figure 6.10 - Critical Shear Surface for Pilarcitos Dam Based on Lowe and Karafiath's Procedure - Using Linear Interpolation to Estimate Strength Envelopes for Anisotropic Consolidation from Strength Parameters for Isotropic Consolidation

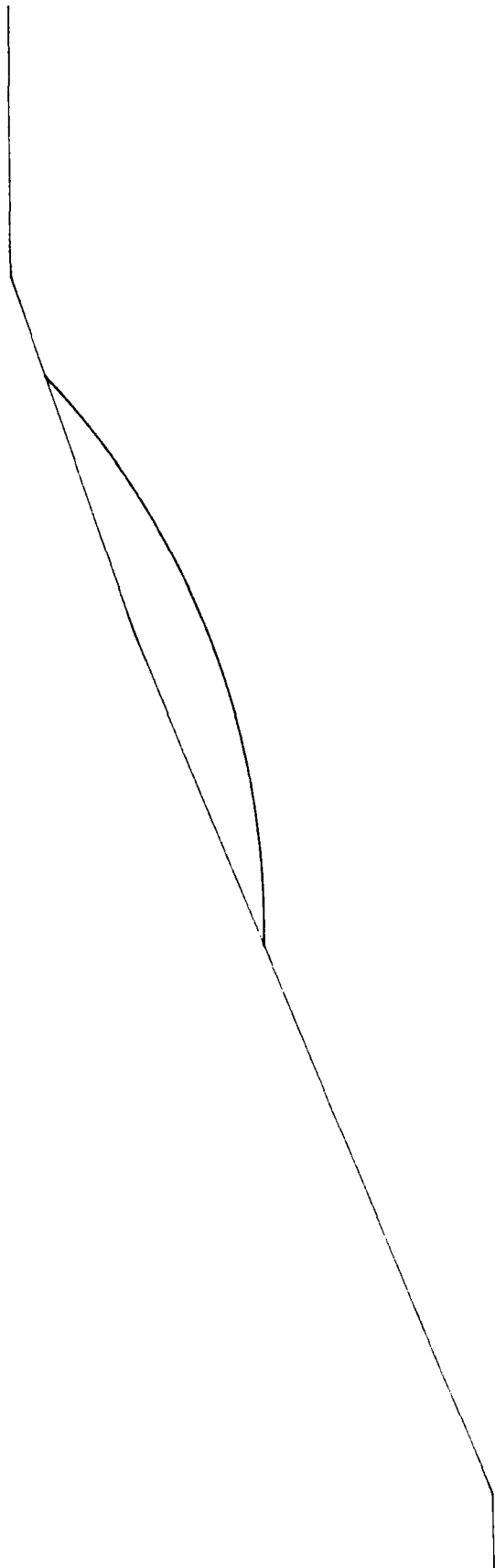


Figure 6.11 - Critical Shear Surface for Pilarcitos Dam Based on a Two-Stage Analysis Employing a Single  
Failure Envelope

TABLE 6.2

SUMMARY OF FACTORS OF SAFETY FOR PILARCITOS DAM  
CALCULATED BY VARIOUS PROCEDURES

| <u>Procedure</u>  | <u>Factor of Safety</u> |
|---|-------------------------|
| Bishop's and Morgenstern's  | 1.160                   |
| Finite Element - A  | 1.117                   |
| Corps of Engineers  | 0.838                   |
| Lowe and Karafiath  | 1.137                   |
| Two-stage with single<br>$\tau_{ff} - \bar{\sigma}_{fc}$ envelope ( $K_c = 2$ ) | 1.097                   |

failure. The second, fourth and fifth of the five procedures listed above produced factors of safety that were in agreement within 2 percent of one another. Such close agreement (2 percent) is encouraging in that the second procedure is an effective stress procedure, while the fourth and fifth procedures are two-stage procedures where the factor of safety after drawdown is actually computed using total stresses and undrained shear strengths. However, all three approaches should reflect the effects of the pore pressures generated by undrained shear during drawdown and the fact that the pore pressure coefficient ( $\bar{A}$ ) varies with the effective consolidation pressure<sup>1</sup>. Accordingly, such close agreement is not surprising.

The factors of safety calculated by the second, fourth and fifth procedures are in close agreement but slightly higher than unity, while the factor of safety calculated by the Corps of Engineer's procedure is somewhat less than unity. The relationship between the factors of safety calculated by these various procedures and a value of unity is as expected: The Corps of Engineers procedure essentially takes a lower-bound, conservative approach for defining shear strengths and effectively ignores higher strengths which would develop at low stresses due to dilatancy. The other approaches (FEM- $\bar{A}$ , Lowe and Karafiath, and Single  $\tau_{ff}-\bar{\sigma}_{fc}$  envelope) on the other hand are based on the assumption

---

<sup>1</sup>Although the pore pressure coefficient is not explicitly considered in the two-stage analysis procedures, the pore pressure coefficients are explicitly expressed. For a given set of effective stress strength parameters ( $c$  and  $\phi$ ) and undrained strength envelope ( $\tau_{ff}-\bar{\sigma}_{fc}$  line or  $c_{Rf}$  and  $\phi_{Rf}$  values) a unique relationship between the pore pressure coefficient and effective stress is implied as discussed in detail in Section 3.

that the soil is undrained and that any effects of dilatancy and the attendant reduction in pore water pressures due to dilatancy can be fully included. In reality conditions somewhere between these two extremes may develop. The consistency and rationality of the results obtained for Pilarcitos Dam should encourage further studies for other case histories.

#### PARAMETRIC STUDIES

The final series of examples was selected and used to perform analyses employing six different procedures. The procedures consisted of the five procedures employed for Pilarcitos Dam plus the procedure based on the solution of the steady-state flow equations as described for the first series of examples. A slope height of 100 feet and side slopes of 1.5:1 and 3.5:1 were used. Four sets of soil properties were used as shown in Table 6.3. The shear strength properties shown are identical to those considered previously in Section 4 where the various procedures for estimating shear strength envelopes for anisotropic consolidation were presented. The initial, pre-drawdown water surface was assumed to be at the crest of the slope and complete, instantaneous drawdown was assumed to occur in all cases and in all procedures.

Factors of safety computed for each set of soil properties (1 through 4) are summarized in Tables 6.4 and 6.5 for 1.5:1 and 3.5:1 slopes, respectively. Two sets of normalized values of the factor of safety are also shown. The first set of normalized values was obtained by dividing the computed factors of safety by the corresponding factor of safety computed using Lowe and Karafiath's procedure. The second set was normalized by dividing the computed factor of safety for each procedure by the corresponding factor of safety computed by the Corps of

TABLE 6.3

SUMMARY OF FOUR SETS OF SOIL PROPERTIES USED  
FOR COMPARATIVE CALCULATIONS WITH VARIOUS PROCEDURES

Property Set Number 1:

Total (saturated) unit weight,  $\gamma$ : 135 pcf

R-Envelope parameters:  $c_R = 60$  psf,  $\phi_R = 23$  degrees

Effective stress strength parameters:  $\bar{c} = 0$ ,  $\bar{\phi} = 45$  degrees

Property Set Number 2:

Total (saturated) unit weight,  $\gamma$ : 130 pcf

R-Envelope parameters:  $c_R = 700$  psf,  $\phi_R = 15$  degrees

Effective stress strength parameters:  $\bar{c} = 200$  psf,  $\bar{\phi} = 31$  degrees

Property Set Number 3:

Total (saturated) unit weight,  $\gamma$ : 135 pcf

R-Envelope parameters:  $c_R = 300$  psf,  $\phi_R = 15.5$  degrees

Effective stress strength parameters:  $\bar{c} = 0$  psf,  $\bar{\phi} = 34$  degrees

Property Set Number 4:

Total (saturated) unit weight,  $\gamma$ : 128 pcf

R-Envelope parameters:  $c_R = 1,400$  psf,  $\phi_R = 22.5$  degrees

Effective stress strength parameters:  $\bar{c} = 0$  psf,  $\bar{\phi} = 35$  degrees

Engineers procedure. Several important observations can be made from the results summarized in Tables 6.4 and 6.5:

1. In six of eight cases the factors of safety computed by Lowe and Karafiath's procedure and by the Finite Element- $\bar{A}$  (FEM- $\bar{A}$ ) procedure were within 15 percent of each other. In one of the cases where the differences were larger (1.5:1 slope, Property Set No. 1) significant errors may have been introduced in extrapolating and interpolating pore pressures at the face of the slope by the FEM- $\bar{A}$  procedure and the results are questionable. In the second case (3.5:1 slope - Property Set No. 4) the cohesion component for the R envelope was substantial. In this case the factors of safety differed by 30 percent. However, the generally small differences between the factors of safety calculated by Lowe and Karafiath's approach and the FEM- $\bar{A}$  procedures are again encouraging. These two approaches differ in that one is an effective stress approach while the other is a two-stage approach, but both reflect the tendency for the soil to either dilate or compress depending on confining stress.

2. The two-stage analysis procedure in which a single envelope ( $\tau_{ff}-\bar{\sigma}_{fc}$ ) was used produced factors of safety which were within 10 percent of the values calculated by Lowe and Karafiath's procedure for six of the eight cases considered. The remaining two cases where the differences were larger occurred for a 1.5:1 slope: In one case (Property Set 1) use of the single envelope resulted in a 17 percent lower factor of safety; in the other case (Property Set No. 4) the single envelope resulted in a factor of safety which was 37 percent higher than the value computed by Lowe and Karafiath's

TABLE 6.4

SUMMARY OF FACTORS OF SAFETY CALCULATED BY VARIOUS PROCEDURES  
METHODS FOR FOUR SETS OF MATERIAL PROPERTIES - 1.5:1 SLOPE

| Property Set | Procedure                                       | Factor of Safety | F / F(Lowe) | F / F(Corps) |
|--------------|---|------------------|-------------|--------------|
| 1            | Bishop/Morgenstern                              | 0.499            | 0.75        | 1.13         |
| 1            | Steady Seepage                                  | 0.501            | 0.75        | 1.14         |
| 1            | FEM-A ( $u \geq 0$ )                            | 0.321            | 0.48        | 0.73         |
| 1            | FEM-A ( $u < 0$ )                               | -                | -           | -            |
| 1            | Corps of Engineers                              | 0.441            | 0.66        | 1.00         |
| 1            | Lowe & Karafiath                                | 0.664            | 1.00        | 1.51         |
| 1            | Single $\tau_{ff} - \bar{\sigma}_{fc}$ envelope | 0.554            | 0.83        | 1.26         |
| 2            | Bishop/Morgenstern                              | 0.564            | 0.77        | 0.84         |
| 2            | Steady Seepage                                  | 0.708            | 0.97        | 1.05         |
| 2            | FEM-A ( $u \geq 0$ )                            | 0.771            | 1.05        | 1.15         |
| 2            | FEM-A ( $u < 0$ )                               | 0.802            | 1.10        | 1.19         |
| 2            | Corps of Engineers                              | 0.672            | 0.92        | 1.00         |
| 2            | Lowe & Karafiath                                | 0.731            | 1.00        | 1.09         |
| 2            | Single $\tau_{ff} - \bar{\sigma}_{fc}$ envelope | 0.787            | 1.08        | 1.17         |
| 3            | Bishop/Morgenstern                              | 0.338            | 0.57        | 0.71         |
| 3            | Steady Seepage                                  | 0.338            | 0.57        | 0.71         |
| 3            | FEM-A ( $u \geq 0$ )                            | 0.528            | 0.89        | 1.12         |
| 3            | FEM-A ( $u < 0$ )                               | 0.549            | 0.93        | 1.16         |
| 3            | Corps of Engineers                              | 0.473            | 0.80        | 1.00         |
| 3            | Lowe & Karafiath                                | 0.591            | 1.00        | 1.25         |
| 3            | Single $\tau_{ff} - \bar{\sigma}_{fc}$ envelope | 0.587            | 0.99        | 1.24         |
| 4            | Bishop/Morgenstern                              | 0.313            | 0.33        | 0.57         |
| 4            | Steady Seepage                                  | 0.316            | 0.33        | 0.57         |
| 4            | FEM-A ( $u \geq 0$ )                            | 0.930            | 0.98        | 1.68         |
| 4            | FEM-A ( $u < 0$ )                               | 0.991            | 1.05        | 1.80         |
| 4            | Corps of Engineers                              | 0.552            | 0.58        | 1.00         |
| 4            | Lowe & Karafiath                                | 0.947            | 1.00        | 1.72         |
| 4            | Single $\tau_{ff} - \bar{\sigma}_{fc}$ envelope | 1.295            | 1.37        | 2.35         |

Note: All factors of safety were calculated using Spencer's limit equilibrium procedure of slices.

TABLE 6.5

SUMMARY OF FACTORS OF SAFETY CALCULATED BY VARIOUS PROCEDURES  
METHODS FOR FOUR SETS OF MATERIAL PROPERTIES - 3.5:1 SLOPE

| Property Set | Procedure                                       | Factor of Safety | F / F(Lowe) | F / F(Corps) |
|--------------|---|------------------|-------------|--------------|
| 1            | Bishop/Morgenstern                              | 1.750            | 1.51        | 1.90         |
| 1            | Steady Seepage                                  | 1.750            | 1.51        | 1.90         |
| 1            | FEM-A ( $u \geq 0$ )                            | 1.145            | 0.99        | 1.24         |
| 1            | FEM-A ( $u < 0$ )                               | 1.145            | 0.99        | 1.24         |
| 1            | Corps of Engineers                              | 0.920            | 0.79        | 1.00         |
| 1            | Low & Karafiath                                 | 1.160            | 1.00        | 1.26         |
| 1            | Single $\tau_{ff} - \bar{\sigma}_{fc}$ envelope | 1.186            | 1.02        | 1.29         |
| 2            | Bishop/Morgenstern                              | 1.340            | 0.97        | 1.14         |
| 2            | Steady Seepage                                  | 1.397            | 1.01        | 1.19         |
| 2            | FEM-A ( $u \geq 0$ )                            | 1.483            | 1.07        | 1.26         |
| 2            | FEM-A ( $u < 0$ )                               | 1.483            | 1.07        | 1.26         |
| 2            | Corps of Engineers                              | 1.174            | 0.85        | 1.00         |
| 2            | Low & Karafiath                                 | 1.383            | 1.00        | 1.18         |
| 2            | Single $\tau_{ff} - \bar{\sigma}_{fc}$ envelope | 1.412            | 1.02        | 1.20         |
| 3            | Bishop/Morgenstern                              | 1.181            | 1.09        | 1.36         |
| 3            | Steady Seepage                                  | 1.181            | 1.09        | 1.36         |
| 3            | FEM-A ( $u \geq 0$ )                            | 1.237            | 1.14        | 1.43         |
| 3            | FEM-A ( $u < 0$ )                               | 1.239            | 1.14        | 1.43         |
| 3            | Corps of Engineers                              | 0.867            | 0.80        | 1.00         |
| 3            | Low & Karafiath                                 | 1.088            | 1.00        | 1.25         |
| 3            | Single $\tau_{ff} - \bar{\sigma}_{fc}$ envelope | 1.134            | 1.04        | 1.31         |
| 4            | Bishop/Morgenstern                              | 1.158            | 0.49        | 0.91         |
| 4            | Steady Seepage                                  | 1.159            | 0.49        | 0.91         |
| 4            | FEM-A ( $u \geq 0$ )                            | 1.667            | 0.70        | 1.31         |
| 4            | FEM-A ( $u < 0$ )                               | 1.669            | 0.70        | 1.32         |
| 4            | Corps of Engineers                              | 1.268            | 0.53        | 1.00         |
| 4            | Low & Karafiath                                 | 2.383            | 1.00        | 1.88         |
| 4            | Single $\tau_{ff} - \bar{\sigma}_{fc}$ envelope | 2.237            | 0.94        | 1.76         |

Note: All factors of safety were calculated using Spencer's limit equilibrium procedure of slices.

more rigorous procedure. No significant correlations between the differences in the factors of safety by the two procedures and the soil properties were evident; the differences would be affected both by the effective principal stress ratio and the magnitude of the effective normal stresses along the shear surface before drawdown. A single  $\tau_{ff} - \sigma_{fc}$  envelope may not be suitable for some cases and, accordingly, should be used cautiously.

3. The factors of safety computed by the Corps of Engineers procedure ranged from approximately 53 percent to 92 percent of the value computed by Lowe and Karafiath's procedure. The largest differences occur for Property Set No. 4 which exhibited the largest cohesion intercept for the R-envelope. The differences between the factors of safety computed by the Corps of Engineers' procedure and Lowe and Karafiath's procedure reflect the conservative nature of the Corps of Engineers' approach. The Corps of Engineers' approach deliberately neglects the higher undrained shear strengths associated with dilatancy at low confining pressures.

4. The factors of safety computed by effective stress procedures employing Morgenstern's approach and the steady-state flow procedure for estimating pore water pressure were generally in agreement within 5 percent or better. The only exception to this agreement occurred for the 1.5:1 slope with Property Set No. 2 where the pore pressures computed by Bishop's and Morgenstern's approach produced a factor of safety approximately 20 percent lower than by the steady-state flow approach. This larger difference (20 percent) is due to the significant effective cohesion value for

Property Set No. 2, which caused the critical shear surface to pass deeper than in other cases. As the depth increases the differences between the pore water pressures by Bishop's and Morgenstern's approach and the steady-state flow approach would be expected to become more pronounced.

5. Factors of safety computed by effective stress procedures based on either Bishop's and Morgenstern's approach or the steady-state flow approach ranged from approximately 33 to 150 percent of the values computed by Lowe and Karafiath's procedure. Similarly the values by these effective stress procedures ranged from 57 to 190 percent of the values computed by the Corps of Engineers procedure. The factors of safety computed by the effective stress approaches generally tended to increase relative to those computed by either Lowe and Karafiath's or the Corps of Engineers procedures as the slope became flatter and as the cohesion intercept for the R-envelope decreased, i. e. as the tendency for dilatancy to occur diminished. The relatively large differences between the factors of safety computed by the two effective stress approaches and by the two-stage approaches should be expected: Both effective stress approaches make no distinction among soil types with regard to the tendency for pore pressures to vary depending on the degree to which the soil tends to compress or expand, while the two-stage procedures are strongly affected by the tendency for pore pressures to develop and affect undrained shear strength.

6. With only one exception Bishop's and Morgenstern's procedure produced factors of safety which were either significantly lower or within 10 percent of the values computed by Lowe and Karafiath's

procedure. Accordingly, the procedure seems to generally meet the intended objective of being at least on the conservative (safe) side. The exception to this conservatism occurred in the case of a 3.5:1 slope with Property Set No. 1, where  $c_R$  was relatively small (60 psf) while  $\bar{\phi}$  was relatively large (45 degrees). In this case Morgenstern's approach produced a factor of safety which was 50 percent higher than the value computed by Lowe and Karafiath's procedure and 90 percent higher than the value computed by the Corps of Engineers procedure.

7. The Corps of Engineers procedure produced factors of safety which were either lower than or within 10 percent of the values computed by all other procedures with only a few exceptions. The exceptions occurred with regard to the effective stress procedures for a 1.5:1 slope and two of the sets of material properties considered. In these cases the effective stress procedures produced much lower factors of safety; however, there is no basis to judge that either the effective stress procedures or Corps of Engineer's procedure were more correct. It appears likely that neither one is correct, but both may be conservative to varying degrees.

## SECTION 7

### SUMMARY, CONCLUSIONS AND RECOMMENDATIONS

(Duncan and Wright)

#### SUMMARY

A number of procedures exist for performing slope stability analyses for sudden drawdown. These various procedures differ principally in the manner in which the shear strength is defined and can be grouped into two general categories. The first category includes those procedures which are based on the use of effective stresses. The effective stress procedures require that pore water pressures be estimated at the end of sudden drawdown and the differences among the various effective stress procedures are related directly to differences in the procedures used to estimate pore water pressures. The second category of procedures for sudden drawdown analysis is two-stage procedure: One set (stage) of calculations is performed for conditions immediately prior to drawdown and is used to estimate effective stresses and corresponding undrained strengths; the second set (stage) of computations is performed for conditions immediately after drawdown and employs undrained shear strengths estimated from the first set of computations.

#### Effective Stress Analysis Procedures.

Most of the effective stress analysis procedures are based on one of two approaches to estimate pore water pressures. One approach employs Skempton's pore pressure coefficients and estimated changes in total stress (due to drawdown) to estimate changes in pore water pressure and subsequently the final pore water pressures. Bishop's and Morgenstern's

procedure and the "new" alternative procedure based on the finite element method to calculate stresses, which was described in Section 5 of this paper, represent the first class of effective stress approaches. The second class of effective stress approaches is based on solutions to some form of the equations for hydraulic flow. Most of these are based on very simplified assumptions and neglect the tendency for soil to change volume and develop pore water pressures due to shear stresses induced by drawdown. Although more rigorous solutions are possible and should lead to improved results, such rigorous solutions have generally not been used. The most common solutions are based on simply solving the equation for steady-state flow and ignoring transient effects.

An alternative procedure has been presented in this paper as an improvement over Bishop's and Morgenstern's procedure whereby the variation in the pore pressure coefficient  $\bar{A}_f$  with effective stress is accounted for and the changes in stress caused by removal of the water load at the slope face are more realistic. However, the procedure has not been tested extensively and requires considerably more effort to use than any of the other procedures, effective stress or two-stage, described in this paper.

#### Two-Stage Analysis Procedures

The only difference among the various two-stage analysis procedures is in the manner in which the undrained shear strength is estimated from the effective stresses before sudden drawdown. Two principal approaches have been used for this purpose: One is the Corps of Engineers procedures, which adopts essentially a "lower-bound" approach for estimating the relationship between undrained shear strength and effective consolidation pressure. The second approach is the one

suggested by Lowe and Karafiath which attempts to account for the effects of anisotropic consolidation on the undrained shear strength. A third approach was suggested by Wong, Duncan and Seed (1983) and was used in the comparative studies in Section 6. The third approach employs a single relationship between undrained shear strength and effective consolidation pressure, which accounts in an approximate manner for the effects of anisotropic consolidation and is somewhat simpler than Lowe and Karafiath's procedure.

Several approaches have been suggested for estimating the effects of anisotropic consolidation on the undrained shear strength of the soil without performing extensive laboratory tests with anisotropic consolidation. Further study and verification of the various procedures would be useful; however, it appears that at least several may be used with reasonable success and confidence at the present time. Accordingly, it appears that the effects of anisotropic consolidation can be accounted for at least in an approximate manner in slope stability analyses without the necessity for very extensive laboratory testing.

#### CONCLUSIONS

This study provides a basis for a number of important conclusions regarding the accuracy and the degree of conservatism of procedures for analyzing rapid drawdown slope stability. The writers believe that the results of the study have brought the state-of-the-art to a point where it is possible to establish what is the most suitable procedure for analysis of rapid drawdown slope stability problems, without need for extensive further studies.

One of the facts brought out clearly by the studies in this paper is that effective stress analysis procedures that use simple pore

pressure assumptions do not properly reflect the actual behavior of the soils in the slope. These procedures (Bishop and Morgenstern, Steady Seepage) use the same estimates of pore water pressure after drawdown no matter what the characteristics of the soil are with regard to development of pore pressures during undrained loading. As estimated by these procedures, the pore pressures after drawdown are the same for all soils, no matter whether they develop high or low pore water pressures during undrained loading. Based on the results of the comparative analyses it appears that these methods may be excessively conservative in some cases, and unconservative in other cases. At best they are suitable only for "quick-and-dirty" analyses, being easy to perform but unreliable with regard to accuracy.

The remaining effective stress method discussed (the FEM-A procedure) resulted in factors of safety that were consistently in good agreement with those calculated using Lowe and Karafiath's procedure. This finding is very significant. It indicates that these two different procedures for approaching the mechanics of the analyses lead to essentially the same results if they are consistent with respect to soil strength parameters and pore water pressures. Pore water pressures are considered explicitly in the effective stress analyses and implicitly in Lowe and Karafiath's procedure. Although the FEM-A procedure is too complex and time-consuming for routine use, it has served a very useful purpose by further validating Lowe and Karafiath's procedure, the most soundly based of the available methods with respect to consistency of mechanics and treatment of soil shear strength.

The Corps of Engineers' procedure is the only one in use that excludes components of strength resulting from negative pore water

pressures. It accomplishes this by using the drained strength envelope in the low stress range where the drained (S) envelope is below the consolidated-undrained (R) envelope. This procedure ensures that the factor of safety will not be overestimated if some drainage occurs during drawdown. If some amount of drainage does occur during drawdown, negative pore pressures that develop in the slope at shallow depths would be reduced in magnitude, and the strength of the soil would be reduced accordingly.

Methods such as Lowe and Karafiath's and others that include components of strength resulting from negative pore pressures give unconservative estimates of factor of safety except for completely undrained conditions. As an example, consider the results of the analyses of Pilarcitos Dam shown in Table 6.2: Lowe and Karafiath's procedure results in a value of  $F = 1.14$ , while the Corps of Engineer's procedure results in a value of  $F = 0.84$ , for the failure condition where the actual factor of safety must have been less than or equal to unity. While it must be recognized that these values of factor of safety might be biased due to unknown inaccuracies in evaluation of the shear strength parameters, it is nevertheless clear that unconservative estimates of safety factor may be calculated when shear strength resulting from negative porepressures are not eliminated.

Based on the results presented in this paper, it is clear that a method of analysis of rapid drawdown slope stability to be used for design of embankment dam slopes should have the following characteristics:

- (1) The procedure should employ a measure of shear strength and pore pressure that reflects the actual properties of the soils in

the slope. Specifically, the tendency of the soils to develop low or high pore pressures during undrained shear should be reflected in the shear strength or pore pressure parameters used in the analyses.

While in principle this aspect of the soil behavior can be included in either effective stress or total stress analyses, in practice it is much easier and more practical to represent it by using a two-stage analysis procedure, with total stress analysis of stability after drawdown.

(2) The procedure should employ a soundly based technique for relating shear strength to effective consolidation pressures. The method of relating the shear stress on the failure plane at failure to the effective stresses at the time of consolidation used by Lowe and Karafiath is, in the writers' opinion, the most logical and fundamentally sound method available for doing this. In contrast, the method now used by the Corps of Engineers, involving use of the R envelope, is fundamentally less sound. Its greatest merit is that it can be shown to be somewhat conservative for most (but not all) conditions.

(3) The procedure should not include strength components due to negative pore water pressures, to avoid overestimating factors of safety for conditions where partial drainage occurs during drawdown. The Corps of Engineers method of using the drained strength envelope in the range of low stresses where the undrained strength exceeds the drained strength is a simple and practical means of accomplishing this objective.

A method with these characteristics can be conceived as a combination of methods currently in use. It could be described as being a modification of the method currently used by the Corps of Engineers, the modification being adoption of Lowe and Karafiath's procedure for representing the undrained strength of the soil, rather than using the R-envelope as is now done. Lowe and Karafiath's procedure relates the shear stress on the failure plane at failure to the effective stress on the failure plane during consolidation and the effective principal stress ratio during consolidation. The new method could also be described as being a modification of Lowe and Karafiath's procedure, the modification being elimination of strength components due to negative pore pressures through use of the drained strength envelope in the low range of stresses where the undrained strength exceeds the drained strength.

#### RECOMMENDATIONS

It is recommended that a computer program be developed incorporating the features outlined above, and adopted for use in analysis and design by the Corps of Engineers. The program should be tested by analyzing the same benchmark cases analyzed in the present study to insure that, as expected, it results in factors of safety that fall between the values computed using the current Corps of Engineers procedure and those calculated using Lowe and Karafiath's procedure. The writer believes that the method described will incorporate the best features of all current procedures, being soundly based with regard to treatment of shear strength, and reliably conservative through adoption of the Corps of Engineers procedure for eliminating strength components resulting from negative pore water pressures.

It is recommended that the linear interpolation method be used to establish the relationships among shear stress on the failure plane at failure, effective stress on the failure plane during consolidation, and effective principal stress ratio during consolidation. This procedure requires only R-bar tests (conventional isotropically consolidated-undrained triaxial tests with pore pressure measurement) for strength evaluation. The required laboratory testing will, thus, be no more difficult than required for the analysis procedure currently used by the Corps of Engineers.

It is recommended that the appropriate minimum factor of safety for use with the new method of analysis is  $F = 1.00$ . The factors supporting use of  $F = 1.00$  for rapid drawdown conditions analyzed by this procedure are:

- (1) Like the method currently used by the Corps of Engineers, the method will provide a conservative bias in the strength evaluations by eliminating components of strength resulting from negative pore pressures.
- (2) There is a further conservative bias in the use of freshly compacted laboratory test specimens for strength evaluations, because compacted soils become harder and stronger with age after compaction. Ignoring this increase in strength and stiffness, as is conventional procedure, results in inherently conservative estimates of shear strengths for compacted fills.
- (3) Most critical failure mechanisms for slope instability during rapid drawdown are shallow. Thus, most rapid drawdown slides do not threaten the integrity of the dam and pose no threat of loss of

the reservoir. The consequence of a rapid drawdown slide in most cases is only the cost of repair, and there is no threat to life.

The positions of slip surfaces should be examined critically when the slope stability analyses are performed, and any slip surface involving possible failure of a large portion of the embankment, or which cuts through the crest and would lead to loss of freeboard, or which has the potential for blocking an outlet works, should have a factor of safety during rapid drawdown greater than unity.

In summary, it is the writers' opinion that the studies presented in this report provide an adequate basis for selection of a method of analysis for rapid drawdown for use by the Corps of Engineers. This new method should incorporate the best features of the method currently used by the Corps, and the method developed by Lowe and Karafiath. It is recommended that a computer program be developed for performing analyses using this procedure, and that the program and the procedure be adopted as standards for use by the Corps.

## REFERENCES

- Adams, Gregory Lee (1982), "Application of the Finite Element Method to Steady-State Flow Through Porous Media." Thesis Presented to the Faculty of the Graduate School of The University of Texas at Austin in Partial Fulfillment of the Requirements for the Degree of Master of Science in Engineering, March, 1982.
- Bazett, L. (1961), "Field Measurements of Pore Water Pressures," Proceedings Twelfth Canadian Soil Mechanics Conference, Vol. 1, Part 3, pp. 2-9, 1961.
- Benjamin, H. F., Jr. (1975), "A Comparison of the Effect of Isotropic vs. Anisotropic Consolidation on the Undrained Shear Strength of Cohesive Soils." Special Project report to Prof. G. W. S. Carter, University of California, Berkeley, Summer, 1975.
- Bishop, Alan W., and A. K. Gamal Eldin (1963), "The Effect of Stress History on the Relation between  $\sigma$  and Porosity in Sand," Proceedings of the Third International Conference on Soil Mechanics and Foundation Engineering, Zurich, Vol. 1, pp. 100-105.
- Bishop, A. W. (1964a), Discussion of the paper, "Shear Characteristics of a Saturated Silt, Measured in Triaxial Compression," by Penman, Geotechnique, Institution of Civil Engineers, Great Britain, Vol. 14, No. 2, 1963, pp. 121-131.
- Bishop, A. W. (1964b), "The Use of Pore Pressure Coefficients in Practice," Geotechnique, The Institution of Civil Engineers, Great Britain, Vol. 14, No. 4, Dec., 1964, pp. 148-150.
- Brahma, S. R. and M. E. Harr (1963), "Transient Development of the Free Surface in a Homogeneous Earth Dam," Geotechnique, Great Britain, Vol. 13, No. 4, 1963, pp. 283-302.
- Browzin, B. G. (1961), "Non-Steady Flow in Homogeneous Earth Dams After Rapid Drawdown," Proceedings of the Fifth International Conference on Soil Mechanics and Foundation Engineering, Paris, Vol. 1, pp. 551-554.
- Federqien, H. H. (1948), "Discussion of 'Investigation of Drainage Rates Affecting Stability of Earth Dams' by F. W. Steed," Transactions, ASCE, Vol. 118, pp. 1285-1293, 1948.
- Federqien, Harry H. (1967), Seepage, Drainage and Flow Nets, John Wiley and Sons, Inc., New York, 1967.
- Forces of Engineers (1970), "Engineering and Design of Stability of Earth and Rock-Fill Dams," Engineer Manual EM 111-2-1000, Department of the Army, Corps of Engineers, Office of the Chief of Engineers, 1 April 1970.
- Desai, Chandrakant G., and Walter S. Sherman (1971), "The Effect of Transient Seepage in Sloping Banks," Journal of the Soil Mechanics and Foundations Division, ASCE, Vol. 97, No. SM2, Feb., 1971, pp. 255-277.

Desai, Chandrakant S. (1972). "Seepage Analysis of Earth Banks Under Drawdown," Journal of the Soil Mechanics and Foundations Division, ASCE, Vol. 98, No. SM11, Nov., 1972, pp. 1143-1162.

Desai, Chandrakant S. (1977). "Drawdown Analysis of Slopes by Numerical Method," Journal of the Geotechnical Engineering Division, ASCE, Vol. 103, No. GT7, July, 1977, pp. 667-676.

Doherty, William P., Edward L. Wilson and Robert L. Taylor (1969). "Stress Analysis of Axisymmetric Solids Utilizing Higher-Order Quadrilateral Finite Elements," Report No. S.E.S.M. 69-3, Structural Engineering Laboratory, University of California, Berkeley, Jan., 1969.

Duncan, J. M., and H. Bolton Seed (1966). "Strength Variation Along Failure Surfaces in Clay," Journal of the Soil Mechanics and Foundations Division, ASCE, Vol. 92, No. SM6, Nov., 1966, pp. 81-104.

Freeze, R. Allan, and John A. Cherry (1979). Groundwater, Prentice-Hall, Inc., New Jersey, 1979.

Glover, R. E., H. J. Gibbs and W. W. Daehn (1948). "Deformability of Earth Materials and Its Effect on the Stability of Earth Dams Following a Rapid Drawdown," Proceedings of the Second International Conference on Soil Mechanics and Foundation Engineering, Rotterdam, Vol. 5, pp. 77-80.

Henkel, D. J. (1960). "The Shear Strength of Saturated Remolded Clays," Research Conference on Shear Strength of Cohesive Soils, ASCE, University of Colorado, Boulder, June, 1960, pp. 533-554.

Holtz, Robert D., and William D. Kovacs (1981). An Introduction to Geotechnical Engineering, Prentice-Hall, Inc., Englewood Cliffs, New Jersey, 1981.

Johnson, Stanley J. (1974). "Analysis and Design Relating to Embankments," Proceedings of the Conference on Analysis and Design in Geotechnical Engineering, Austin, ASCE, 1974, pp. 1-48.

Lowe, John, III, and Leslie Karatiath (1960a). "Stability of Earth Banks upon Drawdown," Proceedings of First PanAmerican Conference on Soil Mechanics and Foundation Engineering, Mexico City, Vol. 1, 1960, pp. 537-552.

Lowe, J. III, and Leslie Karatiath (1960b). "Effect of Anisotropic Consolidation on the Undrained Shear Strength of Compacted Clay," Research Conference on Shear Strength of Cohesive Soils, ASCE, University of Colorado, Boulder, June, 1960, pp. 555-566.

Meyer-Peter, E., and H. M. Neuner (1944). "The Stability of Earth Banks," International Conference on Soil Mechanics and Foundation Engineering, Rotterdam, Vol. 1, 1944, pp. 1-11.

Wang, J. S. (1978). "The Effect of Drawdown on the Stability of Earth Banks," Proceedings of the Conference on Analysis and Design in Geotechnical Engineering, Austin, ASCE, 1978, pp. 1-11.

Nagy, L. (1967), "The Effect of Rapid Water Level Lowering on the Shores of Storage Reservoirs," Transactions of the Ninth International Conference on Large Dams, Istanbul, Vol. 3, pp. 887-893.

Newlin, C. W., and S. C. Rossier (1971), "Embankment Drainage After Instantaneous Drawdown," Journal of the Soil Mechanics and Foundations Division, ASCE, Vol. ??, No. SM1, Jan., pp. 47-58.

Neuman, S. P., and P. A. Witherspoon (1970), "Finite Element Method for Analyzing Steady Seepage with a Free Surface," Water Resources Research, Vol. 6, No. 3, June, 1970.

Newlin, C. W., and S. C. Rossier (1967), "Embankment Drainage After Instantaneous Drawdown," Journal of the Soil Mechanics and Foundations Division, ASCE, Vol. 93, No. SM6, Nov., pp 79-96.

Nonveiller, E. (1957), "Pore Pressure in the Lokvarka Dam," Proceedings of the Fourth International Conference on Soil Mechanics and Foundation Engineering, Vol. 2, London, 1957, pp. 341-347.

Noorany, I., and H. B. Seed (1965), "IN-situ Strength Characteristics of Soft Clays," Journal of the Soil Mechanics and Foundations Division, ASCE, Vol. 91, No. SM2, Mar., 1965, pp. 49-80.

Paton, J. and N. G. Semple (1960), "Investigation of the Stability of an Earth Dam Subjected to Rapid Drawdown Including Details of Pore pressures Recorded During a Controlled Drawdown Test," Proceedings of the Conference on Pore Pressure and Suction in Soils," Butterworth, London, pp. 85-90.

Perloff, W. H., and W. Baron (1976), Soil Mechanics, Principles and Applications, The Ronald Press Co., New York, 1976.

Rowe, P. W. (1962), "The Stress Dilatancy Relation for Static Equilibrium of an Assembly of Particles in Contact," Proceedings of the Royal Society A, 269, pp. 500-527.

Rowe, P. W., L. Barden and I. K. Lee (1964), "Energy Components During the Triaxial Cell and Direct Shear Tests," Geotechnique, Institution of Civil Engineers, Great Britain, Vol. 14, No. 3, 1964, pp. 247-261.

Skempton, A. W. (1954), "The Pore-Pressure Coefficients A and B," Geotechnique, The Institution of Civil Engineers, Great Britain, Vol. 4, No. 4, Dec., 1954, pp. 143-147.

Sowers, George F. (1979), Introductory Soil Mechanics and Foundations: Geotechnical Engineering, Fourth Edition, MacMillan Publishing Co., Inc., New York, 1979.

Terzaghi, Karl, and Ralph B. Peck (1967), Soil Mechanics in Engineering Practice, Second Edition, John Wiley, and Sons, Inc., New York, 1967.

Van Saun, Richard (1985). "An Evaluation of the Use of Pore Pressure Coefficients in the Analysis of Rapid Drawdown in Earth Slopes." Dissertation Presented to the Faculty of the Graduate School of The University of Texas at Austin in Partial Fulfillment of the Requirements for the Degree of Doctor of Philosophy. August, 1985.

Winkley, Thomas Robert (1982). "Embankment Pore Water Pressures and Stability During Rapid Reservoir Drawdown." Thesis Presented to the Faculty of the Graduate School of The University of Texas at Austin in Partial Fulfillment of the Requirements for the Degree of Master of Science in Engineering. August, 1982.

Wong, Kai S., James Michael Duncan and H. Bolton Seed (1983). "Comparison of Methods of Rapid Drawdown Stability Analysis." Report No. UCB/GT/82-05, Department of Civil Engineering, University of California, Berkeley. December, 1982. Revised July, 1983.

Wright, Stephen G. (1986a). "UTEXAS2 (University of Texas Analysis of Slopes - Version 2): A Computer Program for Slope Stability Calculations." Geotechnical Engineering Software GS86-1, Geotechnical Engineering Center, The University of Texas. February, 1986.

Wright, Stephen G. (1986b). "Limit Equilibrium Slope Stability Equations Used in the Computer Program UTEXAS2." Geotechnical Engineering Software GS86-1, Geotechnical Engineering Center, The University of Texas. August, 1986.

END

FEB.

1988

DTIC